The Histone Variant H2Av Regulates Stress Responses and Tissue Development through Interactions with Chromatin Insulator Proteins in *Drosophila melanogaster*

A Dissertation Presented for the

Doctor of Philosophy

Degree

The University of Tennessee, Knoxville

James Ryan Simmons

August 2021

Dedication

I dedicate this doctoral dissertation to my mother, Gloria Simmons, who worked tirelessly as a special education teacher to raise my brother and me. Her work ethic and respect for education always inspired me to push myself further and made this achievement possible for me.

Acknowledgements

I would like to first and foremost acknowledge the support of my dissertation mentor, Dr. Mariano Labrador. His guidance through the various challenges this project presented has been invaluable and I am grateful to have worked under his tutelage. This work has significantly benefited from the input and advice from my committee members Dr. Bruce McKee, Dr. Rachel Patton McCord, Dr. Keerthi Krishnan, Dr. Jae Park, and Dr. Tarek Hewezi. I also thank Dr. Rachel Patton McCord for critical review of our recent manuscript. I would like to express my gratitude to the PEER program for professional development and the BCMB department for financial support. This work was also supported by NIH grant 5R21MH108956-02.

I would also like to acknowledge those associated with the Labrador lab for their support over the years. In addition to her research support, I thank Maria Piedad Plata for her kindness and friendship. I also thank Dr. Thomas Dockendorff for his assistance in the lab and for advice on multiple occasions. It has been a pleasure to work with a number of talented graduate students in our lab. I thank Dr. Emily Stow for her friendship and her contributions to our work on several projects. I would also like to acknowledge Bright Amankwaa for his dedicated work and contributions to my project. It was a privilege to mentor numerous undergraduate students during the course of this work, some of whom made significant contributions that pushed our research forward. I thank Andrea Mancheno Lopez and Shannon Stroud for their countless hours recording and scoring neuroblast karyotypes. I also thank Justin Dale Kemp for his efforts in collecting and analyzing immunostaining data, even continuing his efforts remotely after leaving campus due to the Covid-19 pandemic.

I owe thanks to many of my friends and colleagues for their help, encouragement, and friendship during my time in graduate school. This includes Quitao He, Elsie Adams, and Chris Turpin in the BCMB department. I also thank family friend Lynnville Charles for his friendship and help over the years. Many thanks as well to Alex Edwards for his friendship and our many adventures skiing, camping, and fishing.

My family has been my strongest source of resolve during my time in graduate school. I owe my work ethic and my love of education to my mother, Gloria Simmons, who has given everything she has to support our family. I am forever grateful for her sacrifices and our time spent together. I thank my brother, Jason Simmons, for his emotional support and for being there for me when I needed him throughout my entire life. I would also like to acknowledge my niece, Jennifer Simmons, along with my sister-in-law, Erika, and nephews, EJ and Dempsey, for filling our family home with love and boundless energy. A special acknowledgment goes to Jeremy Watson, to whom I owe much of my success, sanity, and future. Finally, much love goes to my best canine friend and lunchtime companion, Ribgy "Bigrig" Simmons, who is always there to greet me with a wagging tail.

Abstract

The ability of a cell to sense and respond to various forms of stress is essential to maintain integrity of the genome. Numerous pathways have been implicated in cellular responses to environmental and genotoxic stresses, often involving proteins and complexes that bind DNA directly to orchestrate changes in transcription and genome organization. Chromatin insulators describe a class of protein complex that bind specific sequences in the genome and work through two classically described functions: to restrict communication between enhancers and promoters through physical separation into different genomic domains and to prevent the spread of heterochromatin into euchromatic regions of the genome. Insulator sites also demarcate the boundaries between topologically associating domains (TADs). *Drosophila melanogaster* has an array of different insulator complexes, with each complex being recruited to different sequences. Here, we demonstrate an interaction between proteins that associate with the *gypsy* insulator and the phosphorylated histone variant H2Av (γH2Av), a marker of DNA double strand breaks. The *gypsy* retrotransposon contains binding sites for Suppressor of Hair Wing (Su(Hw)), which interacts with and recruits Mod(mdg4)67.2 and CP190. Components of this insulator complex colocalize with γH2Av throughout the genome and at specific *gypsy* insertion sites. Mutation of insulator components prevents stable H2Av phosphorylation in polytene chromatin. Deficiency for Su(Hw) in particular is also associated with chromosomal aberrations in actively dividing larval neuroblasts. PP2A phosphatase inhibition strengthens the association between insulator components and γH2Av and rescues γ localization in insulator mutants. Likewise, mutation of *His2Av* affects binding of *gypsy* insulator components in polytene chromatin. We demonstrate that mutation of *su(Hw)* suppresses the melanotic tumor phenotype associated with the lack of H2Av. We also show that γH2Av is a component of insulator stress bodies, and that phosphatase activity is required for insulator body dissolution after recovery from stress. We propose a model in which H2Av and its phosphorylation are functionally linked with the activity

of insulator binding proteins. Together, our results add to the growing body of evidence linking genome organization to genome stability and provide potential clues to one such mechanism in flies.

Table of Contents

Chapter I: Introduction 1

Chromatin Insulator Function and Regulation in *Drosophila* 1

Drosophila H2Av: Essential Regulator of Development 9

Chapter II: A Phosphorylated Histone H2A Variant Displays Properties of Chromatin Insulator Proteins in *Drosophila* 36

Abstract 36

Introduction 36

Methods and Materials 38

Results 43

Discussion 73

Chapter III: Insulators and DNA damage 81

Abstract 81

Introduction 81

Methods and Materials 82

Results 85

Discussion 92

Chapter IV: Su(Hw) Regulates Hematopoietic Development in *Drosophila* Larvae 97

Abstract 97

Introduction 97

Methods and Materials 98

Results 101

Discussion 110

Chapter V: Fragile X and DNA Damage Repair 113

Abstract 113

Introduction 113

Methods and Materials 115

Results 118

Discussion 126

Final Conclusions 128

References 129

Appendix 162

Vita 166

List of Figures

Figure 1.1. Model of H2AV regulation and activities 35

Figure 2.1. Insulator proteins colocalize with phosphorylated H2Av in *Drosophila* polytene chromosomes 45

Figure 2.2. Phosphorylation of H2Av in polytene chromosomes is inhibited in insulator protein mutants 48

Figure 2.3. Insulator components are interdependent for their colocalization with γH2Av in *Drosophila* polytene chromosomes 50

Figure 2.4. Phosphorylated H2Av is a component of insulator bodies 53

Figure 2.5. Treatment with okadaic acid increases the amount of phosphorylated H2Av on polytene chromosomes 57

Figure 2.6. Phosphatase inhibition restores localization of γH2Av at insulator sites in insulator protein mutants 59

Figure 2.8. Phosphorylated H2Av is present at *gypsy* insulator sites 66

Figure 2.9. H2Av contributes to *gypsy* insulator function 70

Figure 2.10. Phosphorylated H2Av associates with TAD boundaries 74

Figure 3.1. Mutation of *su(Hw)* is associated with chromosomal aberrations. 86

Figure 3.2. Su(Hw) and H2Av phosphorylation increase in polytene chromatin in response to UV irradiation 88

Figure 3.3. Su(Hw) is necessary for H2Av phosphorylation in polytene chromatin after UV irradiation 90

Figure 3.4. Su(Hw) is necessary for the H2Av phosphorylation in polytene chromatin after X-ray irradiation 91

Figure 3.5. Simultaneous mutation of ATR and ATM increases Su(Hw) bound to chromatin 93

Figure 3.6. Su(Hw) enrichment in polytene chromatin after UV irradiation depends on ATR and ATM 94

Figure 4.1. Mutation of *His2Av* has a limited effect on insulator protein binding 103

Figure 4.2. Double mutants show reduced immunostaining of Su(Hw), Mod(mdg4)67.2, and γH2Av. 105

Figure 4.3. Mutation of *su(Hw)* suppresses the *His2Av*^{810} melanotic tumor phenotype 106

Figure 4.4. *su(Hw)*$^{-}$*His2Av*^{810} larvae exhibit overgrowth of lymph glands 108

Figure 4.5. *su(Hw)*$^{-}$*His2Av*^{810} larvae are immunocompetent 109

Figure 4.6. Overexpression of *su(Hw)* in *Antp*-expressing cells results in spontaneous melanization and lethality 111

Figure 5.1. New polyclonal antibodies specifically label FMRP 121

Figure 5.2. Su(Hw) signal is reduced in *dFmr1* mutant larval brains 122

Figure 5.3. dFMR1 remains cytoplasmic in polytene cells during osmotic stress 124

Figure A.1. Genetic crossing and phenotypic selection screen to generate *su(Hw)*^{e04061}*His2Av*^{810} double mutants. 162

Figure A.2. Confirmation of *su(Hw)*^{e04061}*His2Av*^{810} double mutants by PCR 163

Figure A.3. Genetic crossing and phenotypic selection screen to generate *su(Hw)*^{V}*His2Av*^{810} double mutants. 164

Figure A.4. Confirmation of *su(Hw)*^{V}*His2Av*^{810} double mutants by PCR 165

Chapter I: Introduction

Chromatin Insulator Function and Regulation in *Drosophila*

Genome compaction and stability

Eukaryotic genomes can span billions of base pairs of DNA over multiple chromosomes. These chromosomes must be compacted many times over for the entire genome to fit inside the relatively small volume of the nucleus. In humans for example, the diploid genome is approximately two meters long but must fit inside a nucleus that is only 10 µm long. This compaction must happen while still allowing the genome to be functional, i.e. for genes to be accessible to DNA-binding proteins and for long-range contacts between distant loci to form.

Eukaryotic chromosomes achieve this compaction largely through the formation of chromatin. In chromatin, DNA is wrapped up in structures known as nucleosomes. These nucleosomes are formed around an octameric complex of histone proteins. Canonical nucleosomes contain two copies each of the histone proteins H2A, H2B, H3, and H4, although there are variants of histone proteins that can be added to nucleosomes in lieu of the normal protein. Histone variants can have important roles in chromosome structure (e.g. CENP-A helping define the centromere and provide a basis for interactions with the mitotic kinetochore) or in gene regulation (e.g. effects on transcriptional activity upon epigenetic modification of H3.3). Other histone variants are involved in maintaining genome integrity such as the H2AX variant found in humans which becomes phosphorylated in response to DNA double strand breaks (DSBs) (Talbert and Henikoff, 2021).

The integrity of chromosomes must be maintained if cells are to rely on them for proper gene expression and replication/division. Genome instability can manifest itself as aneuploidy, small insertions or deletions (indels), high levels of transposition, or large-scale chromosomal aberrations that can leave chromosomes fragmented. Instability can result in misexpression of genes due to repositioning in the genome or loss of expression altogether if the gene or an essential regulatory element is deleted (Negrini

et al., 2010). Upon sensing extensive damage to the genome many cell types may undergo apoptosis, a programmed cell death with the goal of eliminating that cell from otherwise normal tissue. Genome instability that is not resolved through one of the various DNA damage repair pathways or through apoptosis of damaged cells can have devastating effects on the organism. Chromosome aberrations or fusion of non-homologous chromosomes can result in misexpression of key regulatory genes involved in tissue homeostasis, leading to unregulated cell division and eventually tumor formation. The cell's ability to maintain genome integrity and repair damaged DNA is therefore essential for survival.

Role of insulators, mechanisms/looping

Heterochromatin blocking

How exactly complex eukaryotic genomes are able to coordinate thousands of contacts while sensing and mitigating any potential damage has been the focus of much research in past decades. Through this work it was found that much of genome organization is handled by genome architectural proteins, also known as insulator proteins. These proteins were found to bind DNA at specific sites in the genome known as insulator sites and act as boundaries between neighboring chromatin domains (Schoborg and Labrador, 2014). Insulators were initially described for their ability to prevent the spread of heterochromatin into regions of active transcription and for their capacity to interrupt communication between enhancers and promoters (Labrador and Corces, 2002). Early evidence to support the notion that insulators are refractory to the propagation of heterochromatic marks comes from experiments examining how the presence of insulator sites can affect transcription of a reporter gene. In *Drosophila*, flies with mutations to the *white* gene may lack the red pigmentation normally found in their compound eyes. The mini-*white* gene construct contains a wild-type copy of the *white* gene, resulting in varying degrees of rescue from the white eye phenotype. When inserted randomly into the genome, this construct may end up in heterochromatin and not be expressed or it may end up in actively transcribed euchromatin. If the

construct finds itself in euchromatin there is still the potential for neighboring heterochromatin to spread toward the construct, silencing it. Importantly, it was found that flanking the mini-*white* gene with insulator sites prevents such transcriptional silencing, implying that the insulator acts as a block to heterochromatin (Roseman *et al.*, 1993).

Enhancer blocking

In addition to the ability of chromatin insulators to block the spread of heterochromatic epigenetic marks, insulators also have the effect of either bringing together or separating gene promoters from their distant regulatory elements such as tissue-specific enhancers. Evidence to support the idea that insulators act to block enhancer activity was discovered by studies of the chicken β-globin gene. This locus was found to contain a consensus binding site for the vertebrate CTCF protein that, when inserted between the enhancer and promoter, prevents transcriptional activation (Bell *et al.*, 1999). Further evidence comes from the role that insulators play in the y^2 and ct^6 phenotypes seen in *Drosophila*. Both of these phenotypes are caused by insertion of the *gypsy* retrotransposon between the promoters and specific enhancers. These insertions contain binding sites for Suppressor of Hairy Wing [Su(HW)], which recruits other components to form an insulator complex to prevent interactions between the regulatory sequences on either end (Figure 2.9). This disrupts expression of the *yellow* and *cut* genes in tissues that depend on distal enhancers for expression. Enhancers that fall on the same side of the insulator site as the promoter are unaffected, and expression in these tissues proceeds normally. This ability to direct interactions between regulatory elements through insulator protein binding gives cells a mechanism to regulate expression in complex developmental contexts. Indeed, large-scale morphological development in vertebrates depends on this insulator function, as defects in enhancer blocking by the CTCF insulator was recently demonstrated to result in polydactyly in humans (Lupiáñez *et al.*, 2015). Enhancer blocking

is thus a potent mechanism for driving specific expression of key developmental genes during embryogenesis and understanding the contribution of insulator proteins to this process is crucial.

Drosophila insulator diversity and regulation

Drosophila melanogaster has an array of different insulator complexes, with each complex being recruited to different sequences in the genome (Bushey et al., 2009, Negre et al., 2010). Insulators were first described in fruit flies with the discovery that the scs and scs' sequences function as boundary elements, inhibiting chromosomal position effects (Kellum and Schedl, 1991). Another insulator site, located within the *gypsy* retrotransposon, has been thoroughly characterized for its ability to regulate transcription of neighboring genes (Geyer and Corces, 1992).

A number of *gypsy* retrotransposons are present throughout the *Drosophila* genome (Hoskins et al., 2015), and insertion or transposition of *gypsy* to a new locus may interrupt local transcriptional activity and chromatin dynamics (Jack et al., 1991, Geyer and Corces, 1992). Insulator proteins are recruited to *gypsy* through a 460-bp sequence composed of 12 binding sites for Suppressor of Hair Wing (Su(Hw)) (Geyer and Corces, 1992). The Su(Hw) protein contains an amino-terminal tandem array of a dozen C_2H_2 zinc finger domains (Kim et al., 1996) and a carboxy-terminal leucine zipper domain (Harrison et al., 1993) that is essential for insulator activity through interactions with other insulator proteins (Melnikova, Kostyuchenko, Molodina*, et al.*, 2018). Su(Hw) specifically recruits one of the many isoforms of Modifier of mdg4 (Mod(mdg4)67.2) through interactions between the carboxy-terminal domain of Su(Hw) and carboxy-terminal acidic domain that is unique to the *gypsy*-binding isoform of Mod(mdg4) (Ghosh et al., 2001) and through interactions between the amino-terminal end of Su(Hw) with the glutamine-rich domain of Mod(mdg4)67.2 (Melnikova, Kostyuchenko, et al., 2017). Centrosomal Protein 190 (CP190), another essential component of the *gypsy* insulator (Pai et al., 2004), was originally described through its activity during the cell cycle, dissociating from chromatin during mitotic prophase and localizing to the

centrosome (Ooegema et al., 1995). In chromatin, CP190 is found as an essential part of different insulator complexes (Bushey et al., 2009) and is recruited to the *gypsy* insulator through interactions with Mod(mdg4)67.2 (Pai et al., 2004) and the amino terminal domain of HIPP1 (HP1 and insulator partner protein 1) (Melnikova et al., 2019). HIPP1 is the most recently described member of the *gypsy* insulator complex (Alekseyenko et al., 2014) and functions to stabilize the interaction between Su(Hw) and CP190, but is not required for insulator activity or transcriptional regulation (Glenn and Geyer, 2019, Melnikova et al., 2019).

Insulator activity in *gypsy* is promoted by factors such as the interchromosomal EAST protein (Golovnin *et al.*, 2015, Melnikova, Shapovalov*, et al.*, 2017) and the Chromatin-linked adapter for MSL proteins (CLAMP) (Bag *et al.*, 2019), while activity is negatively regulated by RNA-binding proteins Rumpelstiltskin (King *et al.*, 2014) and Shep (Chen *et al.*, 2019). Insulator-binding proteins in *Drosophila* can form aggregates known as insulator bodies (Gerasimova and Corces, 1998). The role of these bodies in genome organization has been debated, and functions for insulator bodies have been proposed from genome organization hubs to passive storage centers for insulator proteins (Gerasimova et al., 2000, Labrador and Corces, 2002, Golovnin et al., 2012). Previous work in our lab has demonstrated a role for insulator bodies in the cellular response to osmotic stress, with insulator proteins leaving chromatin and forming bodies in the nucleoplasm as the environment becomes more hypertonic (Schoborg et al., 2013).

Of the *gypsy* insulator proteins, Su(Hw) is perhaps the best-characterized. Mutation of *su(Hw)* is associated with female infertility (Klug et al., 1968, Harrison et al., 1993, Baxley et al., 2011, Hsu et al., 2020) and alters the cell's response to DNA damage (Lankenau et al., 2000). Outside of the *gypsy* insulator complex, Su(Hw) binds many sites alone or in conjunction with either Mod(mdg4)67.2 or CP190 (Adryan et al., 2007, Kuhn-Parnell et al., 2008, Bushey et al., 2009, Negre et al., 2010, Soshnev et al., 2012, Baxley et al., 2017).

Apart from its role in chromatin insulator activity, Su(Hw) is also a transcriptional repressor in *Drosophila* oogenesis (Baxley et al., 2011) and regulates the expression of neuronal genes in tissues outside the nervous system, including the ovary (Soshnev et al., 2013). Mutation of *su(Hw)* leads to defects in the formation of ring canals between nurse cells, preventing the proper transport of maternal morphogens during ovary development (Hsu et al., 2015). Ovaries in *su(Hw)* mutants also exhibit malformed microtubule organizing centers and mislocalization of Gurken, a morphogen normally sequestered to one end of the oocyte to direct axis determination in embryos (Hsu et al., 2020). Similar to its role in oogenesis, Su(Hw) is critical for spermatogenesis through its activity as a transcriptional repressor in somatic cyst cells in the male germline (Duan and Geyer, 2018).

Su(Hw) also participates in the DNA damage response, possibly as part of the search for homologous sequences during homologous recombination (Lankenau et al., 2000). A role for insulators in homologous recombination-based DNA repair has been well established with mammalian CTCF, which is recruited to sites of DNA double strand breaks (DSBs) (Han et al., 2017, Hilmi et al., 2017, Lang et al., 2017). Of clinical relevance, mutation of CTCF in humans is associated with various forms of cancer (Docquier et al., 2005, Kemp et al., 2014, Canela et al., 2017, Guo et al., 2018). One of the first steps in the cellular response to DSBs is the phosphorylation of a variant of H2A known as H2AX in mammalian systems and H2Av in *Drosophila* (Rogakou et al., 1998, Baldi and Becker, 2013). H2AX is phosphorylated by ATM (Ataxia-telangiectasia-mutated) kinase and DNA-dependent protein kinase (DNA-PK) in response to ionizing radiation (Stiff et al., 2004) and by ATR (ataxia telangiectasia and Rad3-related) kinase after cells experience replication-induced genotoxic stress (Ward and Chen, 2001). Phosphorylation of H2AX leads to recruitment of numerous proteins involved in the DNA damage response (Sirbu and Cortez, 2013). Upon resolution of the DSB, H2AX is dephosphorylated primarily by PP2A (Chowdhury et al., 2005). H2Av, the sole *Drosophila* H2A variant (Baldi and Becker, 2013), combines the activities of mammalian H2AX and H2AZ. Like H2AX, H2Av is phosphorylated in response to DNA damage (Madigan et al., 2002), and like

H2AZ, phosphorylation of H2Av is involved in transcriptional regulation through activation of poly(ADP-ribose) polymerase 1 (PARP1) (Kotova et al., 2011). Our laboratory previously demonstrated an accumulation of phosphorylated H2Av (γH2Av) signal in the ovaries of *su(Hw)* mutants and the presence of chromosomal aberrations in actively dividing larval neuroblasts lacking Su(Hw), suggesting a significant connection between Su(Hw) activity and genome stability (Hsu et al., 2020). Furthermore, disruption of Mei-41/ATR, a kinase responsible for phosphorylating H2Av among other targets upon DNA damage (LaRocque et al., 2007), partially rescues the defective oogenesis phenotype associated with mutation of *su(Hw)* (Hsu et al., 2020). While insulator-binding proteins have been described for their role in genome organization and regulation in *Drosophila*, the mechanisms linking their activity to DNA repair remain elusive.

Insulator activity may also be affected by post-translational modification of protein components. One recently described example of this involves covalent attachment of poly(ADP-ribose) (PAR) by poly(ADP-ribose) polymerase (PARP). PAR is a negatively charged polymer derived from nicotinamide adenine dinucleotide (NAD^+) that influences protein interactions through its numerous negative charges. PARP localizes to insulator binding sites in polytene chromosomes and Su(Hw), Mod(mdg4)67.2, CP190, and CTCF are PARylated *in vivo*. Inhibition of PARylation by addition of 3AB (3-aminobenzamide) reduces binding of Mod(mdg4)67.2, CP190, and CTCF (Ong *et al.*, 2013) and causes Su(Hw), Mod(mdg4)67.2, CP190, and CTCF to dissociate from the nuclear lamina where they are normally found (Capelson and Corces, 2005), a finding corroborated by RNAi of *Parp*. PARP inhibition also reduces the amount of CTCF associated with CP190 in pull-down assays, suggesting that PARylation increases the stability of insulator complexes *in vivo*. A link between PARP activity and insulator function was demonstrated using the *gypsy* insertion alleles y^2 and ct^6 (Ong *et al.*, 2013). Heterozygosity for the null mutation $Parp^{CH1}$ results in darker pigmentation in the *y2* background and decreased $Parp^{CH1}$ in backgrounds lacking either CP190 or Mod(Mdg4)67.2. Likewise, mutating CP190 at the site of PARylation (K566A) rescues the ct^6 phenotype,

further supporting the idea that PARylation is necessary for insulator function. These findings in *Drosophila* have a parallel in mammalian cells, as PARylation of the maternally imprinted *H19* locus is required for the insulator activity of CTCF but not its ability to bind genomic target sequences (Yu *et al.*, 2004). This relationship was demonstrated in flies by changes in expression of the *white* gene under control of a *Fab-8* insulator site situated between the *white* coding sequence and the eye enhancer (Gerasimova *et al.*, 2007, Mohan *et al.*, 2007). This insulator requires CTCF and CP190 and becomes inactivated in $Parp^{CH1}$ heterozygotes, implying PARylation and regulation of insulator activity is conserved between *Drosophila* and vertebrates.

A version of the following section is currently being prepared for submission for peer review. The manuscript below contains original work by James Ryan Simmons and Dr. Mariano Labrador.

Drosophila H2Av: Essential Regulator of Development

Abstract

Eukaryotic chromosomes are built around the base unit of the nucleosome, whose composition can affect chromosome structure and transcription. Beyond the four canonical core histone proteins, histone variants have evolved that can be exchanged into nucleosomes, imbuing them with for specialized properties. H2Av, the sole H2A variant in *Drosophila*, combines the DNA repair functionality of the vertebrate H2AX variant with the transcriptional regulation activity of the vertebrate H2AZ variant. This makes H2Av activity, its placement into nucleosomes, and its post-translation modification attractive targets for regulation by the cell. H2Av is phosphorylated in a conserved C-terminal domain in response to DNA double strand breaks, promoting the DNA damage response. Phosphorylation of this site also affects transcription of genes regulated by H2Av. Exchange between the canonical H2A and the H2Av variant is highly regulated and depends on acetylation of a lysine in the N-terminal tail. Embryos are supplied with ample H2Av protein from the oocyte that is stored in cytoplasmic lipid droplets. These interactions are dynamic, with H2Av molecules exchanging between different lipid droplets and the cytoplasm, limiting the amount of H2Av available to chromatin in the early embryo. Transcriptional regulation by H2Av is necessary for proper development of numerous fly tissues and maintenance of stem cell populations. H2Av regulates heterochromatin formation and interacts with chromatin architecture proteins as means to influence transcriptional output. This review will summarize our knowledge of H2Av regulation and dynamics with an emphasis on recent results that demonstrate how H2Av function affects fruit fly development.

Introduction

Histone proteins form the base unit of eukaryotic chromosome organization known as nucleosomes. Regulation of chromatin via nucleosomes happens through two routes: post-translational modification of histone amino-terminal tails (Jambhekar *et al.*, 2019) and the substitution of canonical histone proteins for histone variants (Talbert and Henikoff, 2021). Canonical nucleosomes are composed of around 147 base pairs of DNA (Richmond and Davey, 2003) along with two copies each of H2A, H2B, H3, and H4 (Luger *et al.*, 1997), but histone variants are common throughout genomes of archaea and eukaryotes (Kawashima *et al.*, 2015, Jiang and Berger, 2017, Martire and Banaszynski, 2020, Stevens *et al.*, 2020). Histone variants are characterized by sharing high similarity/identity with canonical histones but often contain divergent sequences or extensions that provide unique binding surfaces that allow nucleosomes to recruit specific proteins that influence chromatin activity.

Common roles for histone variants include regulation of transcriptional activity (Loyola *et al.*, 2006, Armache *et al.*, 2020), structural roles such in the chromosome including the centromere (Sullivan *et al.*, 1994) and telomere (Lowell and Cross, 2004, Kim *et al.*, 2019), genome replication (Lai and Pugh, 2017, Maxouri *et al.*, 2018), regulation of stem cell differentiation (Gehre *et al.*, 2020), and the response to DNA damage (Rogakou *et al.*, 1998). Mammalian genomes contain two key histone H2A variants with divergent functions, H2AX and H2AZ. H2AX is phosphorylated in response to DNA double strand breaks; this phosphorylation is one of the earliest steps in the DNA damage repair pathway and serves to recruit DNA repair machinery to damaged loci (Rogakou *et al.*, 1998). In contrast, H2AZ is not involved in DNA damage repair, but instead regulates transcriptional activity by stimulating ATP-dependent chromatin remodelers via an extended acidic patch (Goldman *et al.*, 2010, Dann *et al.*, 2017).

Drosophila provides a unique model to study the function of the H2A histone variants as the fruit fly genome contains only one H2A variant, H2Av, which combines the activities of the mammalian H2AX and H2AZ in one protein (van Daal *et al.*, 1988, van Daal and Elgin, 1992). Initial characterization of H2Av

revealed that, like H2AX, the C-terminal region becomes phosphorylated in response to DNA double strand breaks (Madigan *et al.*, 2002), and that, like H2AZ, transcriptional output of developmentally regulated genes depends on incorporation of this histone variant into nucleosomes (Rust *et al.*, 2018, Scacchetti *et al.*, 2020). Numerous findings have come to light recently that paint an essential role for H2Av in the development and homeostasis of numerous tissues. This review will attempt to summarize what is known about the evolution and function of *Drosophila* H2Av, its regulation though post-translational modification, chromatin remodeling, and storage in lipid droplets, its role in animal development, and interactions with chromatin architectural components.

Drosophila **H2Av combines the functions of vertebrate H2AX and H2AZ**

H2AX

H2AX is distinguished from H2A by the presence of a phosphorylation motif (SQD/EΦ, where Φ represents a hydrophobic residue) appended to the C-terminus (Mannironi *et al.*, 1989). The serine in this sequence becomes phosphorylated in response to DNA double strand breaks (Rogakou *et al.*, 1998). The DNA damage response begins with detection of damage by the MRN complex, which is critical for the subsequent activation of kinases responsible for marking the region as damaged (Lee and Paull, 2004, Difilippantonio *et al.*, 2005). Activation of the ATM kinase requires acetylation by the Tip60 histone acetyltransferase *(Sun et al., 2005, Sun et al., 2007)*. H2AX is phosphorylated in somatic cells of mice and humans by ATM or ATR kinases, depending on whether the break is introduced by ionizing radiation or replicative stress, respectively (Rogakou *et al.*, 1998, Burma *et al.*, 2001, Ward and Chen, 2001). Phosphorylation of H2AX happens within minutes and spreads for megabases in both directions from the site of damage (Rogakou *et al.*, 1999). This serves as a scaffold to recruit enzymes needed to repair the damaged locus, including BRCA1, Rad50/51, 53BP1, and MDC1 (Paull *et al.*, 2000, Rappold *et al.*, 2001, Fernandez-Capetillo *et al.*, 2002, Goldberg *et al.*, 2003, Lou *et al.*, 2003, Stewart *et al.*, 2003, Ward *et al.*,

2003). Phosphorylation of H2AX also stimulates activity of PARP1, leading to the recruitment of further DNA repair proteins (Sharma *et al.*, 2019).

In addition to DNA double strand breaks, H2AX gets phosphorylated in response to programmed chromosomal rearrangements (Chen *et al.*, 2000, Mahadevaiah *et al.*, 2001) and apoptotic DNA laddering (Rogakou *et al.*, 2000), suggesting that this post-translational modification is a widely conserved response to the presence of free DNA ends regardless of their origins. Despite its highly conserved role in the DDR, there is some evidence to support a role in transcriptional regulation for H2AX as well. H2AX is enriched at promoters of rDNA genes in mESCs where it helps repress expression of rDNA transcripts (Eleuteri *et al.*, 2018). H2AX phosphorylation is also essential for chromatin remodeling and silencing of expression during male meiosis (Fernandez-Capetillo *et al.*, 2003).

H2AZ

The other well conserved H2A variant in vertebrates is H2AZ, which is described largely for its activity in transcriptional regulation and its ability to prevent the spread of heterochromatin into actively transcribing euchromatic regions (Meneghini *et al.*, 2003). The situation may not be so simple, as H2A.Z is also involved in maintaining transcriptional silencing of some genes (Dhillon and Kamakaka, 2000, Li *et al.*, 2005, Billon and Côté, 2013) and is enriched in pericentric heterochromatin in early stages of mammal development (Rangasamy *et al.*, 2003). H2AZ regulates transcription by helping to recruit RNA polymerase II (Adam *et al.*, 2001) and nucleosomes with H2AZ separate from DNA more easily than canonical nucleosomes, increasing the accessibility of transcriptional machinery (Weber *et al.*, 2014). H2AZ is frequently enriched in enhancers (Brunelle *et al.*, 2015) and the +1 nucleosome position (the 1st full nucleosome after the transcription start site) in yeast, flies, and vertebrates (Raisner *et al.*, 2005, Zhang *et al.*, 2005, Albert *et al.*, 2007, Mavrich *et al.*, 2008, Kotova *et al.*, 2011, Weber *et al.*, 2014, Rudnizky *et al.*, 2016, Bagchi *et al.*, 2019). This nucleosome has influence over transcriptional activity by

acting as a barrier to promoter escape by RNA polymerase. The presence of H2AZ or its orthologs in the +1 nucleosome increases the rate of successful transcription (Weber *et al.*, 2014). Several studies have indicated that nucleosomes that contain H2AZ are less stable than those with canonical H2A (Abbott *et al.*, 2001, Placek *et al.*, 2005). Indeed, nucleosomes containing H2AZ show lower breaking forces and increased mobility compared to canonical nucleosomes (Rudnizky *et al.*, 2016). Likewise, salt extraction experiments have demonstrated that H2Av nucleosomes in *Drosophila* are soluble in relatively low salt concentrations (Weber *et al.*, 2010).

Drosophila H2Av and its Relation to H2AX and H2AZ

A homolog to vertebrate H2AZ was described in *Drosophila*, where it was first isolated when it was co-purified with canonical H2A in nucleosomal preparations (Palmer *et al.*, 1980). It was later demonstrated that the *Drosophila* histone variant could be incorporated into nucleosomes *in vitro* in place of H2A (Donahue *et al.*, 1986). *Drosophila* H2Av is ubiquitously expressed and is essential for viability (van Daal *et al.*, 1988, van Daal and Elgin, 1992). This was demonstrated by the null allele $His2Av^{810}$ (also known as *l(3)810*), derived from EMS mutagenesis that deleted 311 base pairs including the entire second exon (van Daal and Elgin, 1992). This mutation is homozygous lethal; however, larvae survive through third-instar due to significant maternal contributions (Clarkson *et al.*, 1999, Li *et al.*, 2012). The presence of a carboxy-terminal extension unique to H2Av is required for development and viability in *Drosophila* (Clarkson *et al.*, 1999). This C-terminal extension contains a SQAY phosphorylation site similar to that of vertebrate H2AX. The serine in this extension is phosphorylated in response to DNA damage, demonstrating a conserved function between H2Av and vertebrate H2AX (Madigan *et al.*, 2002).

How *Drosophila* H2Av evolved and its relationship to its vertebrate orthologs sheds light on the roles this variant plays and its mechanisms, and several models have been debated about its origins. One model suggests that H2AX is descended from H2A, having acquired the C-terminal extension along the

way. Another model proposes that H2A is derived from an ancestral H2AX gene that lost the C-terminal SQ[E/D] Φ phosphorylation motif. Under this model, the H2Av variant evolved from H2AZ and acquired its own phosphorylation site later in evolutionary time (Baldi and Becker, 2013). The simplicity of the C-terminal phosphorylation domain is thought to facilitate its addition to H2A-like proteins and supports a model in which multiple H2AX-like proteins evolved independently (Henikoff and Smith, 2015). It is likely that the H2AZ evolved before the canonical H2A in early eukaryotes as H2AZ is more conserved than H2A in many eukaryotes (Talbert and Henikoff, 2010). Yeast lack the canonical H2A but have an H2AX protein that is phosphorylated in response to DNA damage (Downs *et al.*, 2000), supporting the idea that canonical H2A proteins are derived from the primordial H2AX (Henikoff and Smith, 2015). More evidence to support this model comes from the highly conserved role H2AX plays in the DNA damage response and the finding that other vertebrate H2As are derived from an H2AX precursor (Talbert and Henikoff, 2010). Despite this, H2AZ is considered monophyletic due to its conservation across eukaryotes while H2AX is polyphyletic, with functional orthologs having evolved independently in several eukaryotic lineages (Talbert and Henikoff, 2010).

H2AX-like Activity for H2Av

Like vertebrate H2AX, H2Av is a key signaling molecule early in the DNA damage response in *Drosophila*. Several lines of evidence have been described to support this conservation of function and its implications for the animal. H2Av is phosphorylated at serine 137 in the C-terminal extension in response to exogenous DNA double strand break generation by X-ray irradiation (Madigan *et al.*, 2002). Phosphorylation of H2Av has also been noted in response to double strand breaks endogenously generated during meiotic recombination in female flies (Jang *et al.*, 2003, Joyce *et al.*, 2011). Phosphorylation of H2Av occurs after synaptonemal complex formation in meiotic cells of female flies, a process associated with the double strand break formation needed for meiotic recombination (Jang *et al.*, 2003, Mehrotra and McKim, 2006).

H2Av is phosphorylated by ataxia telangiectasia-mutated/ataxia telangiectasia and Rad- related (ATM and ATR) kinases, encoded by the *tefu* and *mei-41* genes in *Drosophila*, respectively. Temperature-sensitive mutation of *tefu* results in mislocalization of Gurken, a developmental morphogen that helps establish the dorso-ventral axis, within the oocyte as a result of unrepaired meiotic DSBs (Joyce *et al.*, 2011). Immunostaining for phosphorylated H2Av in oocytes is more intense in the $tefu^{8}$ mutant but is completely absent in $mei\text{-}W86^{4572}$*; tefu* double mutants, which are unable to produce meiotic DSBs. This demonstrates that ATR activity is sufficient for H2Av phosphorylation in response to unrepaired meiotic DSBs. Additionally, an absence of phosphorylated H2Av was noted in $mei\text{-}41^{D3}$*;* $tefu^{8}$ *double mutants, indicating that these ATM and ATR orthologs serve redundant purposes in regulation of H2Av* (Joyce *et al.*, 2011).

Despite its early role in coordinating the DNA damage response, H2Av phosphorylation at S137 is not essential for viability. Indeed, expression of a C-terminal deletion allele that is missing the phosphosite serine and cannot be phosphorylated is sufficient to rescue viability in *His2Av* null animals (Clarkson *et al.*, 1999). *His2Av* mutant larvae display increased rates of apoptosis after ionizing radiation, however no effect was found on lethality regardless of the developmental stage (Madigan *et al.*, 2002). Despite this, larvae expressing a phosphonull S137A mutation survive to adulthood following irradiation at a lower frequency than wild type. This is associated with a lack of pADPr accumulation, suggesting that H2Av regulates PARP1 activity in the DNA damage response (Kotova *et al.*, 2011).

H2Av phosphorylation has also been noted at sites of underreplication in polytene chromosomes generated as a result of endoreplication (Andreyeva *et al.*, 2008). Polytene chromosomes in *Drosophila* larval salivary glands are generated as a result of endoreplication and can contain over 1,000 copies of each chromosome. Problems for replication can occur with transcriptionally silenced regions of the genome, which replicate slower than actively transcribed regions and may fail to fully replicate before S phase is over (Wallace and Orr-Weaver, 2005). This results in sites of underreplication, which effectively

leaves unresolved DNA double strand breaks amidst the forest of chromosomes. It was shown that the level of H2Av phosphorylation is correlated with the degree of underreplication (Andreyeva *et al.*, 2008). This indicates that these sites are perceived as double strand breaks in the cell and H2Av phosphorylation may be involved in repair of underreplicated polytene DNA. Phosphorylation of H2Av is also a marker for aging in *Drosophila*. In fly muscle tissues, H2Av phosphorylation is positively correlated with muscle degeneration and accumulation of the apoptotic marker cleaved caspase-3, and increased phosphorylation is associated with shorter longevity (Jeon *et al.*, 2015).

H2AZ-like Activity for H2Av

Whereas vertebrates have largely separated the functions that H2A variants serve with respect to the DNA damage response and transcriptional regulation, *Drosophila* H2Av not only acts as a substrate to mark double strand breaks, but also regulates chromatin state and transcriptional activity. Like its vertebrate counterpart, the presence of H2Av in a gene regulatory sequence can either activate or repress transcription (Baldi and Becker, 2013). Under normal conditions, H2Av localizes to many sites in polytene chromatin stains and can be found at genes that are constitutively expressed, genes that are developmentally silenced, and in the heat shock locus (van Daal and Elgin, 1992, Leach *et al.*, 2000). *Drosophila* H2Av is enriched in both transcriptionally silent and heterochromatic regions (Swaminathan *et al.*, 2005) and transcriptionally active regions (Mavrich *et al.*, 2008). H2Av plays an important role in the establishment and/or maintenance of heterochromatin. Mutations in *His2Av* result in reduced H3K9 methylation and HP1 recruitment and disrupt H4K12 acetylation patterns in pericentric heterochromatin (Swaminathan *et al.*, 2005). RNAi reduction of HP1 results in increased H2Av expression in ovaries, indicating a compensation mechanism between these proteins (Park *et al.*, 2019). H2Av is reduced in heterochromatic regions of *Drosophila* diploid chromosomes and but is found in telomere associated sequences where it regulates the chromatin state of telomeres in dividing cells (Frydrychova *et al.*, 2008,

Rong, 2008). H2Av also affects chromatin dynamics in the heterochromatic fourth chromosome by regulating the recruitment of Painting of fourth (POF), an RNA-binding transcriptional regulator (Johansson *et al.*, 2012).

His2Av can be thought of as a member of the Polycomb group of genes. Mutation of *His2Av* enhances the sex comb phenotype associated with mutations in the *Pc* gene and suppresses the phenotypes of trithorax group mutants (Swaminathan *et al.*, 2005). The enhancement of *Pc* phenotypes may involve recruitment of Pc by H2Av as null $His2Av^{810}$ larvae show a reduction in the number of Pc sites identified through immunostaining of polytene chromatin (Swaminathan *et al.*, 2005). Additionally, the homeotic gene *Antennapedia* (*Antp*), whose expression is regulated by the Polycomb complex (Zink *et al.*, 1991, Kassis *et al.*, 2017), is ectopically expressed in the central nervous system of $His2Av^{810}$ null mutants (Swaminathan *et al.*, 2005). This supports a role for H2Av in controlling the expression of Pc-regulated genes and more broadly implicates H2Av as a regulator or development in *Drosophila*.

Immunostaining of polytene chromatin from third instar salivary glands reveals extensive colocalization between H2Av and poly(ADP-ribose) polymerase 1 (PARP1) (Kotova *et al.*, 2011). PARP1 post-translationally modifies its substrates by adding up to over 100 units of ADP-ribose in a process known as poly(ADP ribosyl)ation (PARylation). Chromatin PARylation is involved in several DNA repair pathways (Ray Chaudhuri and Nussenzweig, 2017) and regulates gene expression by making chromatin more accessible to transcriptional machinery (Tulin and Spradling, 2003, Kim *et al.*, 2004). Null mutation of H2Av or of the C-terminal phosphosite serine results in a significant loss of PARylation, however, localization of PARP1 in the chromatin is not affected. Mutation in poly(ADP- ribose)glycohydrolase (*Parg*), an enzyme that catbolizes pADPr, leads to an accumulation of pADPr that is suppressed in a $Parg^{27.1}$; $His2Av^{810}$ double mutant. This loss of PARylation has functional consequences and is enough to prevent cells from activating transcription from the *hsp70* locus in response to heat stress (Kotova *et al.*, 2011). The mechanism behind this involves a conformational change in H2Av upon phosphorylation of

the C-terminal domain that exposes the N-terminal region of H4, which directly stimulates PARP1 activity (Kotova *et al.*, 2011). Expression of wild type H2Av, but not phosphonull or phosphomimetic mutants of H2Av, restored pADPr levels in $Parg^{27.1}$; $His2Av^{810}$ double mutant animals. Expression of the $H2Av^{SE}$ transgene was found to be lethal at the early embryonic stage in $Parg^{27.1}$; $His2Av^{810}$ double mutants. These results emphasize the need of the cell to change the phosphorylation state of H2Av in response to environmental conditions to coordinate a change in transcriptional output (Kotova *et al.*, 2011).

Other post-translation modifications have been discovered in H2Av and its orthologs. Vertebrate H2AX can also be phosphorylated at tyrosine 142 by the WICH chromatin remodeling complex subunit WSTF (Williams-Beuren syndrome transcription factor). This phosphorylation is not necessary to initiate the DNA damage response upon double strand break formation, but is thought to supplement Ser139 phosphorylation by increasing the residency time of DNA repair proteins at the lesion (Xiao *et al.*, 2009). In addition, *Drosophila* H2Av contains two tandem lysine residues, K120 and K121, which are ubiquitylated *in vivo* by Sce, a subunit of the Polycomb repressive complex 1 (PRC1) with E3 ubiquintase activity. Mutation of both residues to arginine abrogated ubiquitination of H2Av, but with no discernable effect on viability, fertility, developmental gene expression, and tissue development (Pengelly *et al.*, 2015). This implies that, in contrast with phosphorylation, ubiquitination of H2Av is not involved in transcriptional regulation, although it may have yet undescribed roles in genome function. These findings would suggest that while other post-translational modifications may impact H2Av/H2AX activity under certain circumstances, phosphorylation of the conserved serine residue in the C-terminal domain remains the predominant mode of regulation.

Nucleosome phasing and composition also affect how H2Av exerts its influence over transcriptional activity. H2Av is enriched in the phased nucleosomes following the transcription start site and may affect polymerase pausing kinetics in active genes (Mavrich *et al.*, 2008). This is supported by the finding that H2Av distributions downstream of TSSs differ between transcriptionally active vs. silenced

genes, with strong phasing of H2Av in active genes gradually becoming weaker over the first few nucleosomes (Zhang and Pugh, 2011). Nucleosomes may either contain one copy of the H2Av variant (heterotypic) or two copies (homotypic) in place of the canonical H2A histone. Homotypic H2Av nucleosomes are more accessible than heterotypic and the 5' ends of actively transcribed genes are enriched for nucleosomes with homotypic H2Av (Weber *et al.*, 2010). The homotypic H2Av nature of nucleosomes and their phasing immediately downstream of the transcription start site of many genes thus work synergistically to facilitate assembly and activation of transcriptional machinery. These results, together with those described above, establish H2Av as a regulator of transcription through multiple distinct mechanisms. Understanding how placement and modification of this histone variant are managed by the cell is therefore crucial to appreciate the contribution that H2Av-based transcriptional regulation has on DNA damage repair and development.

H2Av Histone Exchange

H2Av Exchange in DNA Repair

The substitution of canonical histone proteins for histone variants is a highly regulated process that affects numerous cellular processes. Cells must be able to place the right variants in appropriate positions throughout the genome to ensure homeostasis and viability. Conversely, cells also need to be able to remove histone variants from nucleosomes as the need arises to regulate processes relevant to each variant. In *Drosophila*, H2Av can replace up to 20% of the total cellular complement of canonical H2A (Kotova *et al.*, 2011). H2Av becomes phosphorylated at sites of double strand breaks as part of the DNA damage response; this H2Av is exchanged for unphosphorylated H2Av upon resolution of the DNA damage (Kusch *et al.*, 2004). The *Drosophila* TIP60 chromatin remodeling complex, containing TIP60 and the ATPase Domino, acetylates phosphorylated H2Av at lysine 5, allowing the phosphorylated histone variant to be taken out and replaced with an unphosphorylated H2Av molecule (Kusch *et al.*, 2004).

Decreased expression of TIP60 has no effect on H2Av phosphorylation, but results in accumulation of DNA double strand breaks and the phosphorylated H2Av variant (Kusch *et al.*, 2004). MRG15, another Tip60 complex member, is required for incorporation of H2Av in meiotic chromosomes and is recruited to perform this function after the removal of acetylated γH2Av (Joyce *et al.*, 2011). Phosphorylated H2Av is continuously exchanged for the unmodified form at double strand breaks in meiotic cells. Phosphorylation is maintained, however, by the activity of ATM and ATR kinases (Joyce *et al.*, 2011).

In vertebrates, H2AX is acetylated at a lysine in the 5th position (K5) by the TIP-60 complex in response to DNA damage, and cells lacking TIP-60 acetylase activity are deficient in DNA damage repair (Ikura *et al.*, 2000, Ikura *et al.*, 2007). Acetylation of H2AXK5 by TIP-60 is essential for the recruitment of NBS1 (Nijmegen breakage syndrome protein), a member of the MRN complex that recognizes DNA double strand breaks and recruits enzymes involved in repair (Ikura *et al.*, 2015). Acetylation of H2AX also promotes recruitment of PARP1 to sites of DNA damage in order to regulate exchange of the histone variant; however, phosphorylation of H2AX is not involved in PARP recruitment (Ikura *et al.*, 2016). DNA double strand breaks also induce acetylation of ATM by TIP60 in human cell culture. This is necessary to activate ATM to phosphorylate its downstream substrates in the DNA damage response, including p53 and chk2 (Sun *et al.*, 2005, Sun *et al.*, 2007). This prevent efficient repair and leaves cells vulnerable to the effects of DNA damage.

H2Av Exchange in Transcription

Given that *Drosophila* H2Av plays roles in both DNA damage repair and transcriptional regulation, it is no surprise that the TIP60 complex, which regulates the exchange of H2Av, is involved in both phenomena as well. The TIP60 complex is conserved among eukaryotes and contains the Tip60 lysine acetyltransferase and Domino, a member of the SWI/SNF family of ATPases, among numerous other components (Doyon and Côté, 2004). The H2Av exchange and acetyltransferase activities of the TIP60

complex at the *hsp70* locus are regulated by the methylation state of H3 lysine 4. Trimethylation of H3K4 is associated with actively transcribed chromatin (Santos-Rosa *et al.*, 2002, Collins *et al.*, 2019) and is sufficient to activate the TIP60 complex (Kusch *et al.*, 2014). TIP60 thus incorporates and acetylates H2Av in a transcription-dependent manner to facilitate promoter escape by RNA polymerase. This effectively couples loosening of the chromatin at the transcription start site by TIP60 activity with transcriptional activation, preventing unwarranted destabilization of nucleosomes when genes are transcriptionally silent (Kusch *et al.*, 2014).

Drosophila expresses two isoforms of the SWR1 ortholog Domino (*dom*), DOM-A and DOM-B (Ruhf *et al.*, 2001). Animals containing homozygous a null mutation of *dom* do not survive past second instar, and hypomorphic mutations result in defects in oogenesis, resulting in female sterility (Ruhf *et al.*, 2001). Mutation of either *dom* or *MRG15* in germline stem cell clones results in a decrease in the amount of H2Av (Joyce *et al.*, 2011, Morillo Prado *et al.*, 2013). It was recently discovered that DOM-A is the only described ATP-independent acetyltransferase specific to H4K12 in *Drosophila*, while DOM-B incorporates H2Av into nucleosomes in an ATP-dependent manner (Scacchetti *et al.*, 2020). This finding is supported by results showing that deposition of H2Av in female germline and somatic cells depends DOM-B, but not DOM-A or TIP60. This does not hold true for germline nurse cells, in which DOM-B plays no role in H2Av incorporation while DOM-A promotes H2Av removal in stage 5 nurse cells instead of incorporation (Scacchetti *et al.*, 2020).

Another nucleosome remodeling complex, the remodeling and spacing factor (RSF) complex, is composed of Rsf-1, a histone chaperone, and ISWI, an ATP-dependent nucleosome mobility factor (Loyola *et al.*, 2001, Loyola *et al.*, 2003). Rsf-1 physically interacts with H2Av and the TIP60 complex, and mutation of *Rsf-1* in *Drosophila* results in decreased H2Av occupancy in euchromatic regions positioned next to heterochromatin, suggesting a role for the RSF nucleosome remodeling complex in regulating chromatin dynamics via H2Av exchange (Hanai *et al.*, 2008).

The transcriptional pathways affected by the *Drosophila* TIP60 complex include genes involved in regulating cellular polarity in undifferentiated neuroblasts and genes that regulate the cell cycle in developing tissues. Knockdown of TIP60 components leads to loss of cell polarity and aberrant symmetric divisions of neural stem cells (Rust *et al.*, 2018). In addition, flies carrying the hypomorphic $cycE^{JP}$ allele experience cell proliferation defects during eye development, resulting in a small eye phenotype that is sensitive to E2F activity (Secombe *et al.*, 1998). Heterozygous mutation of either *His2av* or *dom* suppresses the small eye phenotype in $cycE^{JP}$ flies (Lu *et al.*, 2007). Incorporation of H2Av at E2F target promoters depends on both Dom and E2F1, supporting a model in which incorporation of H2Av by Dom prevents activation of transcription through E2F (Lu *et al.*, 2007).

The TIP60 complex also regulates cell cycle progression and the expression of cell cycle genes in differentiating wing cells (Flegel *et al.*, 2016). Inhibition of this complex results in phosphorylation of H2Av and transcriptional activation of DNA damage response genes. Another consequence is reduction in essential cell cycle regulators E2F1 and CycB and an elongation of the cell cycle. These results imply that TIP60 coordinates replacement of phosphorylated H2Av with the unmodified variant before cells enter mitosis (Flegel *et al.*, 2016).

Exchange of H2Av was recently demonstrated to regulate the expression of genes expressed as part of the circadian rhythm pathway (Liu *et al.*, 2019). ChIP data from fly heads examining the promoters of *period* and *timeless*, two key circadian rhythm regulators in *Drosophila* (Dubowy and Sehgal, 2017), revealed the presence of H2Av. H2Av signal increases upon RNAi depletion of *Domino*, indicating that exchange H2A for H2Av at the *period* and *timeless* promoters is essential for proper transcriptional regulation (Liu *et al.*, 2019). This finding expands the range of developmental phenomena that H2Av affects into the realm of adult behavior.

From the experiments described above, it is clear that proper incorporation of H2Av is essential to regulate not only the cell's response to genotoxic stress but also the expression of key developmental

genes. For this reason, H2Av incorporation and removal is a tightly regulated process controlled by a highly conserved family of proteins.

H2Av Phosphorylation Is Dynamically Regulated

Although most H2AX phosphorylation in vertebrates is handled by ataxia telangiectasia-mutated/ataxia telangiectasia and Rad- related (ATM and ATR) kinases, other kinases have also been reported to have activity toward this histone variant. DNA protein kinase phosphorylates H2AX *in vitro* (Park *et al.*, 2003) and *in vivo* mouse models have demonstrated that Polo-like kinase 3 can phosphorylate H2AX in response to osmotic stress (Wang *et al.*, 2014). Like its vertebrate ortholog, *Drosophila* H2Av is phosphorylated by ATM and ATR kinases in response to DNA double strand breaks (Jang *et al.*, 2003, Joyce *et al.*, 2011). H2Av can also be phosphorylated by JIL-1 kinase, although the significance of this is debated (Thomas *et al.*, 2014, Li *et al.*, 2017).

H2AX and its orthologs can potentially be dephosphorylated in the C-terminal domain by a number of phosphatases. In yeast, there is no H2A variant and H2A is phosphorylated itself as part of the DNA damage response (Downs *et al.*, 2000). The yeast orthologs of PP1 and PP4 dephosphorylate H2A as part of the DNA damage checkpoint response (Keogh *et al.*, 2006, Bazzi *et al.*, 2010). This feature is conserved in mammalian PP4, which dephosphorylates H2AX in human cell cultures (Nakada *et al.*, 2008). H2AX phosphatase activity is also seen in PP6, which is also implicated in H2AX dephosphorylation in HeLa cell cultures (Douglas *et al.*, 2010), and the chromatin-associated wild type p53-induced phosphatase 1 (WIP1). Wip1 dephosphorylates H2AX in human cell cultures upon resolution of DNA double strand breaks, thereby regulating the cell's ability to progress through the cell cycle (Macůrek *et al.*, 2010, Moon *et al.*, 2010).

Perhaps the most studied phosphatase with a role in regulated the modification state of H2AX is PP2A. PP2A is highly conserved among eukaryotes and is involved in regulating numerous cellular

pathways by dephosphorylating myriad substrates (Wlodarchak and Xing, 2016). In human cell culture, PP2A directly interacts with and dephosphorylates H2AX, and inhibition of PP2A activity with okadaic acid lengthens the persistence of phosphorylated H2AX foci in response to double strand breaks (Chowdhury *et al.*, 2005, Nakada *et al.*, 2008). Reducing expression of PP2A by RNAi disrupts the DNA damage repair process, leading to more DNA damage and persistence of phosphorylated H2Av foci (Chowdhury *et al.*, 2005, Nakada *et al.*, 2008).

Drosophila PP2A functions in mitosis and *PP2A* mutants display mitotic abnormalities in the dividing neuroblasts (Chen et al., 2007a; Deak et al., 2003). PP2A activity is required for progression through the cell cycle in *Drosophila* (Snaith et al., 1996, Chen et al., 2007) and inhibits self-renewal of neuroblasts by regulating the subcellular localization of several developmental factors in the Polo signaling pathway (Wang *et al.*, 2009). Mutation of the PP2A regulatory subunit gene *tws* results in chromatin bridges during anaphase (Gomes *et al.*, 1993) and chromosomal aberrations as a result of unresolved double strand breaks in dividing neuroblasts (Merigliano *et al.*, 2017). Mutations in *tws* also prevent dephosphorylation of H2Av and impair the cell's ability to respond to ionizing radiation or replicative stress. As mutations to *tefu* and *ku70*, which encodes a key NHEJ protein, are epistatic over *tws*, it was concluded that Ku70 is a substrate of both ATM and PP2A, which maintain a balance necessary to coordinate DNA repair with cell cycle progression (Merigliano *et al.*, 2017).

Aurora A Kinase Regulates Dephosphorylation of H2Av in Response to DNA Damage

There have been conflicting results in human cell culture studies as to whether or not H2AX phosphorylation is regulated by Aurora A kinase, with some experiments supporting this notion (Moretti *et al.*, 2011, Do *et al.*, 2017) and others arguing against it (Shin *et al.*, 2010, Sourisseau *et al.*, 2010). These studies are limited, however, as they were performed in cell lines (most in cancer cell lines) and not in a developing animal. This issue was addressed recently by experiments demonstrating a relationship

between Aurora A kinase and H2Av phosphorylation in *Drosophila*. It was shown that exposing larvae to X-ray irradiation leads to transient phosphorylation of H2Av that lasts for a significantly longer time in the *aurA* mutant compared to wild type (Merigliano *et al.*, 2019). Larvae lacking *aurA* kinase activity also showed increased levels of H2Av phosphorylation under normal conditions. Together, these observations suggest a role for Aurora A kinase in regulating the phosphorylation/dephosphorylation kinetics of H2Av regardless of the source of DNA damage (Merigliano *et al.*, 2019). A further demonstration of this role for Aurora A in maintaining genome integrity was shown by the significant increase in the occurrence of chromosomal aberrations in the dividing neuroblasts of *aurA* mutant larvae. Mutations to *His2av* and *tefu* are epistatic to the chromosomal aberration phenotype in *aurA* backgrounds (Merigliano *et al.*, 2019). This leads to a model where H2Av is phosphorylated by ATM in response to DNA double strand breaks. Upon resolution of the DNA damage, this phosphorylation mark is normally removed by PP2A. PP2A is regulated in turn by AurA kinase, which phosphorylates PP2A to keep it active (Merigliano *et al.*, 2019). This model explains the mechanistic relationship between AurA activity and DNA damage repair and extends our understanding of how H2Av phosphorylation is regulated by the cell under genotoxic conditions.

H2Av Promotes JIL-1 Kinase Activity

There has been some debate in the literature regarding the influence of JIL-1 kinase activity on the phosphorylation state of H2Av. JIL-1 was initially described in *Drosophila* for its ability to regulate chromatin structure in different stages of the cell cycle (Jin *et al.*, 1999). JIL-1 is responsible for phosphorylation of H3S10 and maintaining an open, transcriptionally active chromatin state (Wang *et al.*, 2001). Null mutation of *Jil-1* disrupts chromatin structure in polytene chromosomes (Thomas *et al.*, 2014). One body of research proposes a model in which JIL-1 phosphorylates nucleosome-bound H2AvS137, promoting an interaction between PARP-1 (which is already bound at nucleosomes) and H4, thus

stimulation PARylation. This is thought to change the structure of the nucleosome such that JIL-1 is able to phosphorylate H3S10, resulting in chromatin decondensation and transcriptional activation. It is further argued that the N-terminal domain of H2A has an inhibitory effect on PARP-1 activity and that acetylation of H2AK5 disrupts this inhibition (Thomas *et al.*, 2014). This model is based off the evidence that mutation of *Jil-1* suppresses pADPr accumulation and H3S10 phosphorylation, with both of these phenotypes also being described in *His2Av* null mutants (Kotova *et al.*, 2011). Additionally, flies lacking *JIL-1* show less phosphorylation of H2AvS137, with residual phosphorylation of H3 and H2Av blamed on other kinases. JIL-1 was shown by an *in vitro* assay to phosphorylate H2Av and colocalizes with H2Av, but not H2A, on polytene chromatin. This data suggests that whereas stable H2Av phosphorylation is independent of JIL-1, dynamic phosphorylation requires JIL-1 kinase activity (Thomas *et al.*, 2014).

Some of the key findings of this study were, however, called into question by further experiments into the relationship between H2Av and H3S10 phosphorylation. While some results from the earlier work were validated, including the colocalization between JIL-1 and H2Av in polytene chromosomes and the lack of H3S10 phosphorylation in the $His2Av^{810}$ null background, others argue that JIL-1 phosphorylation of H2AvS137 is not necessary for chromatin decondensation and H3S10 phosphorylation (Li *et al.*, 2017). Despite the lack of H3S10 phosphorylation in the $His2Av^{810}$ null, JIL-1 is recruited to polytene chromosomes at similar levels to wild type, while overexpression of JIL-1::GFP in $His2Av^{810}$ is sufficient to rescue H3S10 phosphorylation (Li *et al.*, 2017). Further, polytene nuclei expressing only CFP::JIL-1-CTD, which lacks kinase activity, show wild type levels of H2Av and γH2Av, suggesting that JIL-1 does not phosphorylate H2AvS137 *in vivo*. It was concluded that while H2Av likely promotes JIL-1 kinase activity, it is not required for phosphorylation of H3S10 by JIL-1 (Li *et al.*, 2017) and that the results reported earlier are based on *in vitro* kinase assays in which other kinases may have had an impact and that these earlier results were based on JIL-1 hypomorphs as opposed to true null alleles (Thomas *et al.*, 2014). It was also argued that PARylation is not required for JIL-1 mediated H3S10 phosphorylation and

that the PolII complex is transcriptionally active at *Hsp70* loci upon heat shock in both JIL-1 and H2Av null backgrounds (Li *et al.*, 2017). Together, these recent findings imply that PARP-1 recruitment is downstream of H3S10 phosphorylation by JIL-1, which might be facilitated by H2Av.

Phosphorylation of H2Av plays crucial roles in both the DNA damage response (Madigan *et al.*, 2002) and in transcriptional regulation (Swaminathan *et al.*, 2005, Kotova *et al.*, 2011). Maintaining the appropriate balance of this post-translationally modified histone variant through the activity of kinases and phosphatases is thus essential for cellular function. By identifying which enzymes modify H2Av and how they affect the cell's ability to induce transcriptional responses or to respond to DNA damage, we may gain a better understanding of the role this histone variant, or by extension its vertebrate orthologs, plays in genome stability and development.

H2Av Availability Is Regulated by Lipid Droplets Early in Development

Numerous experiments have demonstrated that a subset of histone proteins are recruited via electrostatic interactions in high levels to lipid droplets that are found distributed throughout the *Drosophila* embryo (Cermelli *et al.*, 2006, Li *et al.*, 2012). These proteins are thought to be expressed in excess in the mother and localize to lipid droplets during oogenesis and remain throughout early embryogenesis (Cermelli *et al.*, 2006) and function to buffer the maternal supply of histone proteins, which are in great demand as thousands of cells undergo replication during embryogenesis (Li *et al.*, 2012). Indeed, this maternal protein supply is enough to prolong viability through pupation in the absence of zygotic histone expression. The lipid droplets are specifically enriched for H2A, H2B, and H2Av, but not H3 (Cermelli *et al.*, 2006, Li *et al.*, 2014). The presence of histone proteins at these lipid droplets is regulated by the protein Jabba. Mutation of *Jabba*, as well as depletion of the lipid droplets themselves, results in increased amounts of H2Av found in the nuclei of embryonic cells (Li *et al.*, 2014). Zygotic expression of *His2Av* increases in these embryos, and newly expressed H2Av is incorporated into these

lipid droplets alongside the maternal contribution. Transplantation of Jabba-positive lipid droplets were able to recruit H2Av in the recipient cell, further demonstrating the active role lipid droplets play in managing the nuclear concentration of this histone variant (Li *et al.*, 2014).

The dosage of H2Av in these embryonic cells overall is therefore dependent on maternal contributions, zygotic gene expression, and the ability for histones to be temporarily sequestered in lipid droplets. Mis-regulation of the available pool of H2Av can have catastrophic consequences on development: *Jabba*$^{-}$ mutants, in which nuclear accumulation of H2Av is not buffered by the presence of lipid droplets, suffer from nuclear falling (an embryo-specific response to DNA damage) (Li *et al.*, 2012) and lower rates of embryo hatching (Li *et al.*, 2014). These may be the result of disruptions in gene expression due to changes in the nuclear ratio of H2A to H2Av as each of these histones is involved in transcriptional activation and repression.

Further work using live cell Fluorescence photoactivation of H2Av-paGFP in embryos has shown that H2Av can quickly dissociate from LDs and localize to neighboring nuclei (Johnson *et al.*, 2018). Fluorescent photoswitching experiments demonstrate a rapid loss of H2Av from LDs late syncytial blastoderms that is independent of the number of nuclei in the embryo and thus the demand for H2Av. Export of H2Av from the nucleus to the cytoplasm is minimal and has little impact on the cytoplasmic population of H2Av (Johnson *et al.*, 2018). Furthermore, H2Av is actively exchanged between lipid droplets in the cytoplasm. The amount of H2Av that is trafficked into the nucleus is related to the ability of cytoplasmic lipid droplets to recruit H2Av, as increasing Jabba dosage directly correlates with a reduction in nuclear H2Av signal (Johnson *et al.*, 2018). These results, along with the findings that H2Av protein levels are not regulated by translational and post-translational mechanisms similarly to canonical histones, point to a model in which regulation of H2Av trafficking is dominated by lipid droplets. This mode of regulation is tightly associated with the developmental stage of the embryo, as a transition happens in nuclear cycle 14 when H2Av exchange between lipid droplets ceases. This happens when the

embryo passes a threshold in the nuclear to cytoplasmic ratio and may be considered a part of the mid-blastula transition (Johnson *et al.*, 2018).

Recent data in prepublication extends the model of LD-dependent regulation of H2Av in the embryo to the oocyte (Stephenson *et al.*, 2020). It was shown that lipid droplets form first in nurse cells, cells that provide proteins and mRNAs to developing oocytes. These lipid droplets are transported from nurse cells into the oocyte. The oocyte produces most of its own H2Av; however, the Jabba protein delivered to the oocyte via lipid droplets is crucial to prevent degradation of H2Av in the ooplasm (Stephenson *et al.*, 2020). Were it not for this process, oocytes and developing embryos would struggle to keep up with the increasing demand for histones as each animal develops. That cells would evolve a novel mechanism in order to buffer the amount of H2Av available to the nucleus to the appropriate level underscores the importance of this histone variant in development.

H2Av Regulates Tissue Development

Proper development and organogenesis depend on complex networks of transcriptional regulators that dictate the fates of differentiated and undifferentiated cells within tissues. Understanding how these regulators cooperate and compete with each other can yield insight into basic mechanisms of development that may be conserved among complex eukaryotes. As a transcriptional regulator, H2Av is poised at the interface of DNA and epigenetic regulatory networks and thus has broad influence over tissue formation and integrity. As discussed above, inhibition or knockdown of the Tip60 complex prevents correct regulation of H2Av exchange. RNAi depletion of *domino* and *His2Av* leads to aberrant nuclear localization of Prospero, a transcription factor involved in neural stem cell differentiation (Rust *et al.*, 2018). Prospero promotes a transcriptional program that triggers differentiation of neuroblasts in pupae (Ikeshima-Kataoka *et al.*, 1997, Choksi *et al.*, 2006). This is associated with defects in cell polarity and division in larval neuroblasts that result in gross anatomical differences in the central nervous system

(Rust *et al.*, 2018). In addition to this, knockdown of Tip60 or mutation of the histone acetyltransferase domain disrupts cell cycle progression and development of wings in *Drosophila* pupae (Flegel *et al.*, 2016). It is clear from these results that exchange of H2Av in chromatin is essential for development of these tissues and begs the questions of whether this feature is conserved throughout the organism and how the mechanisms differ between tissues.

Misregulation of H2Av was recently shown to have a developmental phenotype in developing larvae. Individuals homozygous for the $His2Av^{810}$ null allele or trans-heterozygous for the $His2Av^{810}$ null allele paired with a chromosomal deficiency lacking the *His2Av* gene (Df(3R)BSC524) (Cook *et al.*, 2012) frequently develop large melatonic masses at their posterior ends (Grigorian *et al.*, 2017). These tumors form out of the lymph gland (the main hematopoietic tissue in flies) and are characterized by loss of differentiated plasmatocytes and crystal cells and the undifferentiated prohemocytes from the primary lobes. Driving RNAi of *His2Av* in prohemocytes resulted in increased differentiation of plasmatocytes and crystal cells in the primary and secondary lymph lobes, while driving RNAi in the posterior signaling center (PSC, a stem cell/tissue organizing hub) showed more normal development of plasmatocytes but fewer crystal cells. Importantly, overexpression of wild type H2Av resulted in less cohesion between PSC cells and fewer differentiated plasmatocytes and crystal cells (Grigorian *et al.*, 2017). This would imply that a precise concentration of H2Av is needed for normal development of this critical tissue, however, the mechanism of this relationship is unclear.

Evidence is also provided in this study that phosphorylation of H2Av is not required for its activity in regulating hematopoietic tissue development (Grigorian *et al.*, 2017). First, expression of a dominant negative mutant allele of *His2Av* lacking the C-terminal 14 amino acid H2AX-like motif ($H2AV^{CT}$) (Clarkson *et al.*, 1999) partially rescues hematopoiesis in the $His2Av^{810}$ null background and allows larvae to survive to adulthood. Second, overexpression of either the phosphomimetic $H2AV^{SE}$ or the phosphonull $H2AV^{SA}$ alleles partially rescues the hematopoietic phenotype seen in the $His2Av^{810}$ null background (Grigorian *et*

al., 2017). The results of this study, along with the finding that H2AZ expression is upregulated during macrophage development in humans (Baek *et al.*, 2009), suggest that regulation of blood cell differentiation is a conserved feature of H2Av function and is independent of the DNA damage response function associated with phosphorylation of the C-terminal domain. This conserved role for H2Av and H2A.Z implies that transcriptional regulation by H2Av in response to developmental stimuli may dictate how these tissues develop.

The H2Av histone variant also plays a vital role in fruit fly spermatogenesis. Examination of the stem cell niche found at the apical end of the testes (Fuller and Spradling, 2007) was performed in adult flies lacking *His2Av* expression. This was achieved using the FLP/FRT system for mitotic recombination in a heterozygous null $His2Av^{810}$/+ background (Morillo Prado *et al.*, 2013). A significant decrease in the population of germline stem cells (GSCs) was noted in the animals along with the appearance of the more differentiated spermatocytes and spermatids. Together, this implies that H2Av is required for maintaining the undifferentiated stem cell fate of the GSCs, but is not required for division and differentiation of daughter cells.

This relationship is not limited to cells of the germline, however, as cyst stem cell (CySC) populations also decrease in the absence of H2Av (Morillo Prado *et al.*, 2013). These cells are responsible for generating the cyst cells that envelop germ cells as they mature (Kiger *et al.*, 2000, Tran *et al.*, 2000), and were still present in the $His2Av^{810}$ homozygous testes, suggesting a conserved role for H2Av in the maintenance of adult stem cells but not in survival or differentiation. This observation was extended still further by abolishing *His2Av* expression in the developing eye with the EGUF/hid system (Stowers and Schwarz, 1999). While flies still generated eyes, they were smaller and rougher. Likewise, mutation of *His2av* suppresses the small eye phenotype observed in $cycE^{JP}$ flies (Lu *et al.*, 2007). These results suggest a highly conserved role for H2Av in the maintenance of adult stem cell populations in different developmental lineages.

Similar results were obtained in a mutant background for the *domino* gene, the ortholog of yeast Swr1 (Ruhf *et al.*, 2001), which exchanges H2A for H2AZ (Kobor *et al.*, 2004, Mizuguchi *et al.*, 2004). The Tip60 chromatin remodeling complex, which includes Domino, also exchanges phosphorylated H2Av with unmodified H2Av in *in vitro* assays (Kusch *et al.*, 2004). Disrupting this process also resulted in an inability to maintain GSC populations, providing further evidence that regulation of and by *His2Av* is crucial for proper tissue maintenance (Morillo Prado *et al.*, 2013). Interestingly, homozygosity for the null $His2Av^{810}$ null allele did not affect the global levels of H3K4 trimethylation (associated with transcriptional activity) or H3K27 trimethylation (associated with transcriptional silencing) (Morillo Prado *et al.*, 2013). This is contrast to the severe effect seen on H3S10 phosphorylation in the absence of H2Av (Kotova *et al.*, 2011, Li *et al.*, 2017). Whatever the epigenetic mechanism, it was proposed that H2Av affects self-renewal of adult stem cells either by repression of genes involved in differentiation or by activation of genes involved in stem cell identity.

γH2Av and Genome Organization

A novel role for H2Av in genome architecture was recently uncovered. Immunostaining data from larval polytene chromatin reveals colocalization between phosphorylated H2Av and Suppressor of Hairy Wing [Su(HW)] insulator complexes throughout the genome (Simmons *et al.*, 2021). Null mutation of the *su(Hw)* gene results in decreased γH2Av staining, suggesting that maintenance of H2Av phosphorylation in polytene chromatin depends on interactions with the Su(Hw) complex. A link between insulator proteins and DNA damage is supported by the finding that *su(Hw)* mutants also display DNA damage in ovaries and chromosomal aberrations in dividing neuroblasts (Hsu *et al.*, 2020). Mutation of *su(Hw)* also results in mislocalization of Gurken within the oocyte, a phenotype caused by DNA damage and observed in mutants of *tefu*/ATM, one of the main H2Av kinases (Joyce *et al.*, 2011). γH2Av enrichment at Su(Hw) insulators is supported by ChIP-seq data from S2 cells, which also reveals an enrichment of γH2Av at

boundaries between topologically associating domains (TADs) (Simmons *et al.*, 2021). These findings support a model in which H2Av aids in establishing or maintaining TAD boundaries within the genome.

γH2Av is enriched in *gypsy* insulator sites, and mutation of *His2Av* partially rescues *gypsy*-related phenotypes in a heterozygous *su(hw)* sensitized background (Simmons *et al.*, 2021). This genetic relationship demonstrates a role for H2Av in regulating the function of *gypsy* insulators. Null $His2Av^{810}$ larvae express *gypsy* retrotransposon mRNA at lower levels than wild type. This effect may be due to the interaction between H2Av and PARP1 as PARP1 protein is enriched at *gypsy* sites and is required for silencing transposon activity (Kotova *et al.*, 2011). Another potential mechanism involves nucleosome phasing. H2Av is enriched in phased nucleosomes at and immediately downstream of transcription start sites (Mavrich *et al.*, 2008, Zhang and Pugh, 2011). Depletion of Su(Hw) decreases nucleosome phasing surrounding *gypsy* loci (Baldi *et al.*, 2018). It may be that the Su(Hw) complex is required to establish the nucleosome phasing needed for this precise H2Av distribution, however, such a relationship has not yet been tested.

Intriguingly, γH2Av is found in insulator bodies, foci that form in the cytoplasm when insulator proteins leave chromatin and aggregate together in response to osmotic stress (Schoborg *et al.*, 2013). No unmodified H2Av is seen in insulator bodies and phosphatase inhibition prevents dissolution of bodies upon return to isotonic conditions (Simmons *et al.*, 2021). This implies that phosphorylation of H2Av regulates insulator body dynamics, though the mechanism remains unknown. These experiments demonstrate a clear relationship between chromatin insulator proteins and H2Av phosphorylation that may regulate local chromatin dynamics.

Conclusions

Chromatin dynamics are largely driven by the composition of nucleosomes and through post-translational modification of chromatin-associated proteins. *Drosophila* H2Av, being a histone variant whose activity

is tightly regulated by multiple modifications, is a prime example of how these processes can work together to coordinate cellular responses to genotoxic stress and developmental signaling pathways. H2Av is involved in diverse cellular processes and is regulated by a complex network of chromatin remodeling complexes and post-translational modifying enzymes (Figure 1.1). Despite decades of significant advances in our understanding of this histone variant, many questions remain regarding mechanisms of H2Av regulation and the downstream target genes whose transcription is affected by H2Av activity. The contribution of some kinases is unclear, while other potential kinases may still be unknown. Further characterization of other potential post-translational modifications on H2Av and the effects they have on H2Av function or S137 phosphorylation is needed. Also, determining the transcriptomic effects of H2Av may put into context the developmental defects observed upon mutation of *His2Av* or its regulators. Further dissection of the mechanisms behind how H2Av influences transcription can also provide crucial insight. H2Av is associated with chromatin architectural proteins and is enriched in TAD boundaries; it will therefore be instructive to determine whether this observation can explain chromatin dynamics and transcriptional regulation associated with H2Av activity. H2Av plays a key role in *Drosophila* biology and provides a unique model to study the function of histone variants on tissue development and homeostasis.

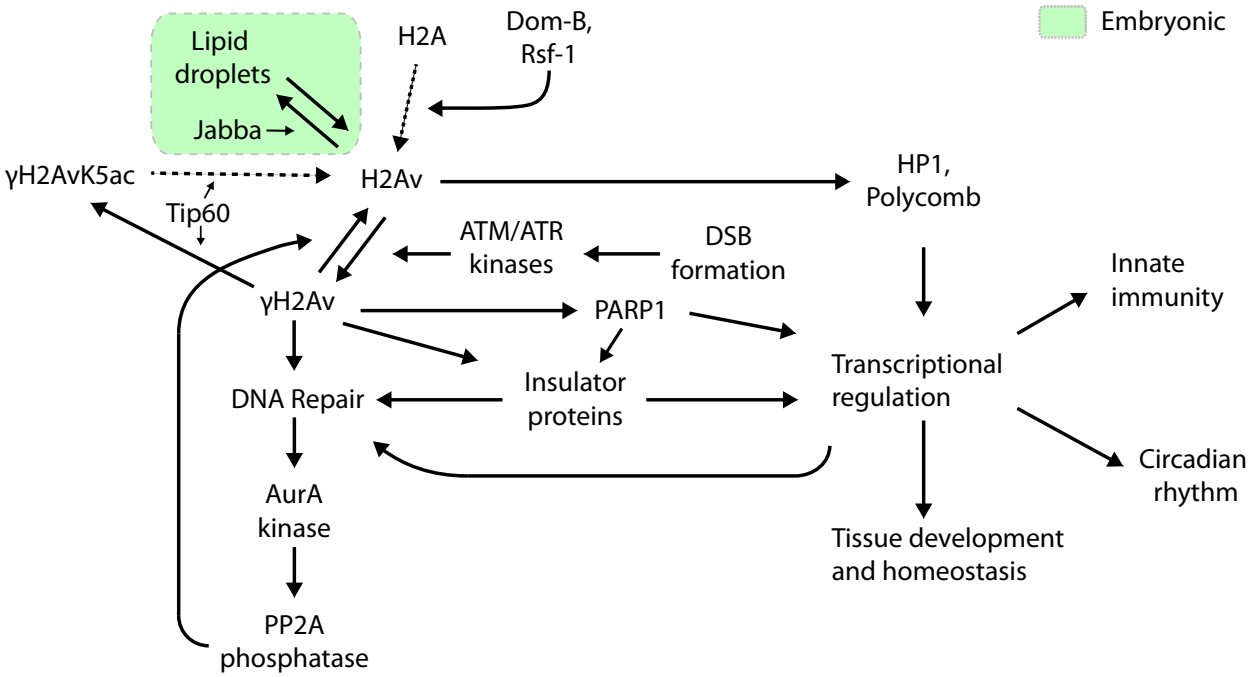


Figure 1.1. Model of H2AV regulation and activities. Dotted arrows represent replacement of one molecule with another. A green background represents activity only reported in embryonic cells.

A version of the following section is being submitted as a research article for peer review. Experiments were performed by James Ryan Simmons, Dr. Ran An, Bright Amankwaa, Shannon Zayac, and Justin Kemp. Data analysis, statistics, creation of figures, and writing was performed by James Ryan Simmons. Dr. Mariano Labrador contributed to experimental design, bioinformatics, manuscript revisions, and funding acquisition.

Chapter II: A Phosphorylated Histone H2A Variant Displays Properties of Chromatin Insulator Proteins in *Drosophila*

Abstract

Chromatin insulators are responsible for mediating long-range interactions between enhancers and promoters throughout the genome and align with the boundaries of topologically associating domains (TADs). Here, we demonstrate an interaction between proteins that associate with the *gypsy* insulator and the phosphorylated histone variant H2Av (γH2Av), a marker of DNA double strand breaks. *Gypsy* insulator components colocalize with γH2Av throughout the genome. Mutation of insulator components prevents stable H2Av phosphorylation in polytene chromatin. Phosphatase inhibition strengthens the association between insulator components and γH2Av and rescues γH2Av localization in insulator mutants. We also show that γH2Av is a component of insulator bodies, and that phosphatase activity is required for insulator body dissolution after recovery from osmotic stress. We further demonstrate a tight association between γH2Av and TAD boundaries. Together, our results indicate a novel mechanism linking insulator function with a histone H2A variant and with genome stability.

Introduction

A highly orchestrated 3D-genome organization is necessary for the proper function and survival of eukaryotic cells. The resulting higher-order chromosome structure in this organization is driven through

the establishment of long-range interactions between different regions of the chromosome. These interactions create domains that may be restricted from interacting with each other, and are based on specific interactions between chromatin-binding proteins (van Berkum *et al.*, 2010, Rao *et al.*, 2014, Fudenberg *et al.*, 2016). Chromatin insulators represent a class of protein/DNA complexes associated to specific sequences in the genome that work through two general functions: to restrict communication between enhancers and promoters through physical separation into different genomic domains and to prevent the spread of heterochromatin into euchromatic regions of the genome (Harrison et al., 1989, Geyer and Corces, 1992, Bell et al., 1999, Schoborg and Labrador, 2014, Ozdemir and Gambetta, 2019). The presence of insulators in the genome is conserved among eukaryotes, with the CTCF insulator being the only known insulator regulating the human genome (Heger and Wiehe, 2014). Insulators have recently been described to help establish the boundaries of topologically associating domains (TADs) and are often found enriched at TAD boundaries (Van Bortle et al., 2014, Fudenberg et al., 2016).

In this work, we show that γH2Av is present at Su(Hw)-binding sites throughout the genome, including at *gypsy* retrotransposons and that mutation of several *gypsy* insulator components disrupts normal H2Av phosphorylation patterns. We show that γH2Av is a component of insulator bodies formed under osmotic stress and that dephosphorylation of γH2Av is required for efficient dissolution of these bodies during recovery. Chromatin immunoprecipitation (ChIP) experiments reveal extensive genome-wide colocalization between Su(Hw) and γH2Av and enrichment for both at TAD boundaries. This association also extends to insulator function as flies doubly heterozygous for $His2Av^{810}$ and mutant alleles of *su(Hw)* showed a partial rescue of phenotypes for $yellow^{2}$ and cut^{6}, two *gypsy* insulator induced mutations. Collectively, these findings point to a model in which γH2Av works with insulators to coordinate genome function and genome-wide responses to genotoxic stress.

Methods and Materials

Fly stocks and husbandry

All stocks were maintained on a standard cornmeal agar fly food medium supplemented with yeast at 20°C; crosses were carried out at 25°C. The following stocks are maintained in our lab and were originally obtained from Victor Corces (Emory University): $y^2w^1ct^6$; $cp190^{H31\text{-}2}$/*TM6B*, Tb^1, $y^2w^1ct^6$; $cp190^{P11}$/*TM6B*, Tb^1, $y^2w^1ct^6$; w^{1118}; $su(Hw)^V$/*TM6B*, Tb^1, $y^2w^1ct^6$; $mod(mdg4)^{u1}$/*TM6B*, Tb^1. The stock w^{1118}; PBac(RB)$su(Hw)^{e04061}$/*TM6B*, Tb^1 was obtained from the Bloomington *Drosophila* stock center (BDSC: 18224). These remaining stocks were provided by our lab: Oregon-R (OR), $y^2w^1ct^6$; PBac(RB)$su(Hw)^{e04061}$/*TM6B*, Tb^1 (derived from BDSC: 18224).

Antibodies

Rabbit polyclonal IgG antibodies against Su(Hw), Mod(mdg4)67.2, and CP190 were previously generated by our lab (Wallace et al., 2010, Schoborg et al., 2013). A rat polyclonal IgG antibody against Su(Hw) generated by our lab was also used. Antibody against the phosphorylated form of H2Av (UNC93-5.2.1) (Lake et al., 2013) was obtained from the Developmental Studies Hybridoma Bank, created by the NICHD of the NIH and maintained at The University of Iowa, Department of Biology, Iowa City, IA 52242. These antibodies were all diluted 1:1 in glycerol (Fisher Scientific, BP229-1, lot 020133) and used at a final dilution of 1:200. Secondary antibodies were all diluted 1:1 in glycerol and used at a final dilution of 1:200. The following secondary antibodies were used in this study: Alexa Fluor 594 goat anti-rabbit (Invitrogen, A-111037, lot 2079421), Alexa Fluor 488 donkey anti-rabbit (Invitrogen, A-21206, lot 1834802), Alexa Fluor 488 goat anti-guinea pig (Invitrogen, A-11073, lot 84E1-1), Texas red donkey anti-rat (Jackson ImmunoResearch Laboratories, 712-075-150), and Alexa Fluor 488 goat anti-mouse (Invitrogen, A-11001, lot 1858182).

Immunostaining of larval tissues

Wandering third instar larvae were dissected in PBS. Tissues were immediately placed into fixative (4%, para-formaldehyde (Alfa Aesar, 43368, lot N13E011), 50% glacial acetic acid (Fisher Scientific, A38-212, lot 172788)) on a coverslip for one minute. Samples were squashed by lowering a slide on top of the sample then turning it over, placing it between sheets of blotting paper, and hitting the coverslip firmly with a small rubber mallet. Slides were dipped in liquid nitrogen, coverslips were removed, and samples were incubated in blocking solution (3% powdered nonfat milk in PBS + 0.1% IGEPAL CA-630 (Sigma-Aldrich, 18896, lot 1043)) for 10 minutes at room temperature. The slides were dried and incubated with primary antibodies overnight at 4°C in a box humidified with wet paper towels. The next day, slides were washed twice in PBS + 0.1% IGEPAL CA-630 before incubation with secondary antibodies for three hours in the dark at room temperature. Slides were washed twice in PBS + 0.1% IGEPAL CA-630, treated with DAPI solution of 0.5 μg/mL (ThermoFisher, D1306) for one minute, and washed one more time in PBS alone.

Samples were mounted with Vectashield antifade mounting medium (Vector Laboratories, H-1000, lot ZF0409) and coverslips were sealed with clear nail polish. All microscopy for immunostaining was performed on a wide-field epifluorescent microscope (DM6000 B; Leica Microsystems) equipped with a 100X (NA 1.35) oil immersion objective and a charge-coupled device camera (ORCA-ER; Hamamatsu Photonics). Image acquisition was performed using SimplePCI (v6.6; Hamamatsu Photonics). Image manipulation was performed in FIJI (Schindelin et al., 2012); all contrast adjustments are linear. Images were further processed in Adobe Photoshop CS5 Extended, Version 12.0 x64. Figures were assembled in Adobe Illustrator CS5, Version 15.0.0. Statistical analyses were performed in GraphPad Prism version 8.0.0 (224) (GraphPad Software, San Diego, CA).

Immunostaining of S2 cells

For normal control conditions, S2 cells were incubated in insect medium (HyClone SFX-Insect Cell Culture Media; Fisher Scientific, SH3027802) supplemented with penicillin (50 units/mL) and streptomycin (50 µg/mL) (Gibco, 15070063) at 25°C. To induce osmotic stress, the istonic media was replaced with hypertonic media supplemented with 250 mM NaCl (Fisher Scientific, BP358-212). Cells were treated in this hypertonic stress media for 30 minutes. Coverslips were pretreated with pure ethanol (Decon Labs, 2716) and coated with concanavalin A (Sigma-Aldrich, C5275) to help S2 cells adhere to the glass surface. Cells were pipetted onto treated coverslips and were allowed to spread and adhere for 30 minutes. After treatment, cells were fixed (4%, para-formaldehyde, 50% acetic acid) for 10 minutes at room temperature, followed by three washes with PBS buffer. Fixed cells were permeabilized with 0.2% Triton X-100 (Fisher Scientific, BP151, lot 014673) for five minutes then washed twice with PBS buffer. Cells were incubated in blocking solution (3% powdered nonfat milk in PBS + 0.1% IGEPAL CA-630) for 10 minutes at room temperature. Primary antibodies were diluted in blocking solution and samples were incubated in antibody solution overnight at 4°C in a box humidified with wet paper towels. Unbound antibodies were washed off three times with PBST buffer (0.1% Triton-X 100). Secondary antibody incubation, DAPI staining, and mounting were performed as described above.

Okadaic acid treatment

For the isotonic control samples, S2 cells were cultured in HyClone SFX-Insect media as above and incubated in 50 nM okadaic acid (Sigma-Aldrich, O9381) for 30 minutes. The hypertonic samples were obtained by shifting S2 cells from isotonic insect media to hypertonic conditions as described above and incubating for 25 minutes. After this, the hypertonic media was supplemented with 50 nM okadaic acid and cells were incubated for five more minutes. The isotonic recovery sample was obtained by first inducing hypertonic stress for thirty minutes, including okadaic acid for the final five minutes as above,

then washing out the hypertonic media twice with isotonic media containing 50 nM okadaic acid. Cells were incubated in isotonic recovery media with okadaic acid for thirty minutes. Control samples were collected throughout the process following the same protocol without addition of okadaic acid. For the polytene chromosome example, salivary glands were dissected from wandering third instar larvae and incubated in 50 nM okadaic acid for 30 minutes before fixation and squashing.

Fluorescence intensity and colocalization analysis

Images were analyzed for the amount of each protein (i.e. the intensity of each channel) using a macro script in FIJI (Schindelin et al., 2012). The DAPI channel was used to automatically generate non-biased ROIs for each cell, which were then manually curated for extra precision. A rolling-ball background subtraction algorithm was used for all images. Intensity measurements were made using the measure function. Numerous images of polytene chromosomes were collected from each salivary gland squash. All acquisition parameters were kept constant between slides within each experiment. Colocalization was quantified using the Coloc2 plugin in FIJI. This analysis uses the Costes method (Costes et al., 2004) to determine appropriate thresholds for each channel. Results are reported in terms of Pearson's Correlation Coefficient (PCC) (Pearson, 1895), which ranges from -1 for perfect anti-correlation to +1 for perfect correlation (Dunn et al., 2011). Another metric of colocalization is the Manders' Colocalization Coefficients (Manders et al., 1992, Manders et al., 1993, Adler and Parmryd, 2010) for each channel – this relates how much of the signal in the green channel overlaps with signal in the red channel (M1) and how much of the signal in the red channel overlaps with signal in the green channel (M2). M1 and M2 may vary from 0, representing no overlap between signals, to 1, representing total overlap.

ChIP-seq and TAD data analysis

The following NCBI publicly available ChIP-Seq datasets were used for the genome wide comparisons: SRX1299942 (γH2Av SRA (Li et al., 2016)), SRX046654 (Su(Hw) SRA (Chen et al., 2012)), SRX186113 (Mod(mdg4)67.2 SRA (Matzat et al., 2012)), SRX2638361 (CP190 SRA (Jox et al., 2017)), SRX2638363 (CTCF SRA (Jox et al., 2017)), and SRX511131 (HIPP1 SRA (Alekseyenko et al., 2014)). The sequencing data was uploaded to the Galaxy web platform, and the public server at usegalaxy.org was used to analyze the data (Afgan et al., 2018). Briefly, the FastQ datasets from NCBI were mapped with Bowtie2 to produce BAM files (Langmead and Salzberg, 2012). Duplicate and unmapped reads were filtered out with SAM tools. Peaks were called with Model-based analysis of ChIP-Seq (MACs) (Zhang et al., 2008). We used SeqMINER version 1.3.4 for the downstream plotting analysis (Ye et al., 2011, Zhan and Liu, 2015).

To compare the distribution of γH2Av with that of nucleosomal H2Av we used the high-resolution distribution of homotypic and heterotypic *Drosophila* H2Av nucleosomes from S2 cells obtained from a previous study (Weber et al., 2010). FastQ datasets from paired-end reads from native micrococcal nuclease–digested chromatin, enriched in homotypic H2Av (SRX019957 (Weber et al., 2010)) or heterotypic H2Av (SRX019953 (Weber et al., 2010)), were mapped with Bowtie2 to produce BAM files mapped to the dm6 *Drosophila* genome. We applied Bamcoverage to BAM files to generate H2Av Hom and H2Av Het bigwig files. SeqMINER was used to generate displays of the distribution of mean read density profiles (tags / 50 bp), using BED files to provide reference coordinates (± 10,000 bp). Bigwig files were generated by applying Bamcoverage to BAM files and peak profiles were visualized with the IGV genome browser (igv.org/app/) (Robinson et al., 2011), using *Drosophila* dm6 as the reference genome. The genomic distribution of TADs in the *Drosophila* genome (Ramirez et al., 2018) was used to produce a BED file generated with all genomic 1Kb fragments containing a TAD boundary at the center.

Phenotypic analysis

Documentation of y^2 and ct^6 phenotypes was performed using a stereomicroscope (MZ16 FA; Leica Microsystems) equipped with a CCD color camera (DFC420; Leica Microsystems). A 150 Watt white light source (KL 1500 LCD; Leica Microsystems) set to a color temperature of 3,000 K was used for illumination. Male flies were selected soon after eclosion and aged for five days at 25°C before imaging. All images within each tissue set were collected with the same parameters using Leica Application Suite (Version 2.4.0 R1; Leica Microsystems). Abdomen images were recorded with a gamma correction of 0.5. Image analysis was performed in FIJI (Schindelin et al., 2012). Intensity of the darkest region within the fifth abdominal tergite was measured using a circular ROI with radius of 15 pixels (= 0.045 mm) (Figure 3.8). Intensity values from abdomens were inverted before analysis so that darker pigmentation provided a higher score. Regions of abdomens that reflected the light source were excluded from analysis. Wing areas were measured in FIJI (Schindelin et al., 2012) using the entire translucent area of the wing (except for the alula, which was sometimes lost in sample preparation) as the ROI.

Results

H2Av Phosphorylation Is Correlated with *gypsy* Insulator Components Genome-wide

Beyond its canonical insulator functions, the *Drosophila* insulator protein Su(Hw) has been implicated in transcriptional regulation and is required for development of testes and ovaries (Soshnev *et al.*, 2013, Duan and Geyer, 2018). Mutation of *su(Hw)* interferes with normal DNA damage repair (Lankenau et al., 2000) and lack of Su(Hw) protein results in chromosomal aberrations in developing neuroblasts (Hsu et al., 2020). While these results point to a role in maintaining genome stability, the mechanistic link between Su(Hw) and DNA repair remains uncharacterized. To investigate this possibility, we performed immunostaining of polytene chromosomes from salivary glands of third instar larvae using an antibody directed against the phosphorylated form of H2Av (γH2Av), a marker of DNA double strand breaks

(Madigan *et al.*, 2002). This procedure reveals a close association between Su(Hw) and γH2Av throughout each polytene chromosome arm. Close inspection shows γH2Av in nearly all of the Su(Hw) bands (Figure 2.1A). Linescans of the 2R polytene chromosome show strong covariance in the fluorescent intensity between γH2Av and Su(Hw) (Figure 2.1A). Likewise, analysis of the immunostaining signal using the entire polytene genome shows a significant colocalization between γH2Av and Su(Hw) (Figure 2.1A). Quantification of colocalization of the two immunostaining signals is reported using Pearson's Correlation Coefficient (PCC), which describes the covariance between the two signals, with positive numbers describing direct correlation between signal intensities, negative numbers representing anti-correlation of the signals, and zero representing no correlation between signals (i.e. random covariance) (Adler and Parmryd, 2010, Dunn et al., 2011). Colocalization is also reported using Manders' overlap coefficient (MOC), which describes the amount of one signal in an image that overlaps with signal from the other channel (Manders et al., 1993). Two values are reported, one for each channel, with values ranging from 0 (representing no spatial overlap between signals) and 1 (representing complete overlap of signals).

An extensive genome-wide association between γH2Av and Su(Hw) is illustrated by the positive PCC values and MOC values above 0.5. Given the fundamental role of γH2Av in DNA repair, the tight association of Su(Hw) with phosphorylated H2Av supports the notion that Su(Hw) is involved in maintaining genome integrity (Lankenau et al., 2000, Hsu et al., 2020). Immunostaining experiments yield similar results for Mod(mdg4)67.2, the isoform of the *mod(mdg4)* locus associated with *gypsy* insulator function (Figure 2.1B). Bands of Mod(mdg4)67.2 are seen to overlap with bands of γH2Av (Figure 2.1B) and linescans reveal a close covariance (Figure 2.1B). The same pattern is recapitulated when examining images and linescans of CP190 (Figure 2.1C), an insulator protein found at *gypsy* and CTCF insulator sites (Pai et al., 2004, Mohan et al., 2007). Quantitative analysis of signal colocalization shows strong positive correlation values when examining genome-wide signal in polytene chromosomes for both Mod(mdg4)

Figure 2.1. Insulator proteins colocalize with phosphorylated H2Av in *Drosophila* polytene chromosomes. A. Colocalization of γH2Av with Su(Hw). **B.** Colocalization of γH2Av with Mod(mdg4)67.2. **C.** Colocalization of γH2Av with CP190. Immunofluorescent micrographs of polytene chromosome squashes obtained from wandering third-instar larvae are shown on the left. Magnified insets are shown in the middle, corresponding to the white boxes in the figures on the left. Scale bars are 5 µm in the figures and 2 µm in the insets. Insets are shown as RGB merge, with DAPI on the blue channel, γH2Av on the green channel, and various insulators on the red channel. Red and green channels are shown independently in grey scale and merged as magenta and green. On the right are linescans performed in FIJI (Schindelin *et al.*, 2012), corresponding to the yellow lines in the merged insets. Linescan intensities were normalized by dividing each value by the maximum intensity recorded on each channel. Arrows in the images and respective linescans denote regions of strong colocalization while arrowheads denote regions enriched for insulator proteins but not γH2Av. Pearson's Correlation Coefficient (PCC) for γH2Av signal with each insulator signal is plotted, with each point representing the polytene genome of each cell. Similarly, Mander's tM1 (the proportion of γH2Av-positive pixels that also contain signal from antibodies against insulator proteins) and tM2 (the proportion of insulator protein-positive pixels that also contain signal from the γH2Av antibody) are plotted in each cell. Error bars represent one standard error of the mean.

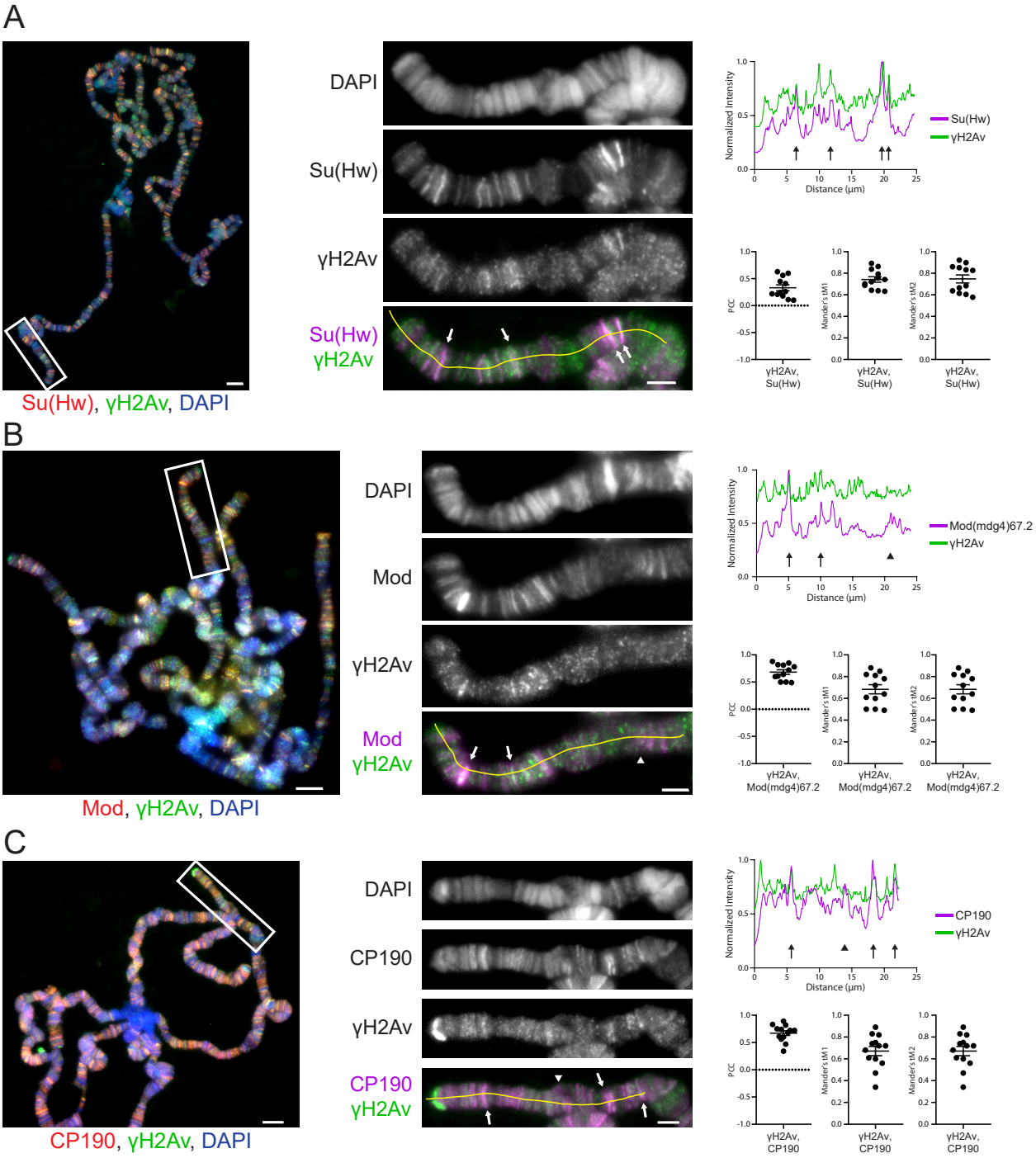


Figure 2.1 continued

and CP190 with γH2Av (Figure 2.1B, C). These findings suggest that γH2Av colocalizes with *gypsy* insulator proteins throughout the genome under normal developmental conditions.

Phosphorylated H2Av Is Stabilized by *gypsy* Insulator Components

To further our understanding of the relationship between γH2Av and insulator complexes we asked whether or not mutation of genes coding for *gypsy* insulator complex members would affect H2Av phosphorylation. Immunostaining of polytene chromatin revealed an almost complete elimination of γH2Av in the chromatin of $su(Hw)^{e04061}$ mutants (Figure 2.2). Mutation of *cp190* also resulted in less γH2Av signal in the immunostained chromosomes, however, the reduction was not as severe as was seen in the $su(Hw)^{e04061}$ mutant (Figure 2.2). In contrast with *su(Hw)* and *cp190*, mutation of *mod(mdg4)* had no significant effect on the amount of H2Av phosphorylation in chromatin (Figure 2.2). These results suggest that Su(Hw) and CP190, but not Mod(mdg4)67.2, are necessary for sustaining H2Av phosphorylation and may hint at a mechanism that depends on specific interactions between H2Av with some but not all *gypsy* insulator components.

As interactions between insulator proteins are generally required for canonical insulator functions (Geyer and Corces, 1992, Bonchuk et al., 2015, Golovnin et al., 2016, Melnikova, Kostyuchenko, Parshikov, et al., 2018, Melnikova et al., 2019), we examined the relationship between each of these insulator proteins and γH2Av in various insulator mutant backgrounds. Notably, the colocalization between Mod(mdg4)67.2 and γH2Av was strongly reduced in the $su(Hw)^{e04061}$ background (Figure 2.3A, F). This is not surprising given both that γH2Av signal is significantly reduced in $su(Hw)^{e04061}$ (Figure 2.2) and that Mod(mdg4)67.2 does not bind at Su(Hw) sites in the absence of Su(Hw) (Ghosh et al., 2001). Linescans of polytene chromosomes and quantitative colocalization analysis show no correlation between the signals from Mod(mdg4)67.2 and γH2Av in $su(Hw)^{e04061}$ mutant polytene chromosomes (Figure 2.3A).

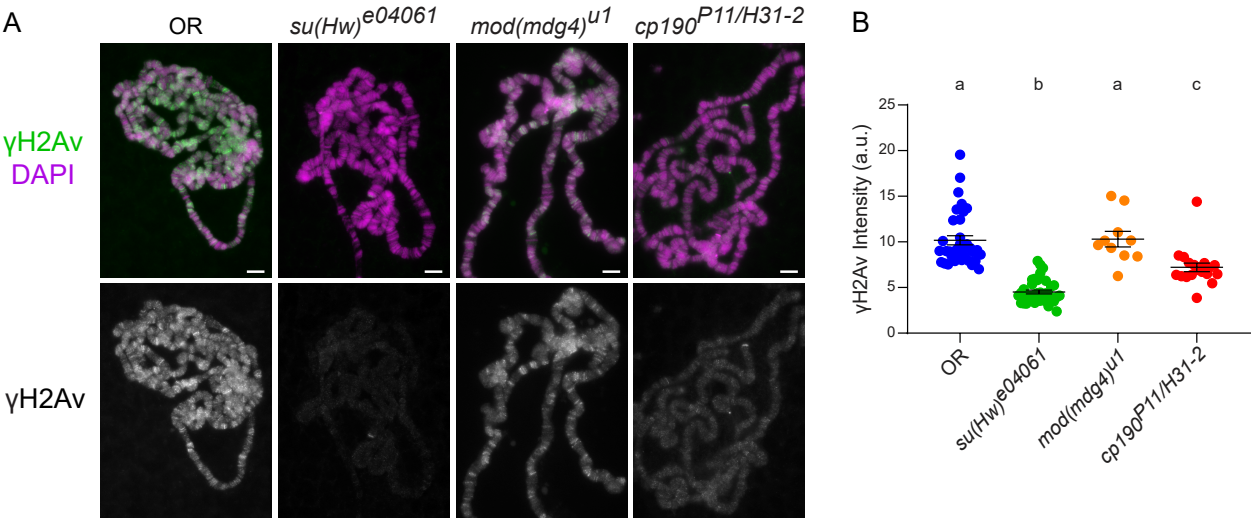


Figure 2.2. Phosphorylation of H2Av in polytene chromosomes is inhibited in insulator protein mutants.

A. Immunostaining of polytene chromosomes from wandering third instar *Drosophila* larval salivary glands from various insulator mutant genotypes (listed above each figure). An antibody against phosphorylated H2Av (γH2Av) was used (green in the merged image, shown alone in greyscale below). Scale bars represent 5 µm. **B.** Quantification of fluorescent signals from immunostains with γH2Av shown in A. Each point represents the polytene genome of an individual cell. Error bars represent one standard error of the mean. Letters above the data indicate statistical groupings as determined using an ANOVA performed with Games-Howell's multiple corrections.

Similarly, immunostaining for Su(Hw) in the loss of function *mod(mdg4)^{u1}* mutant revealed significantly less colocalization as seen by visual inspection, linescans, and quantitative analysis (Figure 2.3B, F). Linescans from immunostains of the *mod(mdg4)^{u1}* mutant with either Su(Hw) (Figure 2.3C) or CP190 (Figure 2.3D) along with γH2Av demonstrate a further disruption of the interaction between γH2Av and insulator complexes. The lack of colocalization between γH2Av and Su(Hw) or CP190 is reflected in decreased PCC values (Figure 2.3F), with negative values for CP190 indicating anticorrelation between the CP190 and γH2Av signals. Su(Hw) was also found to colocalize less with γH2Av in the null *cp190$^{P11\text{-}H31\text{-}2}$* mutant background through the area of chromosome 2R examined (Figure 2.3E) and genome wide (Figure 2.3F). Taken together, these results indicate that stable accumulation of γH2Av in Su(Hw) insulator sites requires having the entire insulator complex intact. It remains unclear which Su(Hw) insulator protein serves as the binding partner of γH2Av, or if this colocalization requires that γH2Av interact with more than one insulator protein or other unknown protein.

H2Av Is Phosphorylated in Insulator Bodies

Upon our finding that γH2Av colocalizes with insulator proteins in the genome in an insulator-dependent manner, we next asked whether or not this interaction was maintained once insulator proteins aggregate into bodies under osmotic stress conditions. Insulator bodies represent a special case for insulator activity: proteins bound to insulator sites in the genome can leave chromatin and associate to form insulator bodies (Gerasimova and Corces, 1998). The exact purpose of these bodies remains unknown, but recent reports have shed new light on their formation and dynamics. In a previous work, our lab demonstrated that insulator bodies form after dissociation of insulator proteins from chromatin and that insulator body formation can be induced under conditions of high osmotic pressure (Schoborg et al., 2013).

Figure 2.3. Insulator components are interdependent for their colocalization with γH2Av in *Drosophila* polytene chromosomes. **A.** Colocalization of γH2Av with Mod(mdg4)67.2 in *su(Hw)*^{e04061}. **B.** Colocalization of γH2Av with CP190 in *su(Hw)*^{e04061}. **C.** Colocalization of γH2Av with Su(Hw) in *mod(mdg4)*^{u1}. **D.** Colocalization of γH2Av with CP190 in *mod(mdg4)*^{u1}. **E.** Colocalization of γH2Av with Su(Hw) in *cp190*$^{P11/H31-2}$. **F.** Pearson's Correlation Coefficient (PCC) for γH2Av signal with each insulator signal is plotted, with each point representing the polytene genome of each cell. Error bars represent one standard error of the mean. PCC values are grouped by genotype (red = *su(Hw)*^{e04061}, green = *mod(mdg4)*^{u1}, blue = *cp190*$^{P11/H31-2}$). Immunofluorescent micrographs of polytene chromosome squashes obtained from wandering third-instar larvae are shown on the left. Magnified insets are shown to the right of each figure, corresponding to the white boxes in the figures on the left. Scale bars are 5 µm in the figures and 2 µm in the insets. Insets are shown as RGB merge, with DAPI on the blue channel, γH2Av on the green channel, and various insulators on the red channel. Red and green channels are shown independently in grey scale and merged as magenta and green. Beneath the insets are linescans performed in FIJI (Schindelin *et al.*, 2012), corresponding to the yellow lines in the merged insets. Linescan intensities were normalized by dividing each value by the maximum intensity recorded on each channel. Arrows in the images and respective linescans denote regions of strong colocalization while arrowheads denote regions enriched for insulator proteins but not γH2Av.

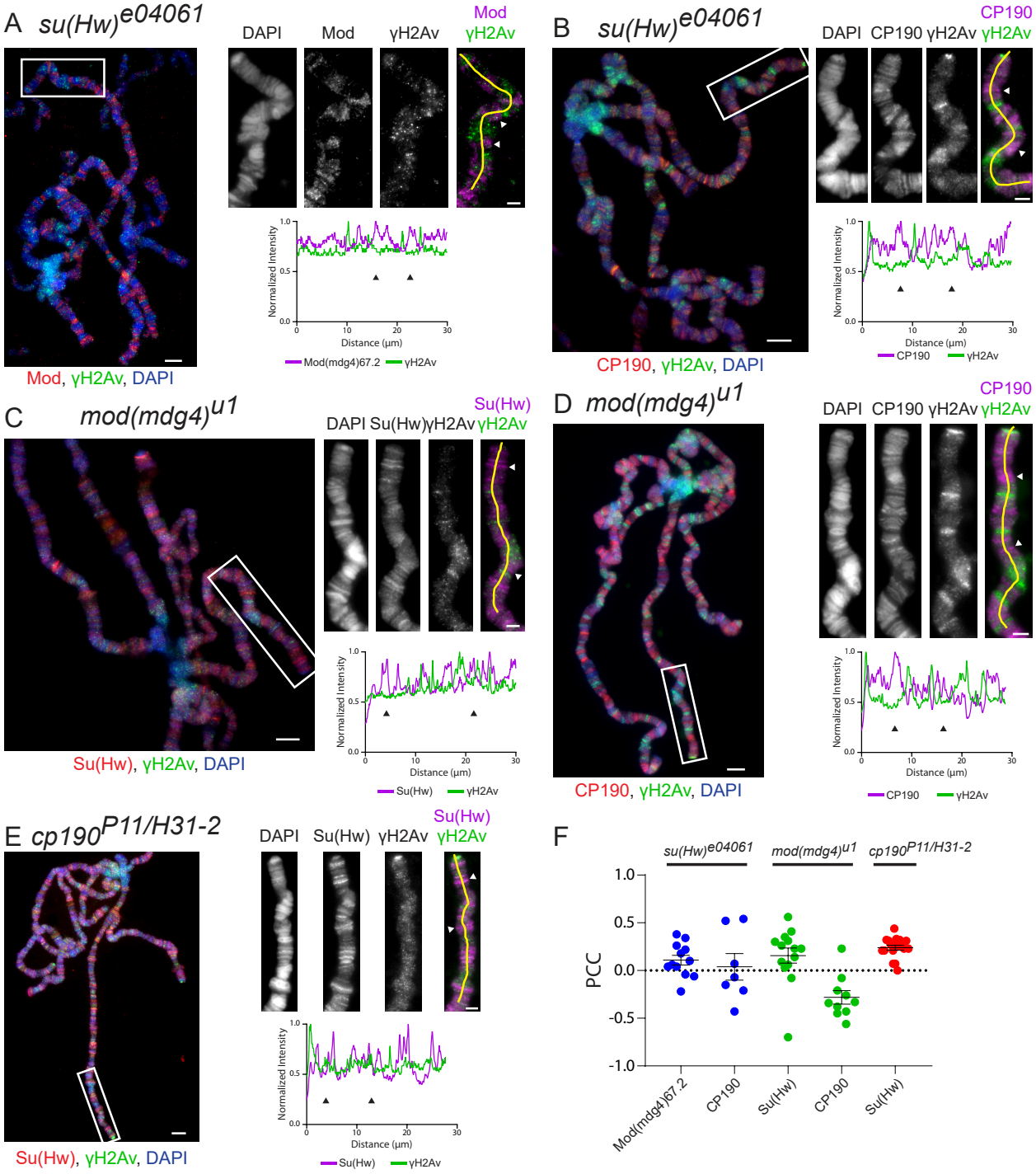
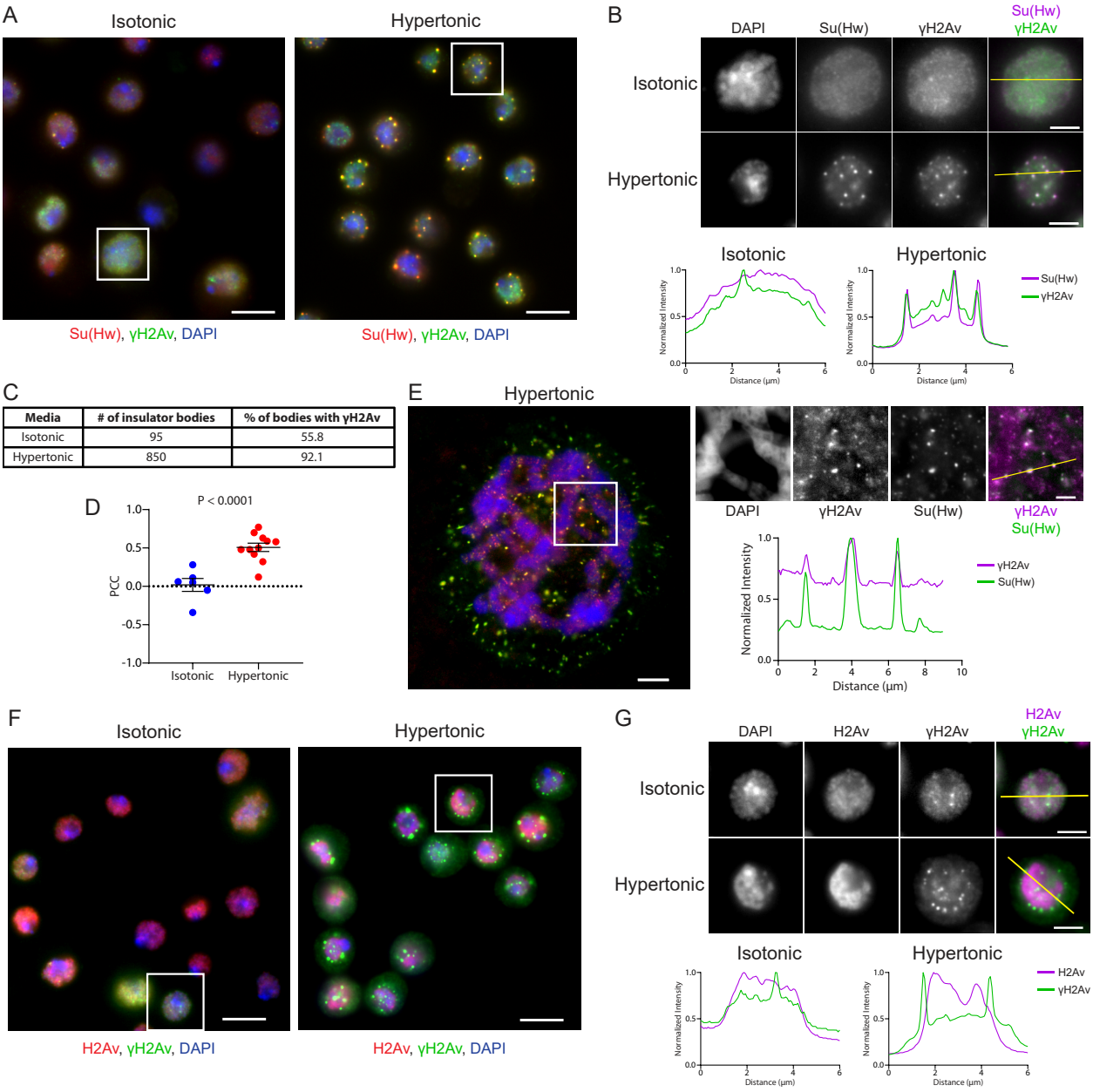


Figure 2.3 continued

Immunostaining of S2 cells for γH2Av and Su(Hw) in isotonic cell culture media shows no visibly apparent pattern between the two proteins (Figure 2.4A). Linescans support this point, with little covariance seen between the signals (Figure 2.4A). Incubation of S2 cells in hypertonic media (containing an additional 250 mM NaCl) induced strong insulator body formation as previously reported (Schoborg et al., 2013). Immunostaining shows clear localization of γH2Av to insulator bodies (Figure 2.4B). Linescans drawn through the insulator bodies confirm this finding, with each signal following the same pattern (Figure 2.4B). The vast majority of observed insulator bodies formed during osmotic stress were positive for γH2Av (92.1%, Figure 2.4C). A number of smaller insulator bodies containing γH2Av also formed under isotonic conditions, implying that some amount of phosphorylated H2Av may be involved in insulator body function during normal cellular conditions. Alternatively, these cells may represent cells undergoing apoptosis (Schoborg et al., 2013). Quantitative colocalization analysis shows a clear and significant increase in colocalization between Su(Hw) and γH2Av after hypertonic stress, whereas there is no colocalization between the two signals in isotonic media (Figure 2.4D).

Insulator bodies have previously been shown to form in other cell types such as the polytene cells of the larval salivary gland (Schoborg et al., 2013). In order to determine whether or not phosphorylated H2Av was present in insulator bodies formed under osmotic stress conditions, larval salivary glands were treated in hypertonic solution and immunostained for Su(Hw) and γH2Av. Analysis of the micrographs reveals strong colocalization of the γH2Av antibody in the insulator bodies labelled by Su(Hw) in salivary gland cells (Figure 2.4E). There is no significant accumulation of unphosphorylated H2Av in these insulator bodies (Figure 2.4F, G), suggesting that phosphorylation of this histone variant is important for its localization to insulator bodies. The mechanism behind how insulators leave chromatin and form bodies is unknown, and the involvement of γH2Av adds an unexpected layer to this question. The presence of γH2Av in insulator bodies may also have implications in how cells respond to DNA damage.

Figure 2.4. Phosphorylated H2Av is a component of insulator bodies. A. Immunostaining of *Drosophila* S2 cells in isotonic media (left) and hypertonic media (right). Insulator bodies formed during osmotic stress are labelled with Su(Hw) (red). Phosphorylated H2Av (green) colocalizes with Su(Hw) in insulator bodies. Scale bars are 5 µm and insets for analysis are delineated by white boxes. **B.** Magnified view of insets showing insulator body formation in hypertonic, but not isotonic, conditions. Insets are shown as RGB merge, with DAPI on the blue channel, γH2Av on the green channel, and Su(Hw) on the red channel. Red and green channels are shown independently in grey scale and merged as magenta and green. Beneath the insets are linescans corresponding to the yellow lines in the merged insets. Scale bars represent 2 µm. **C.** Table showing the ratio of insulator bodies with significant amounts of γH2Av. **D.** Pearson's Correlation Coefficient (PCC) for γH2Av signal with Su(Hw) signal is plotted for isotonic versus hypertonic conditions, with each point representing a field of S2 cells. Error bars represent one standard error of the mean. The P-value was determined using an unpaired Student's T-test. **E.** Polytene chromosomes from wandering third instar larval salivary glands under hypertonic conditions. Colocalization between γH2Av and Su(Hw) is shown in the insets and linescan. The scale bar in the wide view represents 5 µm, the scale bar in the inset represents 2 µm. Linescan intensities in B, E, and G were normalized by dividing each value by the maximum intensity recorded on each channel.



Media	# of insulator bodies	% of bodies with γH2Av
Isotonic	95	55.8
Hypertonic	850	92.1

Figure 2.4 continued

Phosphatase Inhibition Affects Interactions between γH2Av and *gypsy* Insulators

H2Av phosphorylation is tightly regulated by a network of kinases and phosphatases that integrate signals from various aspects of cellular activity including DNA damage repair (Sirbu and Cortez, 2013). Dephosphorylation of mammalian γH2AX is mitigated primarily through Protein Phosphatase 2A (PP2A), but also occurs through the activity of other phosphatases, including Protein Phosphatase 4 (PP4) (Nakada et al., 2008) and Wip1 phosphatase (Macurek et al., 2010). In order to determine how H2Av phosphorylation affects genome dynamics, we used okadaic acid (OA), a potent inhibitor of serine/threonine phosphatases PP1 and PP2A *in vitro* and *in vivo* (Bialojan and Takai, 1988, Haystead et al., 1989). As okadaic acid may affect other phosphatases at high concentrations (Honkanen and Golden, 2002), a concentration of 50 nM was chosen. Third-instar larval salivary glands were dissected then incubated in okadaic acid before fixation, squashing, and immunostaining. Examination of the polytene chromosomes showed no adverse effect of okadaic acid on the binding of insulator proteins or their colocalization with phosphorylated H2Av (Figure 2.5A, C, D). Quantification of the antibody signals indicates a significant increase in the amount of Su(Hw) signal in the presence of okadaic acid compared to untreated samples (Figure 2.5B). Notably, there is also an increase in the amount of phosphorylated H2Av bound to the polytene chromatin in the presence of okadaic acid compared to the untreated control (Figure 2.5B). This would seem to indicate that the okadaic acid is inhibiting PP2A from dephosphorylating γH2Av in chromatin, resulting in a significant accumulation of the modified histone variant. This is in conflict with findings from human cell culture, which were shown to increase cellular levels of H2AX phosphorylation in response to DNA damaging agents in the presence of 25 nM okadaic acid, but not in the presence of okadaic acid alone (Chowdhury et al., 2005). The difference may be a result either of the lower concentration of okadaic acid used in the previous study, or of the innate differences between the two model systems, i.e. the dual nature of *Drosophila* H2Av, which has the combined functions of mammalian H2AX and H2AZ (van Daal et al., 1988). The increased γH2Av signal in the presence of okadaic

acid and in the absence of exogenous DNA damage may therefore support the H2AZ-like transcriptional regulation role in insulator function.

Intriguingly, immunostaining of salivary glands from insulator mutants after incubation in okadaic acid revealed a significant rescue of both H2Av phosphorylation and its colocalization with components of the *gypsy* insulator complex. Close examination of the polytene chromosomes in the *su(Hw)*^{e04061} mutant shows many sites of colocalization between γH2Av with both Mod(mdg4)67.2 and CP190 (Figure 2.6A, B) which were lacking in the untreated mutant (Figure 2.3A, B). This result suggests that in *su(Hw)* mutants, Mod(mdg4)67.2 interacts with CP190 and that this interaction is enhanced by γH2Av. Similar results were obtained when staining for Su(Hw) and CP190 in the *mod(mdg4)*^{u1} mutant, with both proteins showing colocalization with phosphorylated H2Av after incubation with okadaic acid (Figure 2.6C, D). As with the *su(Hw)*^{e04061} mutant, this is in contrast to the untreated mutant samples in which γH2Av and *gypsy* insulator complexes do not colocalize. Staining of the *trans*-heterozygous *cp190*$^{P11/H31-2}$ mutant for Su(Hw) after okadaic acid treatment yielded the same response, with colocalization between Su(Hw) and γH2Av being rescued compared to the untreated mutant (Figure 2.6E). Colocalization analysis over the entire area of the polytene chromosomes showed strong correlation between the γH2Av signal and signals from insulator proteins in the okadaic acid-treated insulator mutants (Figure 2.6F). This is reflected in positive values for Pearson's Correlation Coefficient (PCC), indicating significant correlations between γH2Av and *gypsy* insulator signals. This is in contrast to untreated mutant samples, which show a lack of correlation between γH2Av and *gypsy* insulator proteins (Figure 2.3F). These findings point to a model in which γH2Av acts as a component of *gypsy* insulators. Phosphorylation of H2Av may be required for *gypsy* insulator complex formation or stabilization, and may play an essential role in insulator functions.

Figure 2.5. Treatment with okadaic acid increases the amount of phosphorylated H2Av on polytene chromosomes. Shown are co-immunostains of polytene chromosomes from salivary glands treated with okadaic acid. **A.** Immunostaining of γH2Av with Su(Hw). **B.** Quantification of the immunostaining data show in A. The intensities of Su(Hw) and γH2Av are shown under in the absence and presence of okadaic acid. Each point represents the polytene genome of an individual cell. Error bars represent one standard error of the mean. P-values were determined using unpaired Student's T-tests. **C.** Immunostaining of γH2Av with Mod(mdg4)67.2. **D.** Immunostaining of γH2Av with CP190. Immunofluorescent micrographs of polytene chromosome squashes are shown on the left. Magnified insets are shown to the right of each figure, corresponding to the white boxes in the figures on the left. Scale bars are 5 μm in the figures and 2 μm in the insets. Insets are shown as RGB merge, with DAPI on the blue channel, γH2Av on the green channel, and various insulator proteins on the red channel. Red and green channels are shown independently in grey scale and merged as magenta and green. Beneath the insets are linescans corresponding to the yellow lines in the merged insets. Linescan intensities in A, C, and D were normalized by dividing each value by the maximum intensity recorded on each channel.

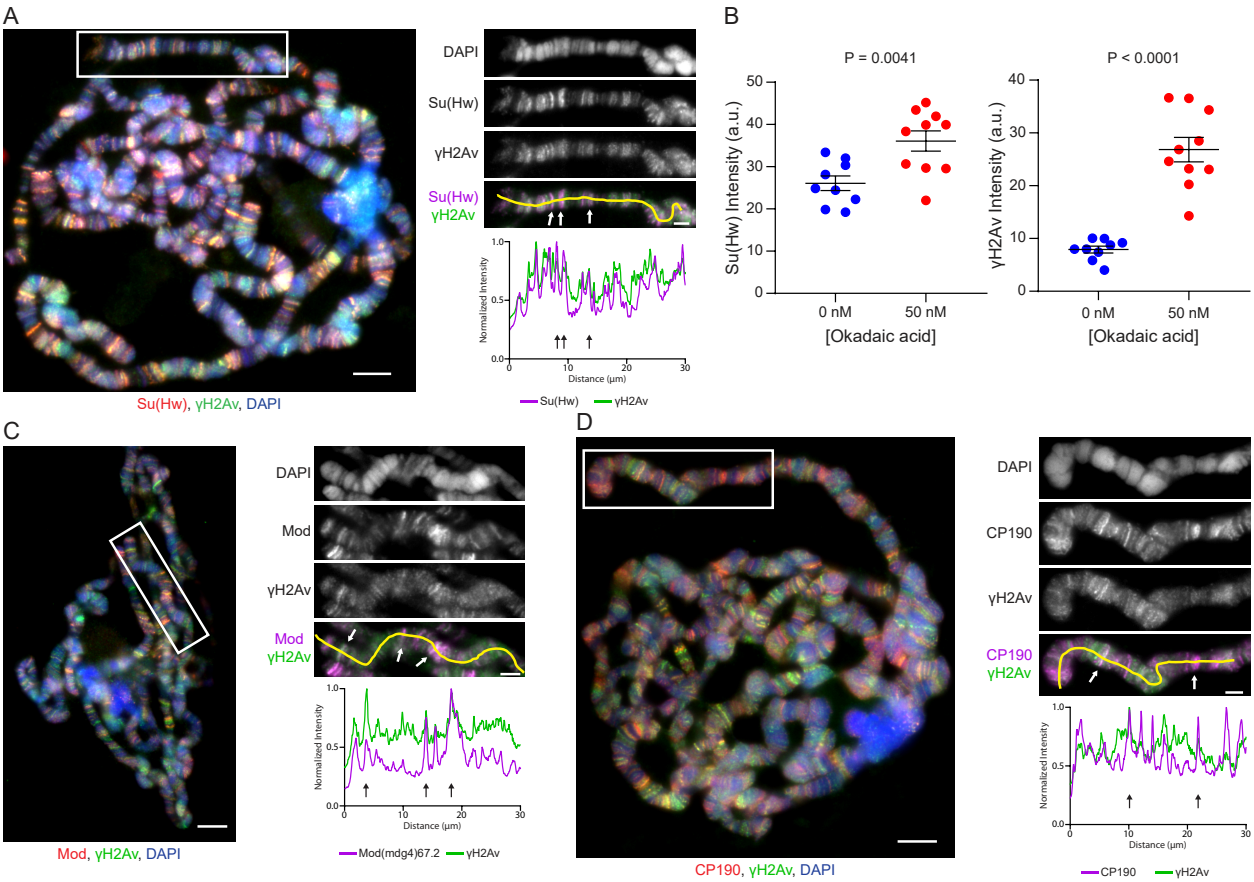


Figure 2.5 continued

Figure 2.6. Phosphatase inhibition restores localization of γH2Av at insulator sites in insulator protein mutants. Shown are co-immunostains of polytene chromosomes from salivary glands treated with okadaic acid. **A.** Colocalization of γH2Av with Mod(mdg4)67.2 in *su(Hw)*^{e04061}. **B.** Colocalization of γH2Av with CP190 in *su(Hw)*^{e04061}. **C.** Colocalization of γH2Av with Su(Hw) in *mod(mdg4)*^{u1}. **D.** Colocalization of γH2Av with CP190 in *mod(mdg4)*^{u1}. **E.** Colocalization of γH2Av with Su(Hw) in *cp190*$^{P11/H31-2}$. **F.** Pearson's Correlation Coefficient (PCC) for γH2Av signal with each insulator signal is plotted, with each point representing the polytene genome of each cell. Error bars represent one standard error of the mean. PCC values are grouped by genotype (red = *su(Hw)*^{e04061}, green = *mod(mdg4)*^{u1}, blue = *cp190*$^{P11/H31-2}$). Immunostaining results from polytene chromosome squashes are shown on the left in each panel. Magnified insets are shown to the right of each figure, corresponding to the white boxes in the figures on the left. Scale bars are 5 µm in the figures and 2 µm in the insets. Insets are shown as RGB merge, with DAPI on the blue channel, γH2Av on the green channel, and various insulators on the red channel. Red and green channels are shown independently in grey scale and merged as magenta and green. Beneath the insets are linescans corresponding to the yellow lines in the merged insets. Linescan intensities were normalized by dividing each value by the maximum intensity recorded on each channel.

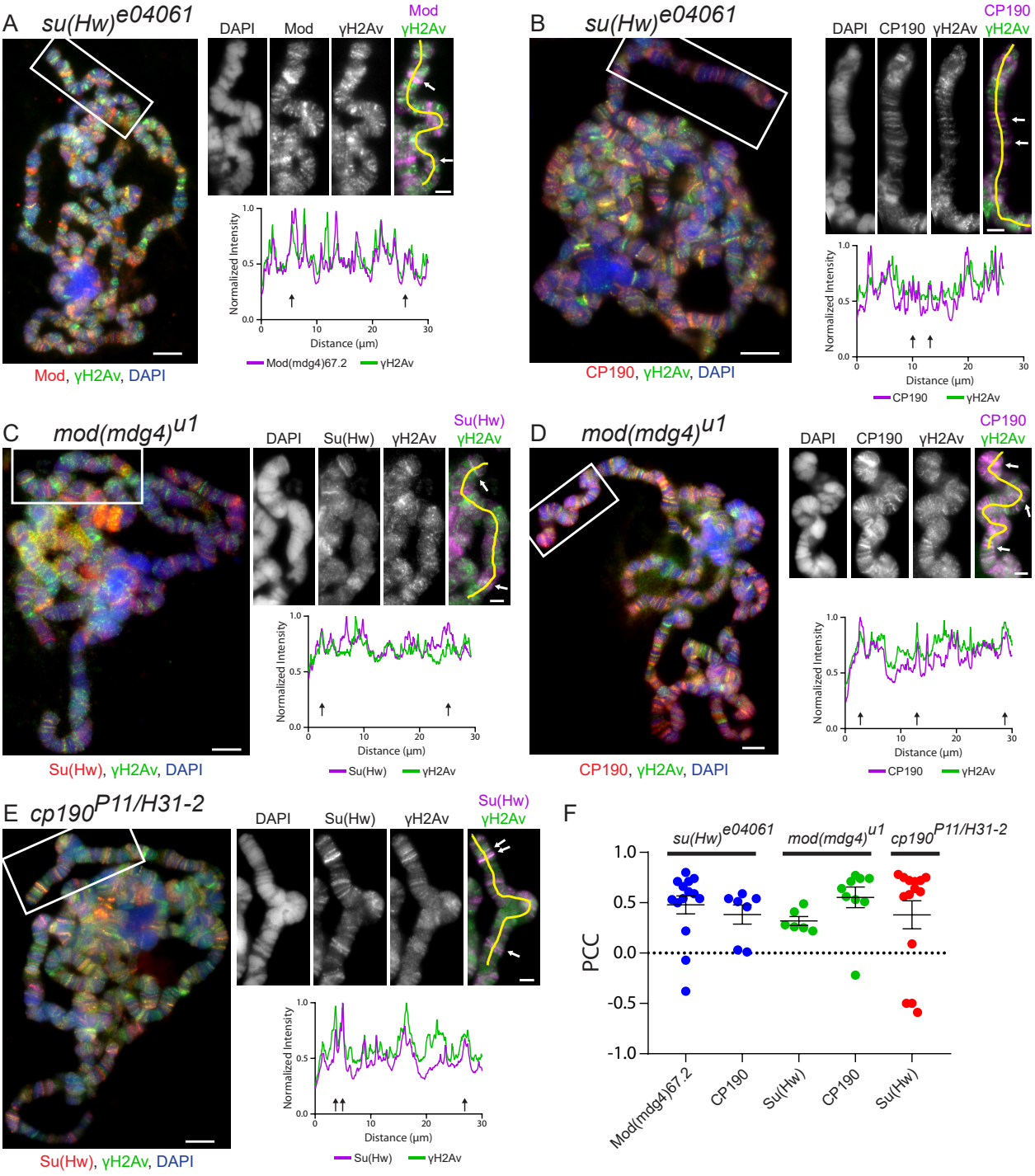


Figure 2.6 continued

We next asked if this role of γH2Av in *gypsy* insulator dynamics is limited to chromatin-bound insulators or if it extends to other cellular functions of insulators. To this end, S2 cells were exposed to osmotic stress to induce insulator body formation with the goal of determining if H2Av phosphorylation is required for insulator body formation or recovery after stress (Figure 2.7A). As a control to ensure okadaic acid alone does not induce body formation, cells were incubated in isotonic media with okadaic acid. These cells showed similarly low numbers of insulator bodies per cell as cells in untreated isotonic media (Figure 2.7B). Osmotic stress was introduced by increasing the salt concentration (Schoborg et al., 2013), resulting in the formation of many insulator bodies (Figure 2.7A, C). No significant difference was seen in the ratio of cells that contained insulator bodies when comparing okadaic acid-treated and -untreated samples (Figure 2.7B). Of particular interest, however, is the finding that after the osmotic stress media is replaced with isotonic media, cells treated with okadaic acid recover significantly less than cells not exposed to okadaic acid, retaining a greater number of insulator bodies throughout recovery (Figure 2.7B, C). These results put into context our finding that γH2Av is present in insulator bodies (Figure 2.3) and imply that phosphorylated H2Av must be maintained in the insulator body as part of the normal osmotic response. Preventing dephosphorylation of γH2Av by phosphatase inhibition prevents resolution of insulator bodies during isotonic recovery, suggesting this is an essential part of the mechanism governing the cellular response to osmotic stress. It remains unclear whether H2Av is phosphorylated after recruitment into insulator bodies or if chromatin-bound H2Av is phosphorylated in response to osmotic stress before localizing to insulator bodies. A third possibility is that the γH2Av observed in insulator bodies originates from H2Av that is already phosphorylated through normal metabolic activity. Further experiments will be necessary to discern which of these models is correct.

A

Treatment	Media	Number of cells	Cells with bodies (%)	Bodies/cell
OA-	Isotonic	650	1.2	0.02
	Hypertonic	510	91.4	5.73
	Recovery	495	2.2	0.04
OA+	Isotonic	596	0.5	0.01
	Hypertonic	487	88.9	4.63
	Recovery	596	63.1	3.11

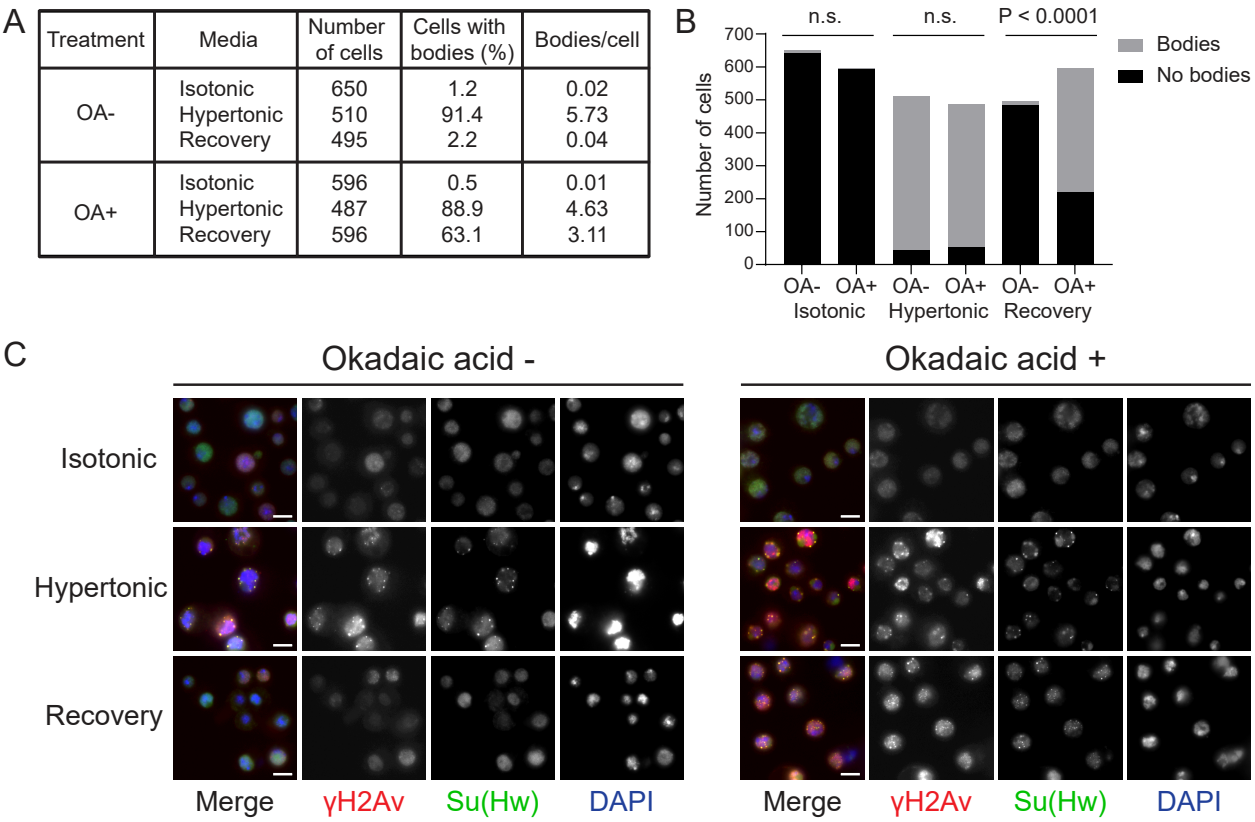


Figure 2.7. Phosphatase inhibition prevents recovery from insulator body formation after osmotic stress. A. Tabulated results from OA (okadaic acid) treatment in osmotic stress and recovery. **B.** Bar graph showing the number of cells displaying bodies (grey) and those not displaying bodies (black). OA- and OA+ treatments are shown for each osmotic condition. P-values were determined using Fisher's exact test. n. s. = not significant. **C.** Osmotic stress and recovery in the absence of okadaic acid (left) in the presence of okadaic acid (right). Representative images are shown of S2 cells in isotonic media, in hypertonic stress media, and recovering in isotonic media. Merged images are shown on the left, with each channel shown independently in greyscale. Scale bars represent 5 µm. Exposure times and contrast settings were kept constant between each sample.

H2Av Is Phosphorylated in *gypsy* Insulator Sites

While a clear correlation is seen between H2Av phosphorylation and insulator binding proteins genome-wide, it is unclear if these interactions are a feature of insulators or sites where insulator proteins bind independently as transcription factors. For example, outside of the canonical *gypsy* insulator, Su(Hw) binds many sites in the genome alone or in conjunction with either CP190 or Mod(mdg4) (Kuhn-Parnell et al., 2008, Bushey et al., 2009, Soshnev et al., 2012, Soshnev et al., 2013). We therefore asked whether or not H2Av phosphorylation is required specifically at *gypsy* insulator sites by looking at two classical examples, y^2 and ct^6 (Figure 2.9A). The former is an allele of the *yellow* (*y*) gene in which a *gypsy* insulator site inserted into the region between enhancers for expression in the wing and body of the fly and the promoter, cutting off contact between the enhancers and promoter upstream of the *yellow* gene promoter and resulting in lowered expression of the *yellow* gene and ultimately lighter pigmentation of the adult fly (Harrison *et al.*, 1989, Geyer and Corces, 1992). The latter example is an allele of the *cut* (*ct*) gene in which a *gypsy* insulator between the wing margin enhancer and *cut* promoter prevents expression of the *cut* gene in the developing wing. This decreases *cut* expression in cells of the wing margin, leading to a jagged appearance of the wing margin (Jack *et al.*, 1991, Kim *et al.*, 1996). As it has previously been demonstrated that a functional gypsy insulator complex composed of Su(Hw), Mod(mdg4)67.2, and CP190 is required for proper function of the insulator (Georgiev and Kozycina, 1996, Cai and Levine, 1997, Gause *et al.*, 2001, Ghosh *et al.*, 2001, Mongelard *et al.*, 2002), these sites serve as known examples of genomic loci associated with binding of each of these components.

To determine if H2Av is phosphorylated at known *gypsy* sites, immunostaining of the X polytene chromosomes of larvae carrying the y^2 and ct^6 alleles were performed in wild-type and mutant backgrounds. Notably, a strong colocalization was observed for phosphorylated H2Av and each *gypsy* insulator component (Su(Hw), Mod(mdg4)67.2, and CP190) at both y^2 and ct^6 sites (Figure 2.8A). Strikingly, this colocalization is lost in $mod(mdg4)^{u1}$ mutants (Figure 2.8B). Su(Hw) is still recruited to *gypsy*

insulator sites in *mod(mdg4)^{u1}* as expected based on previous reports of *mod(mdg4)* mutants (Ghosh *et al.*, 2001, Melnikova, Kostyuchenko*, et al.*, 2017); more significant, however, is the observation that γH2Av is no longer observed colocalizing with Su(Hw) at *y^{2}* or *ct^{6}*. Likewise, H2Av phosphorylation is no longer observed at either *y^{2}* or *ct^{6}* in the *su(Hw)^{e04061}* mutant background (Figure 2.8C). The lack of Mod(mdg4)67.2 at *y2* and *ct6* in the absence of Su(Hw) agrees with previous reports, which implicate Su(Hw) as necessary for recruitment of Mod(mdg4)67.2 to *gypsy* loci (Ghosh et al., 2001, Melnikova, Kostyuchenko, Molodina, et al., 2018), while the lack of γH2Av implies that either Su(Hw) is directly needed to maintain H2Av in a phosphorylated state or that a complete *gypsy* complex containing Mod(mdg4)67.2 is required. To expand on this question, polytene immunostaining from the *trans*-heterozygous *cp190$^{P11/H31-2}$* mutant was performed (Figure 2.8D). This showed a decrease in the amount of Su(Hw) present at *y^{2}* and *ct^{6}*, consistent with a previous report that found reductions in both Su(Hw) and Mod(mdg4)67.2 in the polytene chromatin of *cp190* mutants, (Melnikova, Kostyuchenko, Molodina, et al., 2018). Similar to the mutations in *su(Hw)* and *mod(mdg4)*, mutation of *cp190* also significantly reduced levels of H2Av phosphorylation at the two *gypsy* loci examined. All together, these results indicate that reduction of any of the canonical *gypsy* insulator components is sufficient to disrupt H2Av phosphorylation at these sites. This would argue against this relationship being limited to Su(Hw)-only sites and supports the notion that H2Av phosphorylation is either promoted or stabilized by interactions with intact *gypsy* insulator complexes.

H2Av Contributes to *gypsy* Insulator Function

Our earlier results strongly suggest a correlation between γH2Av and *gypsy* insulator components, including colocalization on polytene chromatin (Figures 3.1 and 3.8) and in insulator bodies (Figure 2.4). Some evidence for a functional relationship was found in the dissolution of insulator bodies (Figure 2.7) but it remained unclear if γH2Av plays any role in canonical insulator functions such as enhancer-blocking.

Based on the correlations described above between *gypsy* insulator proteins and γH2Av, we wondered whether or not mutation of *His2Av,* the sole H2A variant gene found in the *Drosophila* genome (van Daal et al., 1988), would affect *gypsy* insulator function. As the null mutation of *His2Av* is homozygous lethal at the third instar larval stage (van Daal and Elgin, 1992), we were precluded from observing how a complete lack of H2Av would affect the *yellow* and *cut* phenotypes seen in adults. We therefore set up a series of crosses to examine how adult animals that carried heterozygous mutations for both *His2Av* and *su(Hw)*.

The effects of these mutants on the ct^6 allele were measured by examining the wing margins. Wing margins in *Drosophila* contain mechanosensory bristles (Hartenstein and Posakony, 1989) that require expression of the *cut* gene for proper formation (Jack, 1985). Lack of *cut* expression results in decreased specification and differentiation of mechanosensory bristles and increased rates of cell death (Jack et al., 1991, Liu et al., 1991). The ct^6 phenotype is characterized by wings having an incomplete margin due to such defects, resulting in the nominal "cuts" in the wing which can be rescued to near wild type by mutations in *gypsy* insulator genes (Georgiev and Kozycina, 1996, Kim et al., 1996). Wing width was measured as a proxy for *cut* gene activity, as wings with the ct^6 phenotype are less wide due to the decreased cell proliferation associated with this phenotype. Width of the wing is calculated as the area divided by the feret diameter (a measure of length). Notably, flies that contained heterozygous mutations for both $His2Av^{810}$ and $su(Hw)^{e04061}$ displayed wider wings, while both single heterozygotes showed varying degrees of cuts in the margin (Figure 2.9B). To verify this finding, the null $su(Hw)^V$ allele was next tested in conjunction with $His2Av^{810}$. Consistent with the $His2Av^{810}/su(Hw)^{e04061}$ genotype, $His2Av^{810}/su(Hw)^V$ double heterozygotes had significantly wider wings than either single heterozygote (Figure 2.9B). This increased suppression of *gypsy* insulator phenotypes in *su(Hw)* heterozygous backgrounds implies that H2Av is involved in *gypsy* insulator function.

Figure 2.8. Phosphorylated H2Av is present at *gypsy* insulator sites. **A.** Colocalization between γH2Av and Su(Hw) (left), Mod(mdg4)67.2 (center), and CP190 (right) in a wild type y^2wct^6 background. **B.** Colocalization between γH2Av and Su(Hw) in a $mod(mdg4)^{u1}$ homozygous background. **C.** Colocalization between γH2Av and Mod(mdg4)67.2 in a $su(Hw)^{e04061}$ homozygous background. **D.** Colocalization between γH2Av and Su(Hw) in a $cp190^{P11/H31-2}$ *trans*-heterozygous background. Immunostaining results are shown of the X polytene chromosome from wandering third instar larvae in the y^2wct^6 background. Each panel shows an X chromosome, with the y^2 and ct^6 sites labelled and delineated with white boxes. Beneath these are insets showing the y^2 and ct^6 sites in detail. Insets are shown as RGB merge, with DAPI on the blue channel, γH2Av on the green channel, and various insulators on the red channel. Red and green channels are shown independently in grey scale and merged as magenta and green. Beneath the insets are linescans corresponding to the yellow lines in the merged insets. Arrows represent the approximate sites of each *gypsy* locus. Scale bars are 2 μm in the main figures and insets. Linescan intensities were normalized by dividing each value by the maximum intensity recorded on each channel.

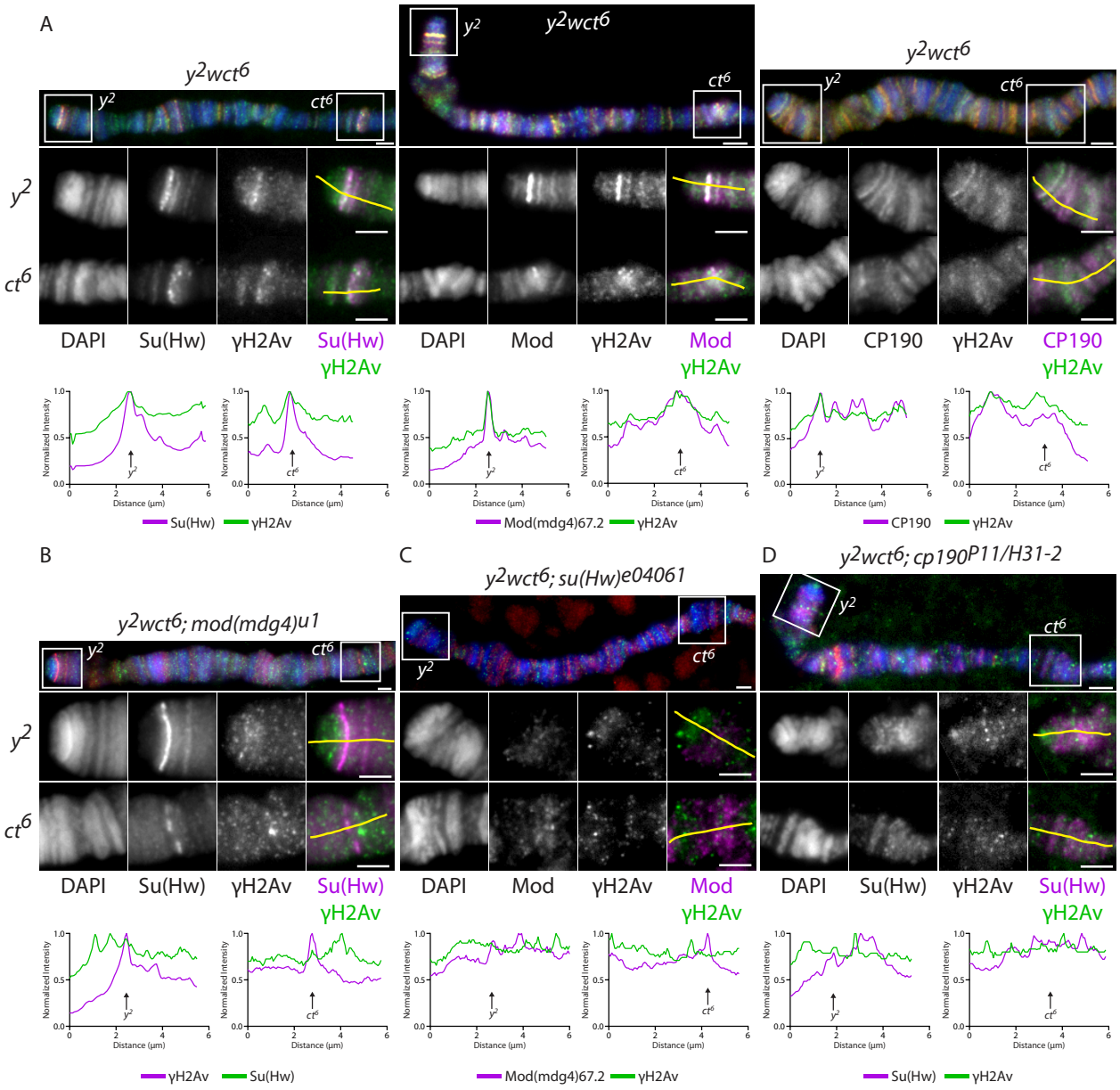


Figure 2.8 continued

In order to determine if this requirement for H2Av in *gypsy* insulator function is specific to the *cut* gene or if it is a general mechanism for *gypsy* insulators, we tested the effect of *His2Av* mutation on the y^2 phenotype. Effects of these mutations on the y^2 allele were tested by measuring the degree of pigmentation in the wings and in the darkened A5 tergite found in male flies. Heterozygous $HisAv^{810}$ or $su(Hw)^{e04061}$ mutations by themselves have little effect on expression of *yellow* in the abdomen (Figure 2.9C). In contrast to this, abdomens in the double heterozygous $His2Av^{810}/su(Hw)^{e04061}$ mutants were significantly darker than the single heterozygous mutants (Figure 2.9C). This implies a reduction in the enhancer-blocking capacity of the *gypsy* insertion upstream of *yellow* and suggests a functional role for H2Av in *gypsy* insulator function. In order to exclude the possibility that second-site mutations in the $su(Hw)^{e04061}$ background were influencing this rescue, we crossed the null $su(Hw)^{V}$ allele with the $His2Av^{810}$ mutant. Flies doubly heterozygous for $su(Hw)^{V}$ and $His2Av^{810}$ showed a statistically significant increase in pigmentation compared to the $His2Av^{810}$ heterozygote, but not the single $su(Hw)^{V}$ mutant (Figure 2.9C). This discrepancy between $su(Hw)^{e04061}$ and $su(Hw)^{V}$ may be due to mutation of the neighboring *RpII15* gene (an RNA Pol II subunit) in the $su(Hw)^{V}$ chromosome (Harrison et al., 1992), which may have an epistatic effect on this phenotype. Taken together, these findings represent the first evidence for the requirement of a histone protein in *Drosophila* insulator function and may hint at a mechanism for how insulators work. There is a correlation between the lack of a balancer chromosome and the rescues seen in this assay. The lack of a balancer is unlikely to be a causative factor in the rescues, as the TM6B and TM6C balancers present in the single heterozygotes carry the $ebony^1$ marker, which significantly increases the degree of pigmentation (Wittkopp *et al.*, 2002), and the single heterozygotes are lighter than the trans-heterozygotes.

γH2Av colocalizes with Su(Hw) at TAD boundaries

Next, given the previous observations indicating that γH2Av and Su(Hw) sites colocalize in polytene chromosomes, we asked whether the colocalization of both proteins is also supported at the molecular level by Chromatin Immunoprecipitation (ChIP) experiments. To answer this question, we used publicly available ChIP data for γH2Av and Su(Hw) from Kc167 cells (SRX1299942 SRA) (Li et al., 2016). We used SeqMiner to compare the two ChIP-seq datasets by heatmap analysis. The peak summits for γH2Av were taken as the reference coordinate for a heatmap and profile analysis comparing Su(Hw) and γH2Av distributions (Figure 2.10A). The profile of mean read densities for both proteins also shows a significant overlap between Su(Hw) and γH2Av peaks at γH2Av peaks flanked by 10,000 bp (Figure 2.10B). These results support our observation that the genomic distribution of Su(Hw) and γH2Av overlap in polytene chromosomes.

Because insulator proteins are frequently associated with the boundaries of Topologically Associating Domains (TADs), we next asked whether γH2Av is also enriched at TAD boundaries. To address this question, we used publicly available data and obtained a map of all *Drosophila* TADs as determined by Hi-C using *Drosophila* Kc167 cells (Ramirez et al., 2018). We used this data to generate a BED file consisting of 1,000 bp DNA fragments containing all TAD boundaries in the *Drosophila* genome flanked by 500 bp at both sites of the boundary. The 1 kb TAD boundary BED file was used as a reference coordinate for a heatmap comparing the density distribution of nucleosomes containing the histone variant H2Av, either homotypic (H2Av Hom) or heterotypic (H2Av Het), as well as the densities of γH2Av and Su(Hw) in the *Drosophila* genome (Figure 2.10C). The distribution of H2Av nucleosomes was obtained from a previous study (Weber et al., 2010). The heatmap analysis shows there is a strong association between the density distribution of H2Av nucleosomes and TAD boundaries (Figure 2.10C). Generally, we found homotypic H2Av nucleosomes are enriched at the boundaries, whereas heterotypic nucleosomes have a significant density drop at TAD boundaries.

Figure 2.9. H2Av contributes to *gypsy* insulator function. **A.** Illustration of the upstream regulatory elements found in the ct^6 and y^2 alleles. Gene coding sequences (purple) are regulated by coordinated contacts between enhancers (blue) and promoters (green). In each case, the *gypsy* retrotransposon (denoted with the thick black bar) has been inserted between a promoter and at least one enhancer. LTR = long terminal repeats, RT genes = retrotransposon genes (*gag*, *pol*, and *env*), IBS = insulator binding site, IBPs = insulator binding proteins (Su(Hw), Mod(mdg4)67.2, and CP190). When the IBS is bound by a complete insulator complex, it interrupts communication between the promoter and distal enhancers. In cut^6 this prevents expression of *cut* by the wing margin enhancer (En-wm), while in $yellow^2$ the insulator prevents expression of *yellow* directed by the wing enhancer (En-w) and the body enhancer (En-b) but not the bristle enhancer (En-br) between the *yellow* promoter and transcription start site. Genomic distances are not drawn to scale. **B.** The average length of wings along the feret axis was used as a metric for the *cut* phenotype. Wing area in mm^2 (yellow shaded area) was divided by feret diameter (red line). Examples of wings are displayed above their respective genotypes. **C.** y^2 phenotype scoring in the male abdomen. The illustration on the left shows the male abdomen with abdominal segments 3-6 labelled. A circular ROI (yellow circle) was sampled from the a5 tergite of each male to determine the degree of pigmentation. The graph depicts the mean pixel intensity from individual flies by genotype. Example pictures of abdomens are displayed above their respective genotypes. In B and C, Green dots represent *su(Hw)* heterozygotes, orange dots represent $His2Av^{810}$ heterozygotes arising from each cross, and red dots indicate flies doubly heterozygous for $His2Av^{810}$ and *su(Hw)*. Above each data set is the sample size and single letter statistical codes from an ANOVA performed with Dunnett's T3 multiple comparisons, with significant differences at $P \leq 0.05$.

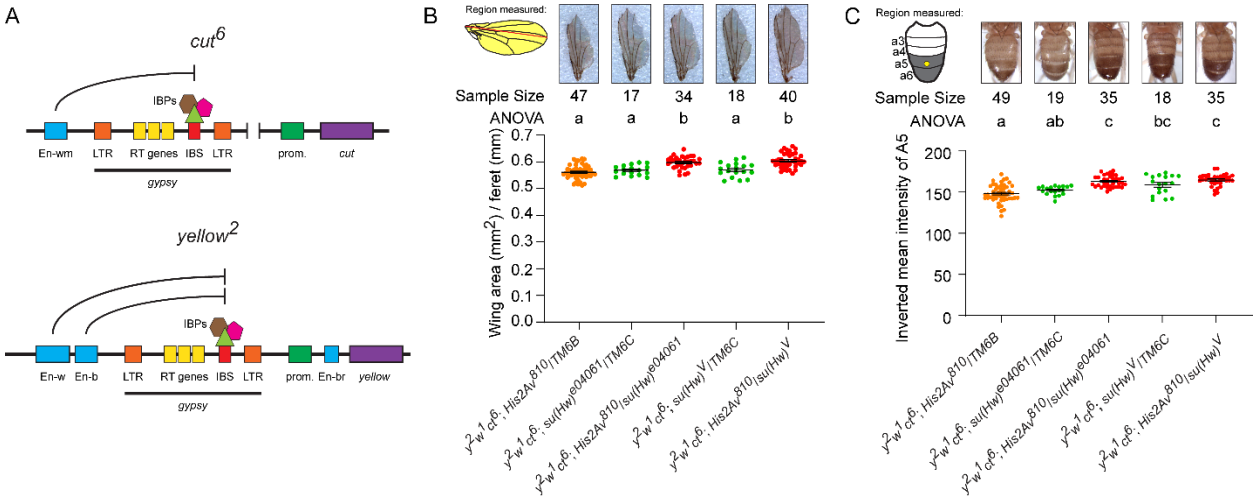


Figure 2.9 continued

Interestingly, enrichment in γH2Av and Su(Hw) is also observed at the TAD boundaries (Figure 2.10C). Signal enrichment can be grouped in two major clusters, where the most significant difference is the relative enrichment of Su(Hw) and γH2Av at the boundaries (Figure 2.10D, E). In cluster 2, heterotypic H2Av and γH2Av have similar enrichment levels through the DNA flanking the boundary. At the center of the boundary, however, is the homotypic instead of the heterotypic H2Av that has an enrichment similar to that of γH2Av, with both intensity profiles (H2Av Hom and γH2Av) significantly more elevated than in the flanking DNA (Figure 2.10E). Interestingly, Cluster 1 has the opposite pattern. In cluster 1, homotypic H2Av and γH2Av have similar enrichment densities through the DNA flanking the boundary and remain elevated at the boundary center. However, γH2Av and Su(Hw) intensities are similar and higher than that of the homotypic and heterotypic H2Av nucleosomes (Figure 2.10D).

The functional significance of the association of γH2Av with TAD boundaries is intriguing. Interestingly, we found that the association of γH2Av with TAD boundaries is very similar to that of Su(Hw) and other insulator proteins in that is found as an enriched peak. One such example of this is a TAD boundary that flanks a TAD containing the homeotic gene *Abdominal A* (*Abd-A*). Like other boundaries associated with the homeobox gene cluster (Postika *et al.*, 2018, Ozdemir and Gambetta, 2019), this boundary is enriched in the insulator proteins Su(Hw), Modifier of Mdg4, CP190, CTCF, and HIPP1. Here, we show this boundary is equally enriched in γH2Av (Figure 2.10F). Moreover, when observing the distribution of H2Av nucleosomes at this site, it appears that the γH2Av peak does not colocalize with a nucleosome, suggesting the possibility that γH2Av may be non-nucleosomal. In another example, two boundaries flank a TAD that contains the developmentally regulated pair rule gene *eve* (Figure 2.10G). Each boundary is enriched in γH2Av; however, in the left boundary the γH2Av peak overlaps at least partially with the nucleosomal H2Av, whereas in the right boundary the γH2Av peak seems to be non-nucleosomal as well. This particular boundary corresponds to the well characterized Homie insulator

(Fujioka et al., 2013). These findings show that the distribution of γH2Av in the *Drosophila* genome display all the properties of insulator proteins, suggesting that γH2Av may be required for insulator function.

Discussion

Our results have demonstrated a clear relationship between the phosphorylated histone variant γH2Av and chromatin insulator proteins. γH2Av colocalizes with Su(Hw) insulator complexes throughout the genome, and both are enriched at TAD boundaries. Disruption of insulator complex formation prevents stable phosphorylation of H2Av that can be overcome by phosphatase inhibition. Importantly, we provide evidence that this histone variant is involved in insulator activity, as dephosphorylation of γH2Av is necessary for dissolution of insulator bodies and reducing the genetic dose of H2Av in a sensitized *su(Hw)* heterozygous mutant background partially rescues *gypsy* insulator phenotypes.

Chromatin insulator proteins were initially characterized by their enhancer-blocking properties and their ability to prevent the spread of heterochromatin, and more recently by their role in large-scale genome organization (Harrison *et al.*, 1989, Geyer and Corces, 1992, Bell *et al.*, 1999, Bushey *et al.*, 2009). In addition to these canonical properties, however, our lab has uncovered roles of insulators in other aspects of cell metabolism including the osmotic stress response (Schoborg *et al.*, 2013) and genome stability (Hsu *et al.*, 2020). It is now established that mutation of the only insulator protein found in humans, CTCF, predisposes cells to cancer formation (Docquier *et al.*, 2005, Kemp *et al.*, 2014, Guo *et al.*, 2018) through increased rates of unrepaired DNA damage. Despite this knowledge, the mechanisms linking insulator activity to the maintenance of genome stability remain enigmatic. Here, we report a functional relationship between a *Drosophila* insulator and H2Av, the sole histone H2A variant in fruit flies. H2Av in *Drosophila* performs functions associated with both the mammalian histone variants H2AX and H2AZ (Baldi and Becker, 2013), and misregulation of H2Av in *Drosophila* is associated with severe

Figure 2.10. Phosphorylated H2Av associates with TAD boundaries. **A.** Heatmap comparing the intensity distributions of yH2Av and Su(Hw) using yH2Av peaks as reference. **B.** Mean read density profiles of yH2Av and Su(Hw) centered at yH2Av peaks. **C.** Heatmap comparing the intensity distributions of H2Av nucleosomes, yH2Av and Su(Hw) and Su(Hw) using TAD boundaries as a reference. **D.** and **E.** Mean read density profiles of two major clusters from heatmap on C, centered at TAD boundaries. **F.** Peak profile of Insulator proteins, including yH2Av and the H2Av nucleosome distribution at the left boundary of the *abd-A* TAD. **G.** Peak profile of Insulator proteins, including yH2Av and the H2Av nucleosome distribution at the Homie insulator flanking the pair rule gene *eve*. **H.** This model shows the interaction between *gypsy* insulator components and H2Av phosphorylation. We propose that binding of the Su(Hw) insulator complex promotes phosphorylation of neighboring H2Av. This stabilizes binding of the insulator complex and promotes spread of the H2Av phosphorylation mark through neighboring nucleosomes. (i.) Case in which Su(Hw) complexes interact with nucleosomal γH2Av. (ii.) Case in which Su(Hw) complexes interact with non-nucleosomal γH2Av. (iii.) Case in which Su(Hw) is absent. Phosphorylation of H2Av is significantly reduced. **I.** During osmotic stress, insulator complexes leave chromatin and form insulator bodies. These bodies contain γH2Av that must be dephosphorylated during recovery so that insulator proteins can return to their genomic binding sites.

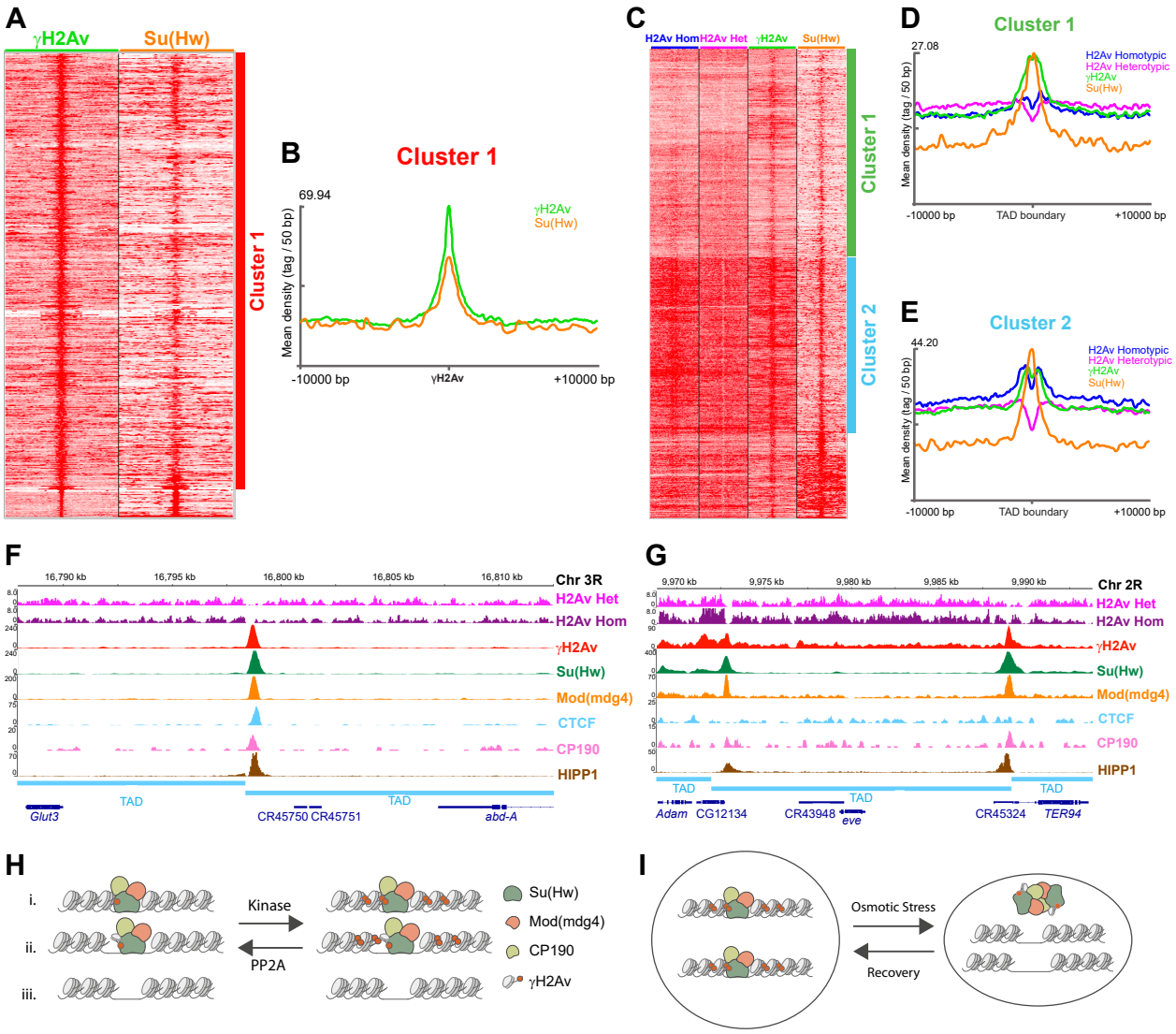


Figure 2.10 continued

developmental phenotypes including nuclear falling in embryos (Li *et al.*, 2014), the formation of necrotic tumors in the larval lymph gland (Grigorian *et al.*, 2017) and an inability to maintain stem cell populations in adult tissues (Morillo Prado *et al.*, 2013). Like H2AX, H2Av is phosphorylated in response to DNA double strand breaks (DSBs) and serves as a chromosomal mark to recruit DNA repair proteins (Madigan *et al.*, 2002, Joyce *et al.*, 2011).

Our initial experiments in *Drosophila* polytene chromosomes revealed a striking correlation between the binding sites of phosphorylated H2Av and insulator proteins at *gypsy* insulator sites (Figure 2.8) and at Su(Hw) sites elsewhere in the genome (Figures 3.1, 3.10). Importantly, this colocalization depends on having a complete and stable Su(Hw) insulator complex, as mutating any of the three core insulator components reduces the coincidence of γH2Av signals with the remaining insulator proteins (Figure 2.3). Some insight into the mechanism behind this phenomenon comes from experimental inhibition of PP2A, the phosphatase responsible for dephosphorylating γH2Av after resolution of double strand breaks (Merigliano *et al.*, 2017). We found that the amount of γH2Av in undamaged polytene chromosomes increases after PP2A inhibition. This was as expected due to the known role of PP2A in regulating H2Av phosphorylation. Surprisingly, the amount of Su(Hw) bound to the polytene chromosomes also significantly rose when tissues were treated with the PP2A inhibitor (Figure 2.5). This seems to imply that *gypsy* insulator complex formation or stability is driven at least in part by the phosphorylation state of H2Av, although we cannot rule out the potential impact that other PP2A substrates may have on insulator complexes. Indeed, we show that inhibition of PP2A rescues *gypsy* insulator complex formation in tissues missing one of the three core insulator binding proteins (Figure 2.6). This supports the notion that Su(Hw) insulators are stabilized by the presence of phosphorylated H2Av.

To further explore the relationship between insulator binding proteins and γH2Av, we performed immunostains on polytene chromosomes in the background of mutations in genes encoding for insulator

proteins. We observed significant reductions of γH2Av signal in *su(Hw)*^{e04061} and *cp190*$^{P11/H31-2}$ (Figure 2.2), suggesting a relationship between γH2Av and *gypsy* insulator components in terms of recruitment to the chromatin. Notably, the reduction of γH2Av in *su(Hw)*^{e04061} was more extreme than in other mutants. From this we postulate that the interaction between γH2Av and Su(Hw) insulator sites may be largely mediated through interactions with Su(Hw) itself, although interactions with Mod(mdg4)67.2 and CP190 may also contribute to the overall stability of the complex. A large fraction of Su(Hw) binding sites do not include Mod(mdg4)67.2 or CP190 based on chromatin immunoprecipitation data (Negre *et al.*, 2010). It will thus be informative for future experiments to determine whether or not the presence of H2Av or γH2Av is required for insulator activity or transcriptional regulation at other loci bound by Su(Hw).

Our results to this point showed numerous correlations between *gypsy* insulators and γH2Av in chromatin, but it remained unclear if there was a functional relationship. Therefore, our final round of experiments sought to determine if γH2Av influences insulator function. These experiments are limited by the lethality of adults H2Av homozygous mutant, but one key finding is the partial rescue of the *ct*^{6} phenotype in *su(Hw)*^{e04061}/*His2Av*^{810} double heterozygotes (Figure 2.9). Significant increases in pigmentation in the abdomens of male flies were also found in this genotype in the *y*^{2} background, and the *ct*^{6} phenotype rescue was replicated in the *su(Hw)*^{V}/*His2Av*^{810} background (Figure 2.9). This demonstrates that H2Av influences the activity of insulator complexes in multiple tissues and therefore could be considered an insulator protein itself.

Our findings point to a model in which *gypsy* insulator components and γH2Av stabilize each other in the chromatin (Figure 2.10H). Based on our results and the fact that Su(Hw) makes direct interactions with DNA while Mod(mdg4)67.2 and CP190 are recruited by interactions with Su(Hw) (Harrison *et al.*, 1993, Gdula *et al.*, 1996, Ghosh *et al.*, 2001, Pai *et al.*, 2004, Melnikova, Kostyuchenko*, et al.*, 2017), we propose that Su(Hw) is the main site of the interaction with γH2Av and that Mod(mdg4)67.2, and potentially CP190, stabilize this interaction. Further biochemical analysis will be required to determine if

γH2Av is in direct physical contact with Su(Hw) and, if so, which domains are the contact points between these proteins. Another possibility is an indirect association between γH2Av and Su(Hw), possibly via another yet unknown protein. Interactions with RNA may be another mechanism by which these proteins associate based on the recent finding that *Shep* RNA is required for *gypsy* insulator function (Chen *et al.*, 2019). Direct binding with Mod(mdg4)67.2 or CP190 cannot be ruled out either, though such interactions are likely to have less effect on γH2Av recruitment than that with Su(Hw), based on results from the ct^6 and y^2 phenotypic rescue experiment (Figure 2.9).

Our model also proposes that γH2Av localizes in insulator bodies that form as a result of osmotic stress (Figure 2.10I). The mechanism remains unknown with possibilities including disassembly of the complex and reassociation as nucleoplasmic bodies or the entire complex translocating from chromatin into insulator bodies. It is not yet clear, however, if the γH2Av found in insulator bodies comes from the same population as found in chromatin or if these proteins are recruited from the non-chromatin bound nucleoplasmic H2Av population.

An interaction between Su(Hw) and nucleosomes was recently reported in which *gypsy* insulators serve to position nucleosomes and establish regular nucleosome phasing (Baldi *et al.*, 2018). Our observations may relate to this finding if such Su(Hw)-based nucleosome positioning interactions depend on the presence of γH2Av. Another possibility is a potential relationship between contacts with *gyspy* insulator proteins and whether neighboring nucleosomes are heterotypic or homotypic for this histone (Weber *et al.*, 2010). Our ChIP-seq analysis shows enrichment for homotypic H2Av along with Su(Hw) and other insulator proteins at TAD borders (Figure 2.10). This raises the question of whether *gypsy* insulator proteins affect the composition of nearby nucleosomes, or conversely, if these insulator proteins are preferentially recruited to homotypic nucleosomes. It is also possible that H2Av is acting as an insulator protein outside of a nucleosome, as ChIP-seq peaks enriched for γH2Av and insulator proteins do not necessarily align to nucleosomes (Figure 2.10). While the mechanistic relationship between these groups

of proteins remains unknown, our data add to a growing consensus that interactions between histone proteins and insulator proteins are required for cellular homeostasis and maintenance of genome integrity.

Recent results from mammalian cell culture studies highlight an interaction between H2AZ, the histone variant associated with transcriptional regulation (Giaimo *et al.*, 2019), and CTCF, the sole insulator protein in mammals (Wen *et al.*, 2020). As *Drosophila* H2Av serves orthologous functions to both mammalian H2AZ and H2AX, our findings regarding insulators and the early DSB marker γH2Av may be relevant to human health as CTCF is frequently mutated in various cancers (Kemp *et al.*, 2014, Canela *et al.*, 2017, Guo *et al.*, 2018). Mutation of CTCF in *Drosophila* is associated with instability in ribosomal DNA found in the nucleolus (Guerrero and Maggert, 2011). If the relationship between insulator proteins and the DNA damage repair pathway is conserved from flies to humans, testing for interdependence of these components may provide clinically useful information. Indeed, it was recently described that CTCF sets the boundaries for phosphorylated H2AX spreading in human cell culture (Natale *et al.*, 2017) and that CTCF and γH2AX are both recruited to sites of DSBs in mouse embryonic fibroblasts (MEFs) (Lang *et al.*, 2017). Unlike our findings with Su(Hw), CTCF depletion in MEFs increases H2AX phosphorylation but, similar to Su(Hw) depletion in flies, induces genome instability (Lang *et al.*, 2017), possibly indicating a different mechanism linking CTCF to H2AX phosphorylation. The link between DNA damage repair and insulator proteins is further corroborated by the recent finding that TAD boundary strength and CTCF insulation strength both increase in an ATM-dependent manner in human cell culture after X-ray-induced DNA damage (Sanders *et al.*, 2020).

Other questions generated from our results here will need to be addressed in future experiments. One example is determining how H2Av or its phosphorylated form affect other phenotypes associated with lack of *su(Hw)* expression. Importantly, *su(Hw)* has been shown to regulate genome stability (Lankenau *et al.*, 2000) and we recently described the presence of chromosomal aberrations in actively

dividing neuroblasts of *su(Hw)*-deficient larvae (Hsu *et al.*, 2020). How these aberrations arise is still unclear, however, our finding here that *su(Hw)* homozygotes show significantly less phosphorylated H2Av may shed light on a mechanism. Cells that are unable to phosphorylate H2Av in response to DNA damage may be unable to recruit essential DNA damage repair proteins to the site of DSBs. If left alone, these unrepaired DSBs become obvious candidates for the source of the chromosomal aberrations seen in larval neuroblasts. Further studies will address this question, along with examining the role of Su(Hw) in repair of induced DNA damage, as well as the role of γH2Av in boundary function and genome organization. Our results so far provide a foundation for understanding how the interplay between chromatin insulators and histones influences gene regulation and genome stability.

Acknowledgements

We would like to thank former members of the Labrador lab, including Dr. Emily Stow, for collaboration and discussion. We thank Dr. Rachel Patton McCord for critical review of the manuscript. Stocks obtained from the Bloomington *Drosophila* Stock Center (NIH P40OD018537) were used in this study. S2 cell culture was obtained from the *Drosophila* Genomics Resource Center (NIH 2P40OD010949).

Chapter III: Insulators and DNA damage

Abstract

Genome architecture is regulated by chromatin insulator proteins, and misregulation of insulator function is associated with genome instability caused by defects in the DNA damage response. Indeed, mutations of the sole insulator protein in humans, CTCF, are carcinogenic. Here, we demonstrate roles for the Su(Hw) chromatin insulator complex in the DNA damage response in *Drosophila melanogaster*. Lack of Su(Hw) results in chromosomal breaks in mitotic larval neuroblasts. Su(Hw) and Mod(mdg4)67.2 immunostaining signals increase on polytene chromatin in response to UV irradiation, and Su(Hw) is necessary for both the increased Mod(mdg4)67.2 and H2Av phosphorylation in response to UV treatment. Su(Hw) is also necessary for H2Av phosphorylation in polytene chromatin in response to X-ray irradiation, although Su(Hw) is not needed for the response to UV or X-rays in neurons, where Su(Hw) is not normally expressed. Mutation of the ATR/*mei-41* and ATM/*tefu* DNA damage response kinases increases Su(Hw) binding to polytene chromatin under native conditions but prevents the increase of Su(Hw) chromatin binding in response to UV irradiation. These findings support a critical role for the Su(Hw) insulator complex in the DNA damage response through the regulation of H2Av phosphorylation.

Introduction

Chromatin insulators help mitigate the response to DNA damage in human cells and previous work by our lab characterized the relationship between the phosphorylated form of the H2A variant in *Drosophila*, γH2Av, and insulator proteins. Our study revealed a close association between Su(Hw) insulator proteins and γH2Av throughout the genome by a combination of immunostaining and ChIP-seq analysis of publically available datasets (Simmons *et al.*, 2021). Mutation of any component of the Su(Hw) insulator complex was enough to disrupt the interaction of this complex with γH2Av, and *su(Hw)* mutants displayed significantly less γH2Av in polytene chromatin than wild type. The association between insulator proteins

and γH2Av was strengthened by treatment with an inhibitor of protein phosphatase 2A (PP2A). We also show that γH2Av is a component of insulator bodies that form during osmotic stress and that recovery of the bodies after stress can be prevented by inhibition of PP2A (Simmons *et al.*, 2021). Mutation of *His2Av* suppressed the ct^6 *gypsy* phenotype in a sensitized *su(Hw)* heterozygous background, demonstrating that H2Av and Su(Hw) function in the same developmental pathway in the wing. Several questions were still left after these experiments, including which kinases might promote this interaction and how lack of H2Av might affect insulator protein recruitment to chromatin.

Methods and Materials

Fly stocks and husbandry

All stocks were maintained on a standard cornmeal agar fly food medium supplemented with yeast at 20°C; crosses were carried out at 25°C. The following stocks are maintained in our lab and were originally obtained from Dr. Victor Corces (Emory University): w^{1118}; $su(Hw)^{V}$/*TM6B*, Tb^{1}. The stock w^{1118}; PBac(RB)$su(Hw)^{e04061}$/*TM6B*, Tb^{1} was obtained from the Bloomington *Drosophila* stock center (BDSC: 18224). These remaining stocks were provided by our lab: OR, $y^{2}w^{1}ct^{6}$; PBac(RB)$su(Hw)^{e04061}$/*TM6B*, Tb^{1} (derived from BDSC: 18224).

Antibodies

A rabbit polyclonal IgG antibody against Su(Hw) was previously generated by our lab (Wallace et al., 2010, Schoborg et al., 2013). Antibody against the phosphorylated form of H2Av (UNC93-5.2.1) (Lake et al., 2013) was obtained from the Developmental Studies Hybridoma Bank, created by the NICHD of the NIH and maintained at The University of Iowa, Department of Biology, Iowa City, IA 52242. These antibodies were all diluted 1:1 in glycerol (Fisher Scientific, BP229-1, lot 020133) and used at a final dilution of 1:200. Secondary antibodies were all diluted 1:1 in glycerol and used at a final dilution of 1:200. The following

secondary antibodies were used in this study: Alexa Fluor 594 goat anti-rabbit (Invitrogen, A-111037, lot 2079421), Alexa Fluor 488 donkey anti-rabbit (Invitrogen, A-21206, lot 1834802), and Alexa Fluor 488 goat anti-mouse (Invitrogen, A-11001, lot 1858182), and a Texas Red anti-mouse (Jackson Laboratories).

Immunostaining of larval tissues

Wandering third instar larvae were dissected in PBS. Tissues were immediately placed into fixative (4%, para-formaldehyde (Alfa Aesar, 43368, lot N13E011), 50% glacial acetic acid (Fisher Scientific, A38-212, lot 172788)) on a coverslip for one minute. Samples were squashed by lowering a slide on top of the sample then turning it over, placing it between sheets of blotting paper, and hitting the coverslip firmly with a small rubber mallet. Slides were dipped in liquid nitrogen, coverslips were removed, and samples were incubated in blocking solution (3% powdered nonfat milk in PBS + 0.1% IGEPAL CA-630 (Sigma-Aldrich, 18896, lot 1043)) for 10 minutes at room temperature. The slides were dried and incubated with primary antibodies overnight at 4°C in a box humidified with wet paper towels. The next day, slides were washed twice in PBS + 0.1% IGEPAL CA-630 before incubation with secondary antibodies for three hours in the dark at room temperature. Slides were washed twice in PBS + 0.1% IGEPAL CA-630, treated with DAPI solution of 0.5 µg/mL (ThermoFisher, D1306) for one minute, and washed one more time in PBS alone.

Samples were mounted with Vectashield antifade mounting medium (Vector Laboratories, H-1000, lot ZF0409) and coverslips were sealed with clear nail polish. All microscopy for immunostaining was performed on a wide-field epifluorescent microscope (DM6000 B; Leica Microsystems) equipped with a 100X (NA 1.35) oil immersion objective and a charge-coupled device camera (ORCA-ER; Hamamatsu Photonics). Image acquisition was performed using SimplePCI (v6.6; Hamamatsu Photonics). Image manipulation was performed in FIJI (Schindelin et al., 2012); all contrast adjustments are linear. Images were further processed in Adobe Photoshop CS5 Extended, Version 12.0 x64. Figures were assembled in

Adobe Illustrator CS5, Version 15.0.0. Statistical analyses were performed in GraphPad Prism version 8.0.0 (224) (GraphPad Software, San Diego, CA).

Fluorescence intensity and colocalization analysis

Images were analyzed for the amount of each protein (i.e. the intensity of each channel) using a macro script in FIJI (Schindelin et al., 2012). The DAPI channel was used to automatically generate non-biased ROIs for each cell, which were then manually curated for extra precision. A rolling-ball background subtraction algorithm was used for all images. Intensity measurements were made using the measure function. Numerous genomic images were collected from each sample. All acquisition parameters were kept constant between slides within each experiment.

Chromosomal aberration (CAB) assay

Wandering third instar larvae were selected and quickly dissected in PBS to obtain the brain with ventral nerve cord attached. Brains were incubated in 0.5% sodium citrate, pH 6.00, for 10 minutes. Tissues were fixed in 4% paraformaldehyde for 1 minute. Tissues were squashed between a slide and a coverslip before DAPI staining. To determine the frequency of metaphasic cells that show CABs in larval brains, pictures were taken of fifty fields of view that contained at least one metaphasic cell. Each metaphasic cell was scored manually for the presence of CABs based on DAPI staining.

Western blotting

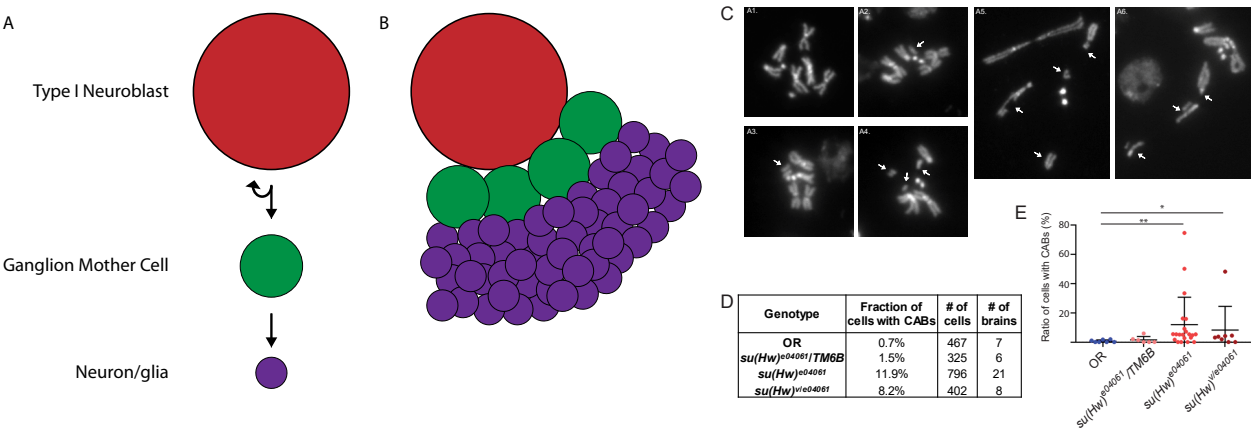
Tissues were dissected from wandering third instar larvae in 1X PBS. Tissues were collected in RIPA buffer (150 mM NaCl, 1% NP-40, 0.5% sodium deoxycholate, 0.1% SDS, 50 mM Tris-HCl, pH 8.0) supplemented with protease inhibitor (A32953, Thermo Scientific) and a phosphatase inhibitor (A32957, Thermo Scientific). Samples were homogenized in a 500 µL PCR tube with a motorized pestle, mixed with 5X

loading buffer (0.5 M Tris-HCl, pH6.8, 5% SDS, 0.0125% bromophenol blue, 12.5% β-mercaptoethanol, 50% glycerol) and 15% per volume β-mercaptoethanol, and boiled for 10 minutes. Protein samples were separated on 8% polyacrylamide gels and transferred onto 0.45 µm PVDF membranes. Membranes were blocked in a solution of 20% Odyssey Blocking Buffer (LI-COR, 927-50000) in TBS at room temperature for one hour. Membranes were incubated in primary antibodies diluted in TBST at 4 °C overnight. Primary antibodies used in these western blots include the mouse α-γH2Av (1:5,000), our rabbit polyclonal α-H2Av antibody (1:500). Next, membranes were washed four times in TBST, 5 minutes each wash. Membranes were then incubated in secondary antibodies diluted in TBST at room temperature for one hour. Secondary antibodies used in these western blots include Goat α-rabbit 680 RD (1:10,000) and Donkey α-mouse 800 CW (1:10,000). Membranes were washed four times in TBST followed by two washes in TBS, 5 minutes each wash. Blots were imaged on an Odyssey CLx scanner (LI-COR). Image files were manipulated in FIJI for analysis and presentation (Schindelin *et al.*, 2012).

Results

Mutation of *su(Hw)* is associated with chromosomal aberrations (CABs)

Based on previous results demonstrating a relationship between Su(Hw) and DNA damage (Lankenau *et al.*, 2000, Hsu *et al.*, 2020), we sought to determine the effect of *su(Hw)* null mutation on genome integrity. One common method used to assay repair of double strand breaks is by karyotyping of mitotic chromosomes from actively dividing neuroblast cells in the larval brain (Gatti and Goldberg, 1991). Neuroblasts are stem cells in the central nervous system of *Drosophila* that divide to give rise to a copy of itself alongside a more differentiated cell such as the ganglion mother cell, which later divides to generate terminally differentiated neurons and glia (Figure 3.1A). Using this assay we found that mutation of *su(Hw)* is associated with the presence of chromosomal aberrations (Figure 3.1 C-E). This was true for both $su(Hw)^{e04061}$ homozygotes and for $su(Hw)^{V/e04061}$ trans-heterozygotes (Figure 3.1 D, E) and supported



Genotype	Fraction of cells with CABs	# of cells	# of brains
OR	0.7%	467	7
su(Hw)^{e04061}/TM6B	1.5%	325	6
su(Hw)^{e04061}	11.9%	796	21
su(Hw)$^{v/e04061}$	8.2%	402	8

Figure 3.1. Mutation of *su(Hw)* is associated with chromosomal aberrations. A. Cartoon illustrating the developmental pathway of Type I neuroblasts in the larval central nervous system. **B.** Illustration of clusters of central nervous system cells derived from the same neuroblast. **C.** Examples of wild type chromosomes (A1, labelled with chromosome numbers) and those with chromosomal aberrations (A2-A6). Chromatid deletions (A2) and isochromatid deletions (A3) are frequently found in *su(Hw)* mutant backgrounds. (A4-A6) Genomes showing multiple CABs per cell. White arrows denote the sites of chromosomal breaks. **D, E.** The fraction of cells showing CABs from each brain was tabulated and plotted according to genotype. A significant frequency of chromosomal aberrations is seen in *su(Hw)^{e04061}* homozygotes and *su(Hw)$^{e04061/v}$* trans-heterozygotes but not for wild-type or *su(Hw)^{e04061}* heterozygotes. Error bars represent one standard error. * $P < 0.05$, ** $P < 0.01$.

other findings from our lab that demonstrate a role for Su(Hw) in maintaining genome integrity (Hsu *et al.*, 2020).

Polytene chromosomes require Su(Hw) to respond to DNA damage

In order to determine whether the interaction between chromatin insulator proteins and H2Av is related to the histone variant's role in the DNA damage response, third instar larvae were treated with UV irradiation and allowed three hours to recovery. Immunostaining of salivary gland polytene chromosomes revealed a significant increase in the amount of H2Av phosphorylation in the wild type OR strain after UV treatment when compared to the unexposed control (Figure 3.2 C, D), indicating the presence of DNA damage. Additionally, the immunostaining intensity of Su(Hw) protein on polytene chromatin increased significantly after UV irradiation of wild type larvae (Figure 3.2 C, D). This finding was not replicated in diploid cells in the larval brain that express little *su(Hw)*, however, where no significant increase in Su(Hw) signal was seen despite increased H2Av phosphorylation after UV treatment (Figure 3.2 A, B), suggesting this response is not conserved between the specialized polytene cells and diploid neuronal cells that do not typically express much Su(Hw).

The level of Su(Hw) protein on polytene chromatin was significantly decreased in the $su(Hw)^{e04061}$ mutant larvae compared to the wild type, as was the level of Mod(mdg4)67.2, which depends on Su(Hw) for recruitment to chromatin (Figure 3.3 A,B). Like Su(Hw), Mod(mdg4)67.2 levels increase significantly in polytene chromosomes in response to UV irradiation (Figure 3.3 A,B). This increase in Mod(mdg4)67.2 is dependent on Su(Hw), as no significant change in Mod(mdg4)67.2 levels is seen in the $su(Hw)^{e04061}$ mutant after UV treatment (Figure 3.3 A,B). More significantly, the increase in H2Av phosphorylation that occurs in wild type polytene chromosomes in response to UV irradiation is abolished in the $su(Hw)^{e04061}$ mutant (Figure 3.3 A,B), hinting at a mechanism in which Su(Hw) is required for H2Av phosphorylation upon DNA damage.

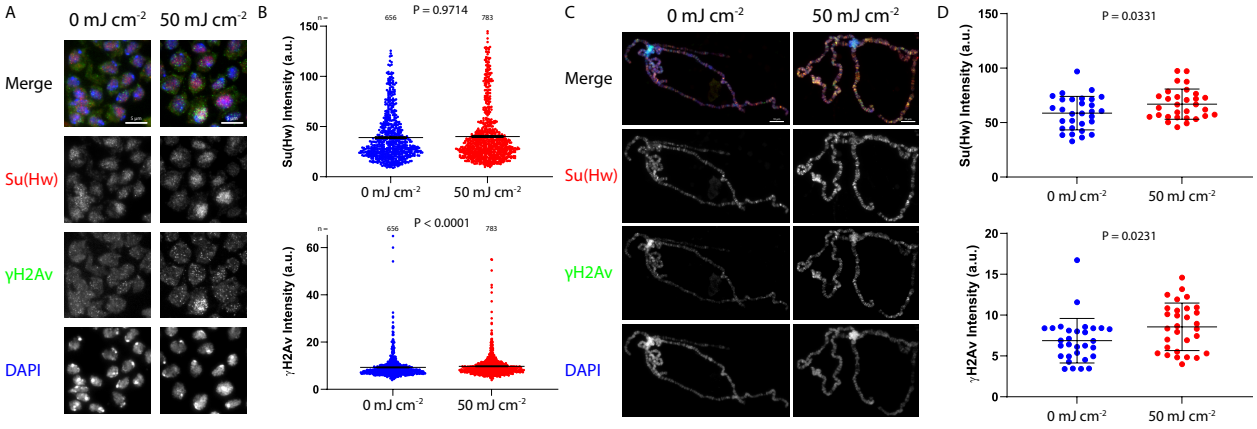


Figure 3.2. Su(Hw) and H2Av phosphorylation increase in polytene chromatin in response to UV irradiation. A. Immunostaining results for Su(Hw) and γH2Av antibodies in neural cells with and without UV treatment. The scale bars are 5 µm each. **B.** Fluorescent intensities of the Su(Hw) and γH2Av antibody signals in neural cells. P-values were determined using unpaired ANOVA with Dunn's multiple comparison test. **C.** Immunostaining results for Su(Hw) and γH2Av antibodies in polytene chromatin with and without UV treatment. The scale bars are 10 µm each. **D.** Fluorescent intensities of the Su(Hw) and γH2Av antibody signals in polytene chromatin. Each dot in B and D represents a single cellular genome. P-values were determined using unpaired Welch's T-tests.

To determine if Su(Hw) is involved in the cellular response to ionizing radiation, third instar larvae were subjected to a 10 Gy dose of X-rays and allowed to recover for four hours. Immunostaining of diploid cells from the larval brain revealed a significantly lower degree of H2Av phosphorylation in the unexposed *su(Hw)^{e04061}* control as compared to the unexposed wild type control (Figure 3.4 A, B), a finding consistent with previous results in polytene chromatin (Figure 2.2). Upon X-ray irradiation, phosphorylated H2Av immunostaining levels increased significantly in both the wild type larvae and the *su(Hw)^{e04061}* mutant (Figure 3.4 A, B). Likewise, western blotting of larval brains demonstrates a similar degree of H2Av phosphorylation upon X-ray treatment in the wild type and *su(Hw)^{e04061}* mutant larvae (Figure 3.4 C). Immunostaining reveals a near complete absence of Su(Hw) in the *su(Hw)^{e04061}* mutant, and there is no change in Su(Hw) staining levels in wild type after X-ray irradiation (Figure 3.4 A, B). These findings suggest that Su(Hw) is not necessary for H2Av phosphorylation in neuronal cells in response to ionizing radiation. Immunostaining in polytene chromosomes shows the expected pattern for Su(Hw), with significantly lower levels in *su(Hw)^{e04061}* mutants compared to the wild type control (Figure 3.4 D, E). Like diploid cells, the level of nuclear Su(Hw) does not change in polytene chromosomes after X-ray treatment (Figure 3.4 D, E). As expected, the level of H2Av phosphorylation increases significantly in polytenes after X-ray treatment (Figure 3.4 D, E). Unlike diploid cells, however, this response is inhibited in *su(Hw)^{e04061}* mutants, which show little γH2Av after irradiation (Figure 3.4 D, E). This is similar to the response seen after UV irradiation in the *su(Hw)^{e04061}* mutants, hinting at a mechanism in which Su(Hw) is required for H2Av phosphorylation upon various forms of double strand break formation in polytene cells.

Simultaneous mutation of ATR and ATM disrupts Su(Hw) binding dynamics on polytene chromatin

Based on our previous results, phosphorylation of H2Av stabilizes insulator protein complexes in polytene chromatin. Several kinases have been reported to phosphorylate H2Av, with the *Drosophila* homologs for ATR (*mei-41*) and ATM (*tefu*) being the key examples (Joyce *et al.*, 2011). We therefore sought to

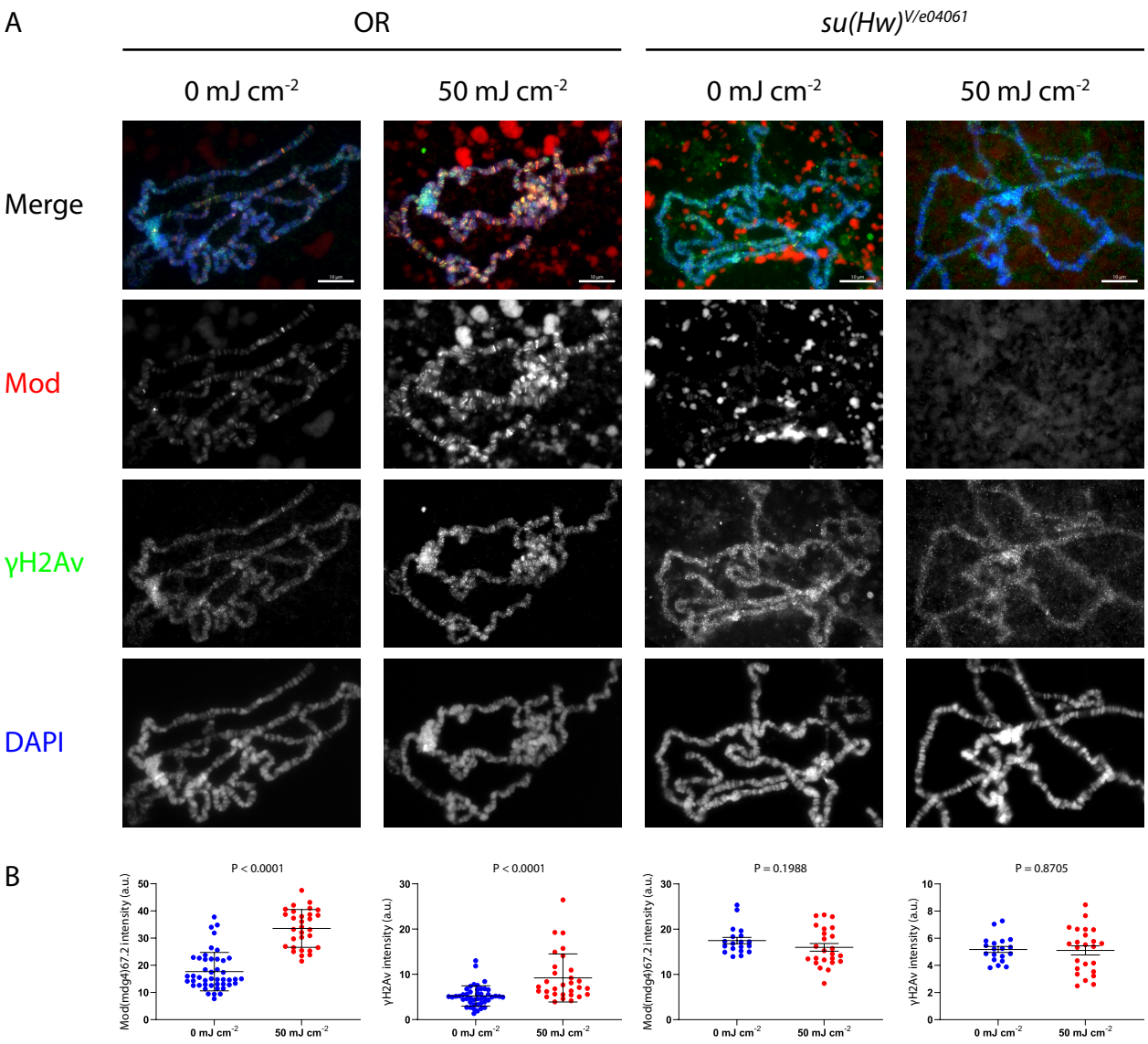


Figure 3.3. Su(Hw) is necessary for H2Av phosphorylation in polytene chromatin after UV irradiation. A. Immunostaining results for Mod(mdg4)67.2 (abbreviated as Mod) and γH2Av antibodies on polytene chromosomes with and without UV treatment. The scale bars are 10 µm each. **B.** Fluorescent intensities of the Mod(mdg4)67.2 and γH2Av antibody signals. Each dot represents a single polytene genome. P-values were determined using unpaired Welch's T-tests.

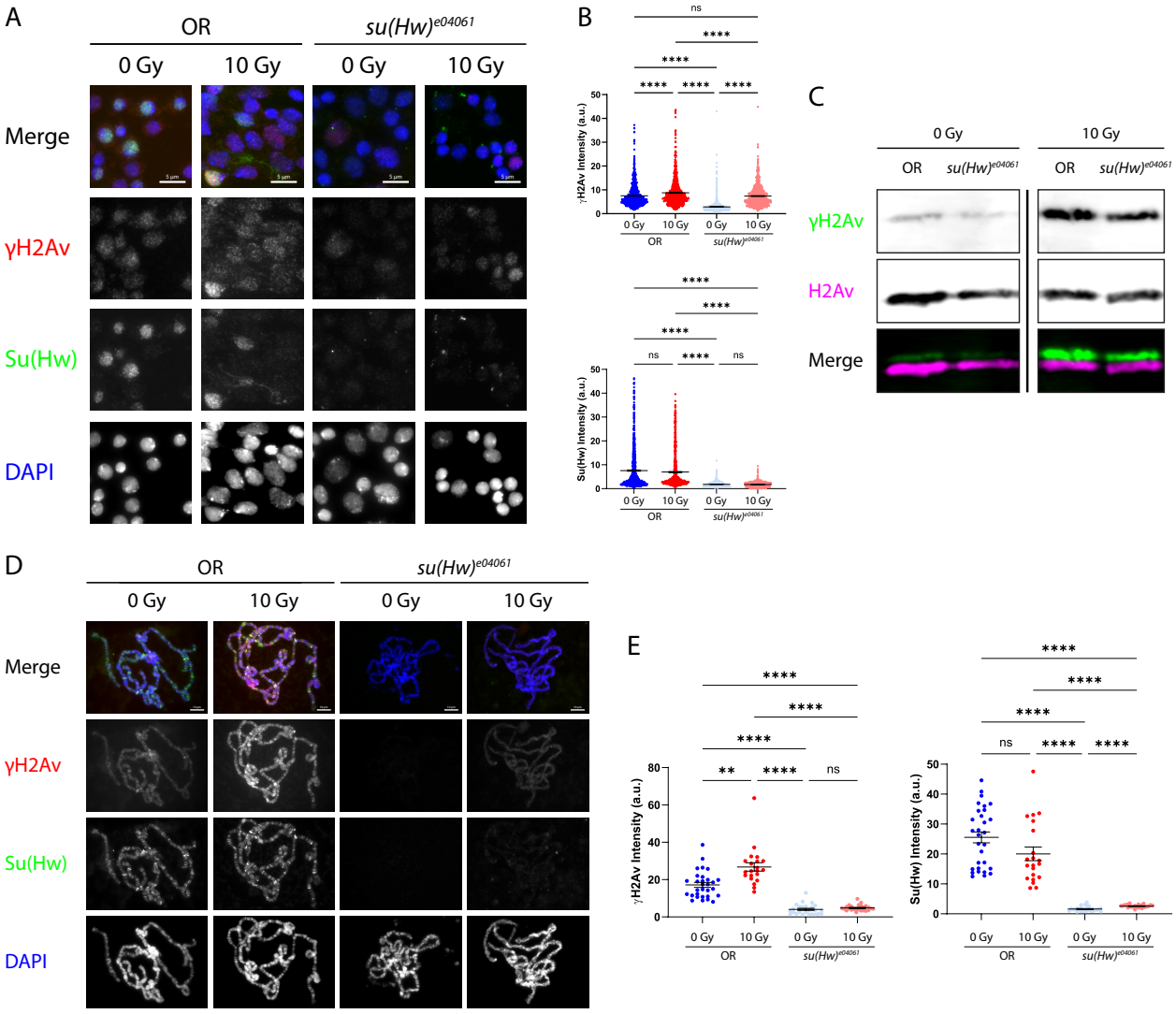


Figure 3.4. Su(Hw) is necessary for the H2Av phosphorylation in polytene chromatin after X-ray irradiation. A. Immunostaining results for Su(Hw) and γH2Av antibodies in neural cells with and without UV treatment. The scale bars are 5 μm each. **B.** Fluorescent intensities of the Su(Hw) and γH2Av antibody signals. P-values were determined using unpaired ANOVA with Dunn's multiple comparison test. **C.** Western blotting results for central nervous systems from control and X-ray irradiated larvae. **D.** Immunostaining results for Su(Hw) and γH2Av antibodies in polytene chromatin with and without UV treatment. The scale bars are 5 μm each. **E.** Fluorescent intensities of the Su(Hw) and γH2Av antibody signals. P-values were determined using unpaired ANOVA with Dunnett's T3 multiple comparison test. Each dot in B and E represents a single polytene genome. ** P < 0.01, **** P < 0.0001.

determine the effect of mutation of each of these kinases by immunostaining polytene chromatin for Su(Hw). We found no difference in the amount of Su(Hw) bound to chromatin in either single mutant (*mei-41*^{D5} and *tefu*$^{atm-3}$); however, there was a significant increase in the amount of Su(Hw) in the double mutant (Figure 3.5 A, B). In addition, we measured the effect of these mutations on H2Av phosphorylation in polytene chromatin. We found a significant increase in H2Av phosphorylation in the ATR/*mei-41*^{D5} mutant but not the ATM/*tefu*$^{atm-3}$ mutant (Figure 3.5 A, B). The double mutant also showed significantly more H2Av phosphorylation than wild type, though there was no difference between the double mutant and the ATR/*mei-41* single mutant, suggesting the difference is due to the *mei-41* mutation alone (Figure 3.5 A, B).

Due to our data showing increased Su(Hw) binding in polytene chromosomes in the double mutant (Figure 3.5) and after UV irradiation (Figure 3.2), we questioned what the response to UV irradiation would be in these mutants. Su(Hw) immunostaining intensity increased after UV treatment in the ATR/*mei-41*^{D5} mutant but not the ATR/*mei-41*^{D5} ATM/*tefu*$^{atm-3}$ double mutant (Figure 3.6 A, B). The lack of response in the double mutant may be due to natively high levels of Su(Hw) observed in the strain (Figure 3.5 A, B). H2Av phosphorylation increased in response to UV irradiation in both the ATR/*mei-41*^{D5} mutant but not the ATR/*mei-41*^{D5} ATM/*tefu*$^{atm-3}$ double mutant (Figure 3.6 A, B), suggesting one or more other kinases may be acting redundantly with ATR and ATM in the UV response.

Discussion

Chromatin insulators play an essential role in setting up and maintaining genome architecture during animal development by establishing long-distance interactions. These interactions help preserve the integrity of the genome against the threat of genotoxic stress, and chromatin insulators actively respond to DNA damage in higher eukaryotes. Here, we have demonstrated that the Su(Hw) insulator complex is involved in the DNA damage response in multiple cell types in *Drosophila* larvae. In addition to the

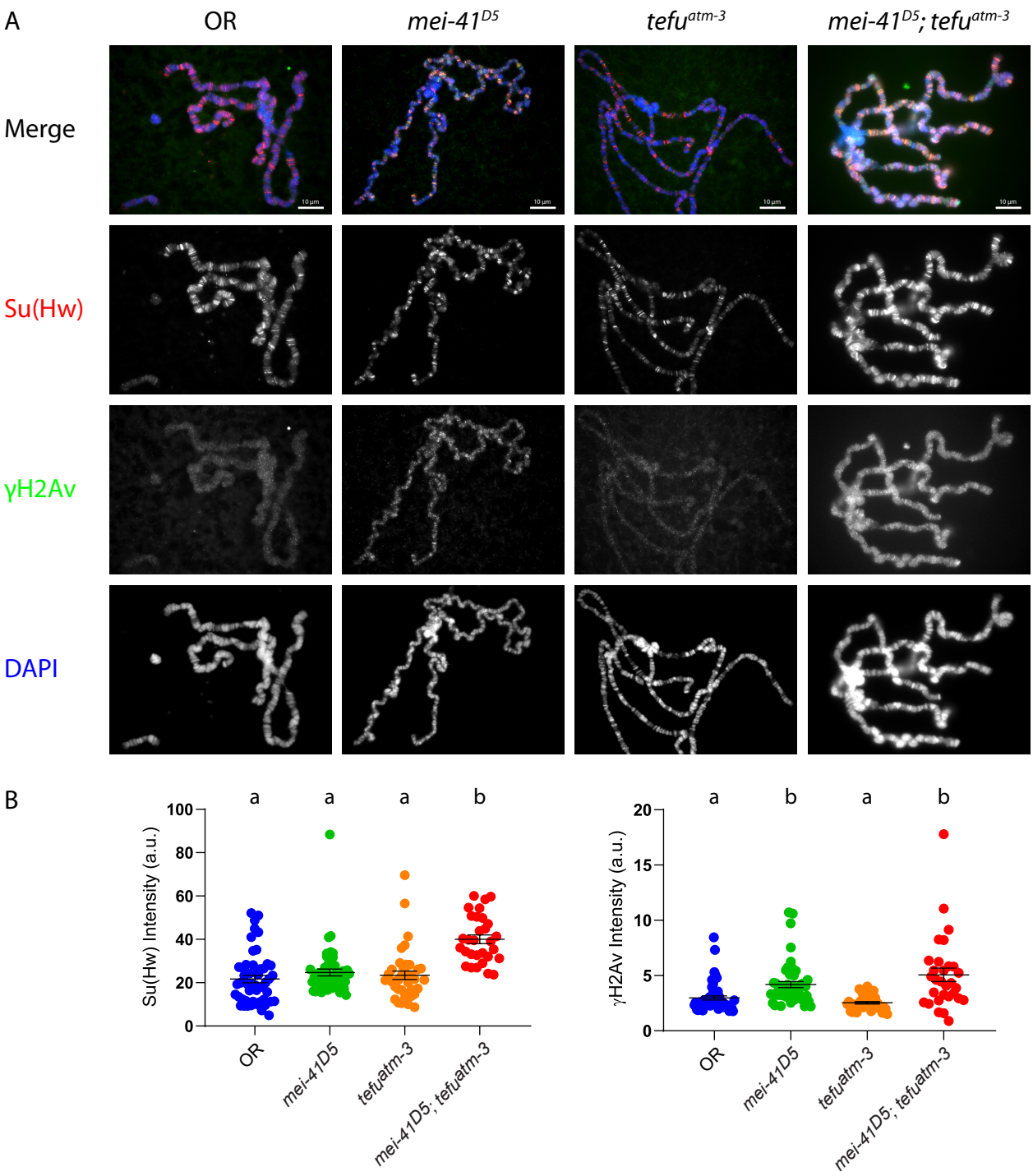


Figure 3.5. Simultaneous mutation of ATR and ATM increases Su(Hw) bound to chromatin. A. Immunostaining results for Su(Hw) and γH2Av antibodies on polytene chromosomes. The scale bars are 10 µm each. **B.** Fluorescent intensities of the Su(Hw) and γH2Av antibody signals. Each dot represents a single polytene genome. Letters above the graphs represent statistical groupings based on a one-way ANOVA with Dunn's multiple comparisons test with significances at $P < 0.05$.

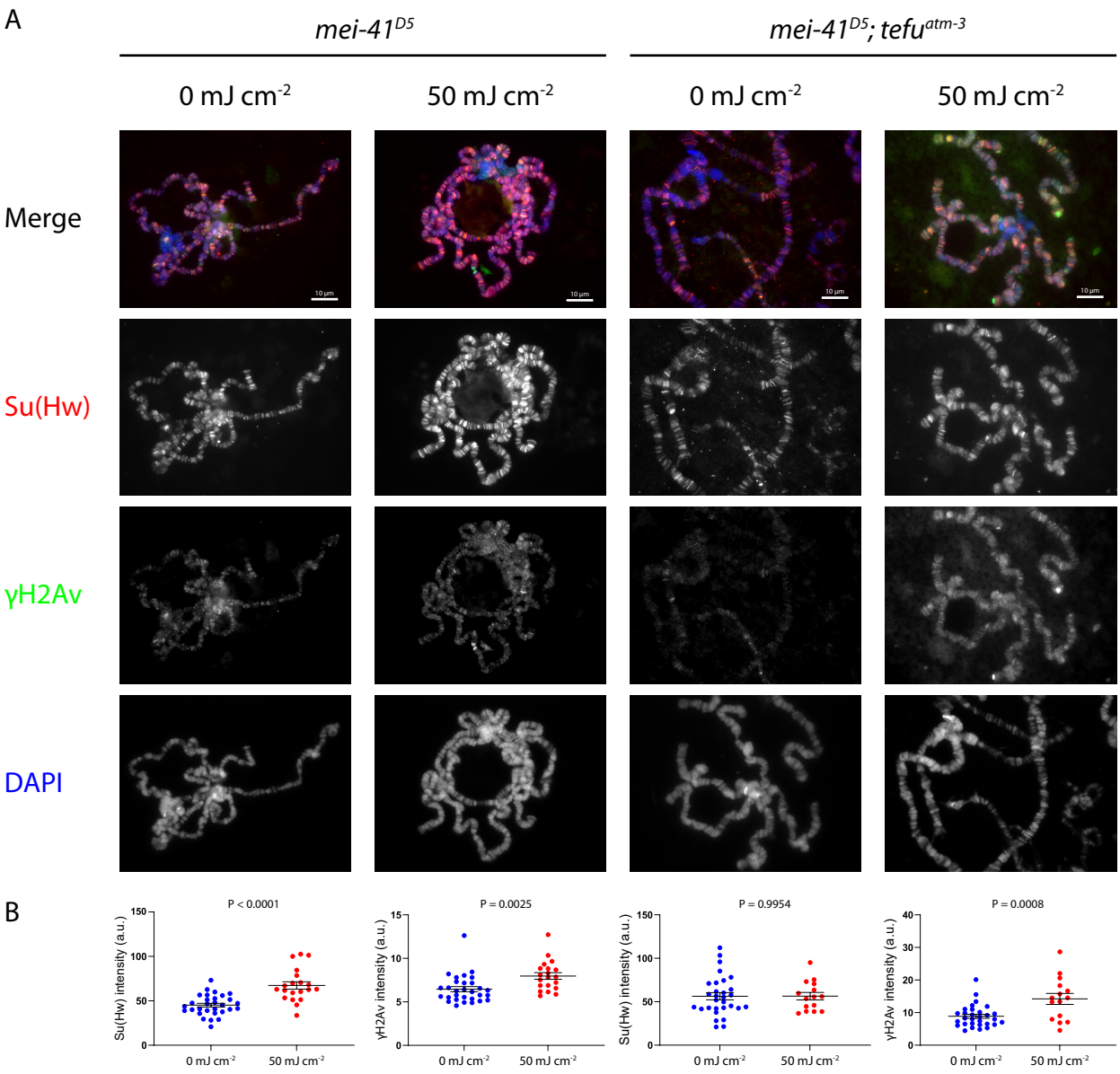


Figure 3.6. Su(Hw) enrichment in polytene chromatin after UV irradiation depends on ATR and ATM. A. Immunostaining results for Su(Hw) and γH2Av antibodies on polytene chromosomes with and without UV treatment. The scale bars are 10 µm each. **B.** Fluorescent intensities of the Su(Hw) and γH2Av antibody signals. Each dot represents a single polytene genome. P-values were determined using unpaired Welch's T-tests.

previously described role in *Drosophila* oocytes (Hsu *et al.*, 2020), we find that null mutation of *su(Hw)* results in generation of gross chromosomal aberrations in dividing larval neuroblasts. This mutant phenotype is common among genes that are involved in detection, marking, and resolution of double strand breaks, including the Aurora A kinase (*aurA*), ATR (*mei-41*), ATM (*tefu*), Twins (*tws*, a PP2A specificity factor), and the topoisomerase gene *Top2* (Gatti and Goldberg, 1991, Mengoli *et al.*, 2014, Merigliano *et al.*, 2017, Merigliano *et al.*, 2019). This fits in with a model in which Su(Hw) also helps regulate the cellular response to DNA damage.

To test this model, the larvae were subjected to UV and X-ray irradiation, which cause DNA damage through different mechanisms that is corrected through distinct pathways depending on the nature of the lesion. Our work shows significant enrichment of the Su(Hw) protein and Mod(mdg4)67.2, which is recruited to chromatin through interactions with Su(Hw), on polytene chromatin after UV irradiation but not after X-ray treatment. Despite this, null mutation of *su(Hw)* significantly reduced the degree of H2Av phosphorylation in polytene chromatin in response to DNA damage by either UV or X-ray irradiation. This suggests that Su(Hw) is involved in the DNA damage response at the early step of labeling double strand breaks with H2Av phosphorylation regardless of the source of damage. Su(Hw) enrichment after UV treatment may reflect a mechanism that depends on insulator activity to respond to issues with transcription and replication that arise from pyrimidine dimer formation that are absent in the damage seen with ionizing radiation. It remains unclear if the enrichment of Su(Hw) in response to UV irradiation is due to specific binding of Su(Hw) at sites of DNA damage/DSBs or if the enrichment reflects a genome-wide response of chromatin insulators to large-scale damage to aid repair through architectural changes. Next-generation techniques such as ChIP-seq and HI-C may provide further clues as to the exact mechanism in future studies. The reliance on Su(Hw) for H2Av phosphorylation was not conserved in diploid cells of the larval central nervous system, which express little Su(Hw). These cells are still able to

phosphorylate H2Av after UV or X-ray irradiation even in the absence of Su(Hw), suggesting that specialized roles may exist for certain insulator complexes in specific tissues.

Our findings on H2Av phosphorylation in polytene cells (Figure 3.5) also conflicts with findings from meiotic cells in *Drosophila*, which show more H2Av phosphorylation in the absence of ATM/*tefu* but not ATR/*mei-41* (Joyce *et al.*, 2011). Other results in mitotic neural cells show decreased frequency of γH2Av foci formation in the $tefu^{atm-6}$ mutant but not the $mei\text{-}41^{29D}$ mutants (Merigliano *et al.*, 2017). The reason for these discrepancies may be due to the difference in cell types, as meiotic cells, mitotic cells, and polytene cells undergo significantly different developmental programs. The increase in Su(Hw) binding to polytene chromatin in the ATR/$mei\text{-}41^{D5}$ ATM/$tefu^{atm-3}$ double mutant would imply that more Su(Hw) accumulates in chromatin as DNA damage accrues in the absence of these two crucial DNA damage sensors. One possibility for a mechanism is that the ATR and ATM kinases may be regulating the activity of a phosphatase needed to diminish the amount of H2Av phosphorylation as DNA damage repair proceeds.

Chapter IV: Su(Hw) Regulates Hematopoietic Development in *Drosophila* Larvae

Abstract

Hematopoiesis, the formation the of lymph glands and circulating hematocytes that constitute the fly circulatory and immune systems, is essential for organismal growth during larval stages and for maintaining homeostatic conditions and fighting infections from exogenous insults. H2Av regulates formation of the larval lymph gland, and reduction of H2Av causes formation of large melanotic tumors in third instar larvae. Here, we show that mutation of *su(Hw)* in the *His2Av*^{810} mutant background rescues the melanotic tumor phenotype. *su(Hw)*$^{-}$ *His2Av*^{810} double mutants are immunocompetent and form supernumerary lymph gland lobes that are larger than those found in wild type. Overexpression of Su(Hw)::GFP in *Antennapedia*-expressing cells results in lethality and spontaneous melanization in larvae. We hypothesize that Su(Hw) regulates expression of *Antennapedia* in the larval lymph gland to affect the differentiation of prohemocytes and lymph gland development.

Introduction

Differentiation and cell fate are crucial decisions that cells in complex, multicellular animals must make. These choices regulate cell morphology and the biochemistry available to any given cell type and are largely influenced by complex signaling networks that affect transcription of different sets of genes depending on the developmental context and needs of the tissue. Transcriptional changes are often driven by epigenetic modifications that adjust the expression of genes, driving cell specification and tissue formation. The circulatory system of *Drosophila* larvae is composed of circulating hemocytes, pockets of sessile hemocytes scattered throughout the animal, and the lymph gland which generates most cells of the hemolymph. The lymph gland of a third instar larvae is comprised of three sets of lobes that run from anterior to posterior along the dorsal vessel, which acts as the heart by moving hemocytes through the larvae. The posterior two lobes, the secondary and tertiary lobes, are small and generate few hemocytes

at this stage. The anterior-most primary lobe, however, is the largest and contains many undifferentiated prohemocytes in addition to differentiated hematocytes, crystal cells, and lamellocytes. Differentiation of prohemocytes is regulated by Hedgehog signaling generated from cells in the posterior signaling center (PSC). PSC cell identity is determined by expression of *Antennapedia*, the lack of which results in unregulated division of prohemocytes in the primary lobe.

Misregulation of H2Av was recently shown to have a striking phenotype in developing larvae. Individuals homozygous for the $His2Av^{810}$ null allele, or trans-heterozygous for the $His2Av^{810}$ null allele paired with a chromosomal deficiency lacking the *His2Av* gene (Df(3R)BSC524), frequently develop large melanotic masses at their posterior ends (Grigorian *et al.*, 2017). These tumors are derived from cells of the lymph gland (the main hematopoietic tissue in flies) and are characterized by loss of differentiated plasmatocytes and crystal cells and the undifferentiated prohemocytes from the primary lobes. It was proposed that H2Av is necessary for prohemocytes to be competent to respond to Hedgehog signaling from PSC cells, suggesting an inhibited transcriptional response in prohemocytes (Grigorian *et al.*, 2017). Based on our previous results showing extensive colocalization of H2Av with Su(Hw) insulator proteins throughout the genome, we questioned whether interactions between H2Av and Su(Hw) are responsible for proper hematopoiesis in *Drosophila* larvae. Our results imply a significant role for Su(Hw) in larval hematopoiesis and a genetic interaction with H2Av that influences growth and differentiation of cells in the lymph gland.

Methods and Materials

Fly stocks and husbandry

All stocks were maintained on a standard cornmeal agar fly food medium supplemented with yeast at 20°C; crosses were carried out at 25°C. The following stocks are maintained in our lab and were originally obtained from Dr. Victor Corces (Emory University): w^{1118}; $su(Hw)^{V}/TM6B$, Tb^{1}. The stock w^{1118};

PBac(RB)*su(Hw)*^{e04061}/*TM6B*, *Tb*^{1} was obtained from the Bloomington *Drosophila* stock center (BDSC: 18224). The His2Av::mCherry stocks were obtained from the Bloomington *Drosophila* stock center. These remaining stocks were provided by our lab: OR, *y*^{2}*w*^{1}*ct*^{6}; PBac(RB)*su(Hw)*^{e04061}/*TM6B*, *Tb*^{1} (derived from BDSC: 18224).

Antibodies

Rabbit polyclonal IgG antibodies against Su(Hw), Mod(mdg4)67.2, and CP190 were previously generated by our lab (Wallace et al., 2010, Schoborg et al., 2013). An antibody against the phosphorylated form of H2Av (UNC93-5.2.1) (Lake et al., 2013) was obtained from the Developmental Studies Hybridoma Bank, created by the NICHD of the NIH and maintained at The University of Iowa, Department of Biology, Iowa City, IA 52242. These antibodies were all diluted 1:1 in glycerol (Fisher Scientific, BP229-1, lot 020133) and used at a final dilution of 1:200. Secondary antibodies were all diluted 1:1 in glycerol and used at a final dilution of 1:200. The following secondary antibodies were used in this study: Alexa Fluor 594 goat anti-rabbit (Invitrogen, A-111037, lot 2079421), Alexa Fluor 488 donkey anti-rabbit (Invitrogen, A-21206, lot 1834802), and Alexa Fluor 488 goat anti-mouse (Invitrogen, A-11001, lot 1858182).

Fluorescence intensity and colocalization analysis

Images were analyzed for the amount of each protein (i.e. the intensity of each channel) using a macro script in FIJI (Schindelin et al., 2012). The DAPI channel was used to automatically generate non-biased ROIs for each cell, which were then manually curated for extra precision. A rolling-ball background subtraction algorithm was used for all images. Intensity measurements were made using the measure function. Numerous genomic images were collected from each sample. All acquisition parameters were kept constant between slides within each experiment.

Generation of *su(Hw)*$^{-}$ *His2Av*^{810} double mutant genotypes

Briefly, flies with null mutations of *su(Hw)*^{e04061} and *His2Av*^{810} in the third chromosome were crossed (See appendix, Figure A1). Female F1s in which recombination between the two mutant chromosomes happened were crossed against the *His2Av*^{810}/*TM6B* mutant background and potential recombinant chromosomes were isolated in F2 males over the *TM6B* balancer. F2 males were selected for the presence of the *su(Hw)*^{e04061} mutation based on eye color and used to establish isogenic lines after two more generations of crossing. These lines were genotyped by PCR to determine the presence or absence of the *His2Av*^{810} mutation. Gel electrophoresis of the PCR products revealed three double recombinant *su(Hw)*^{e04061} *His2Av*^{810} mutant lines (Figure A2). As a control for potential second-site mutations on the *su(Hw)*^{e04061} chromosome, double mutants were also generated using the *su(Hw)*^{V} mutations. Flies with null mutations of *su(Hw)*^{V} and *His2Av*^{810} were crossed in the background of the *y*^{2}*ct*^{6} *gypsy* insulator mutations (Figure A3). Female F1s in which recombination between the two mutant chromosomes happened were crossed against the *su(Hw)*^{e04061}/*TM6B* mutant background and potential recombinant chromosomes were isolated in F2 males over the *TM6B* balancer. F2 males were selected for the presence of the *su(Hw)*^{V} mutation based on the rescue of the *y*^{2}*ct*^{6} mutant phenotype and used to establish isogenic lines after two more generations of crossing. These lines were genotyped by PCR to determine the presence or absence of the *His2Av*^{810} and *su(Hw)*^{V} mutations. Gel electrophoresis of the PCR products revealed multiple double recombinant *su(Hw)*^{V} *His2Av*^{810} mutant lines (Figure A4).

Crystal cell detection and lymph gland phenotyping

Crystal cells in wandering third instar larvae were visualized by incubating between 5-10 larvae in 40 µL 1X PBS buffer in a 200 µL PCR tube in a thermocycler set to 70 °C for 10 minutes. Samples were left overnight at 4 °C to increase the intensity of the melanization product for easier detection of crystal cells and lymph glands. Larvae were placed in halocarbon oil 700 (Sigma, H8898) and photographed using a

stereomicroscope (MZ16 FA; Leica Microsystems) equipped with a CCD color camera (DFC420; Leica Microsystems). A 150 Watt white light source (KL 1500 LCD; Leica Microsystems) set to a color temperature of 3,000 K was used for illumination. Images were collected using Leica Application Suite (Version 2.4.0 R1; Leica Microsystems). Image analysis was performed in FIJI (Schindelin et al., 2012) by counting the number of crystal cells visible on the dorsal side of each larvae. The frequency at which lymph glands become visible after this treatment was recorded, as were measurements of the number of lobes in each lymph gland and the size of each lobe.

Sterile wound assay

To determine whether mutant larvae had functional innate immune responses, a sterile wound assay was performed. Wandering third instar larvae were selected, washed briefly in 1X PBS buffer and 70% ethanol, and placed on a soft pad constructed of black construction paper (for contrast) taped to a folded-up paper towel. Larvae were stabbed on the dorsal side along the midline approximately between abdominal segments A3 to A4 (Galko and Krasnow, 2004) using an insulin syringe needle (Beckton, Dickinson, and Company, Micro-fine IV 28G1/2, 0.36 mm diameter). In some cases, the needle penetrated all the way through the ventral side of the larvae and clots were visible on both sides. Larvae were incubated in a vial of fly food overnight at 25 °C before scoring. Larvae that died immediately after stabbing due to unintentional damage were discarded from the count.

Results

Mutation of *su(Hw)* suppresses the *His2Av^{810}* melanotic tumor phenotype

Drosophila H2Av is involved in both DNA damage repair and in transcriptional regulation. As we previously explored the relationship between Su(Hw) and H2Av phosphorylation in insulator protein mutants, we next questioned how insulator activity and binding are affected by mutation of His2Av. As discussed

previously, heterozygous mutation of *His2Av* in a heterozygous *su(Hw)* mutant background partially rescues defects observed in the wing margins of ct^6 mutants (Figure 3.9). Based on this, and on previous immunostains showing extensive colocalization between Su(Hw) insulator components and γH2Av (Figure 3.1), we examined binding of insulator proteins to polytene chromatin in the $His2Av^{810}$ null background. Quantification of immunostaining signals revealed a slight but statistically significant increase in Su(Hw) binding when comparing $His2Av^{810}$ homozygotes with $His2Av^{810}$/*TM6B* heterozygotes (Figure 4.1). No difference was observed in the binding of the two other key components of the Su(Hw) insulator complex, Mod(mdg4)67.2 and CP190, implying the effect of H2Av mutation on insulator binding to polytene chromatin is minimal.

Our next question was to determine the effect of mutating insulator proteins on the phenotype of *His2Av* mutants. To further explore this relationship between Su(Hw) and H2Av, we generated the double mutant genotype $su(Hw)^-$ $His2Av^{810}$ using established null mutations of *su(Hw)*. As both genes reside on the third chromosome, double mutant generation was performed by taking advantage of meiotic recombination of chromosomes that is largely limited to female *Drosophila* (see methods and the appendix for details). Double mutant $su(Hw)^-$ $His2Av^{810}$ strains were confirmed by PCR and subjected to immunostaining for insulator proteins and γH2Av. Staining for Su(Hw), Mod(mdg4)67.2, and γH2Av were all significantly reduced in the $su(Hw)^{e04061}$ $His2Av^{810}$ mutants when compared to heterozygotes (Figure 4.2 A, B, and E); however, CP190 and CTCF staining were unaffected (Figure 4.2 C, D).

$His2Av^{810}$ null mutants were recently described to form large melanotic masses in their posterior ends as third instar larvae (Grigorian *et al.*, 2017). Inspection of the new double homozygous $su(Hw)^-$ $His2Av^{810}$ genotypes revealed a nearly complete rescue of the melanotic tumor phenotype presented by $His2Av^{810}$ homozygotes, implying a genetic interaction between the two genes that influences the outcome of the hematopoiesis. Whereas the vast majority of $His2Av^{810}$ homozygous larvae developed large melatonic tumors in their posterior ends, none of the examined $su(Hw)^{e04061}$ $His2Av^{810}$ homozygous

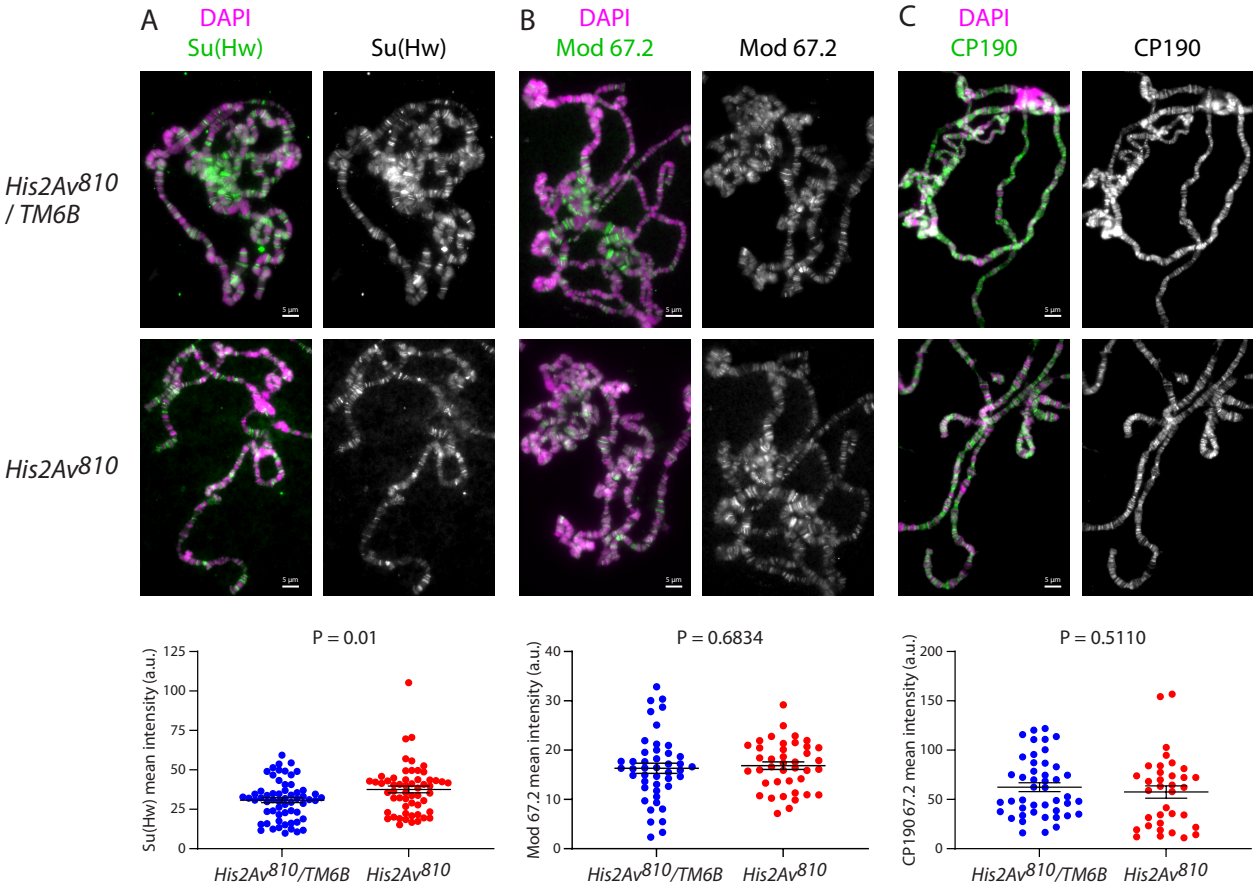


Figure 4.1. Mutation of *His2Av* has a limited effect on insulator protein binding. Immunostaining results for **A.** Su(Hw), **B.** Mod(mdg4)67.2, and **C.** CP190 antibodies on polytene chromosomes. The scale bars are 10 µm each. Beneath each figure are graphs showing fluorescent intensities of the antibody signals. Each dot represents a single polytene genome. P-values were determined using unpaired Welch's T-tests.

larvae showed such masses (Figure 4.3). This result was replicated in the other double homozygous mutant *su(Hw)^{e04061} His2Av^{810}*, suggesting that the rescue is most likely due to mutation of the *su(Hw)* gene specifically and not due to a second-site mutation on the same chromosome. Crossing the double mutants against the single *His2Av^{810}* mutant allowed us to monitor how a partial reduction in the dose of *su(Hw)* affects formation of melanotic tumors in the *His2Av^{810}* homozygote. Unlike the double homozygote, larvae generated from this cross showed large masses but at a significantly lower frequency than the *His2Av^{810}* mutants alone. These results demonstrate that these masses form in the presence of Su(Hw), and that reducing the amount of Su(Hw) available in the cell is associated with decreased tumor size and frequency.

su(Hw)$^{-}$ His2Av^{810} larvae exhibit overgrowth of lymph glands

To further characterize the relationship between Su(Hw) and H2Av in the hematopoietic lineage, third instar larvae were subjected to heat treatment at 70°C. This heat treatment triggers catalysis of the prophenoloxidase enzymes found in crystal cells, resulting in melanin production and subsequent darkening of the cell (Banerjee *et al.*, 2019). This provides a convenient means to visualize the numbers and distribution of crystal cells in heat-treated larvae (Figure 4.4 A). Heat-treated wild type larvae show around 50 crystal cells visible from the dorsal side, while *su(Hw)^{e04061}* homozygous larvae display significantly more crystal cells with around 200 visible per larvae (Figure 4.4 B, C). *His2Av^{810}* homozygous larvae show similar numbers of crystal cells as wild type; however, this mutant was reported to have reduced lymph glands and exhibits large melanotic tumors that contain many crystal cells (Grigorian *et al.*, 2017), obfuscating interpretation of this genotype. *su(Hw)^{e04061} His2Av^{810}* homozygous double mutant larvae generate significantly more crystal cells as the wild type but a similar number compared to the *su(Hw)^{e04061}* single mutant (Figure 4.4 B, C).

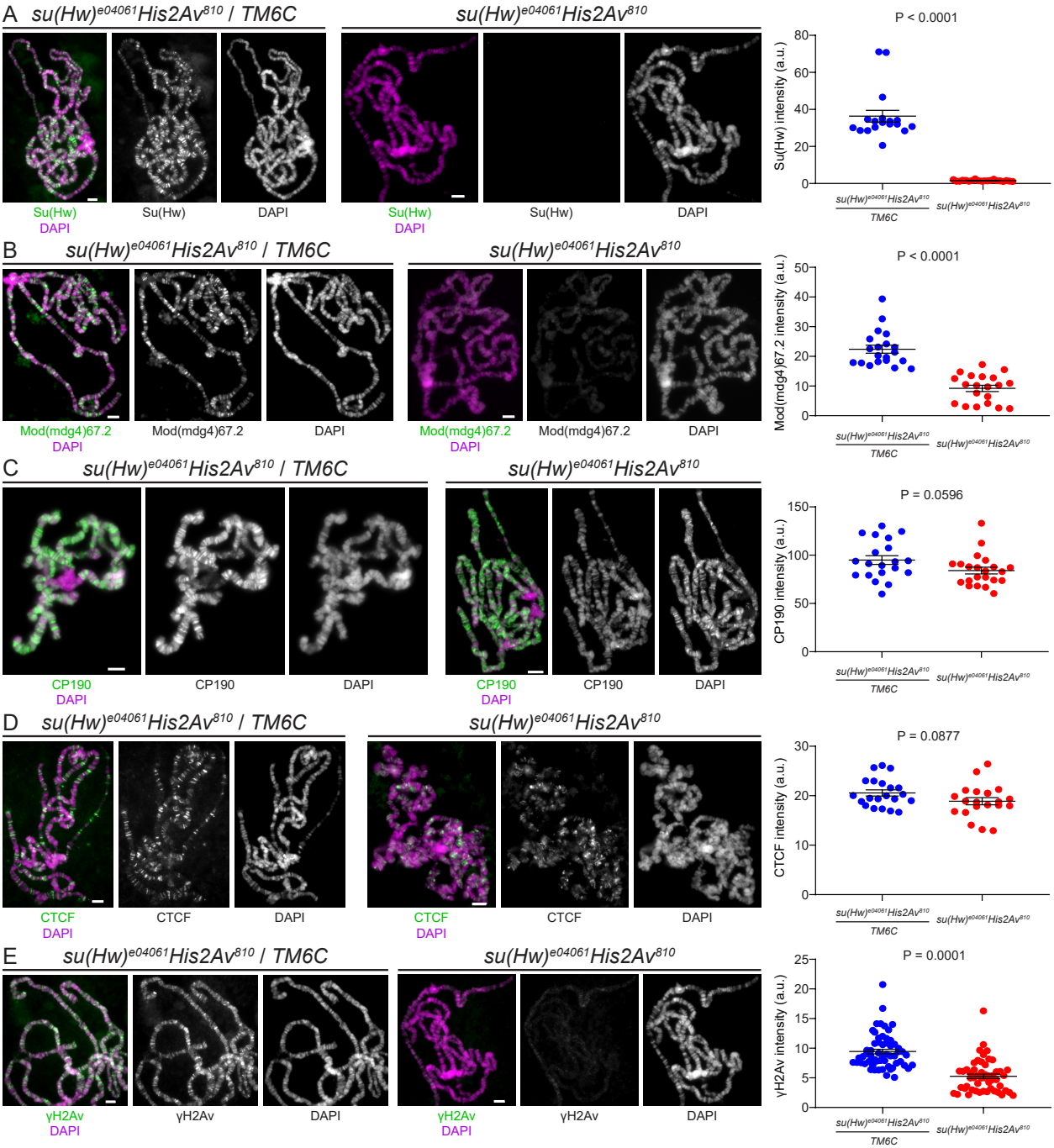


Figure 4.2. Double mutants show reduced immunostaining of Su(Hw), Mod(mdg4)67.2, and γH2Av. Immunostaining results for **A.** Su(Hw), **B.** Mod(mdg4)67.2, **C.** CP190, **D.** CTCF, and **E.** γH2Av antibodies on polytene chromosomes in *His2Av*^{810} heterozygotes (left) and homozygotes (right). The scale bars are 10 µm each. To the right of each figure are graphs showing fluorescent intensities of the antibody signals. Each dot represents a single polytene genome. P-values were determined using unpaired Welch's T-tests.

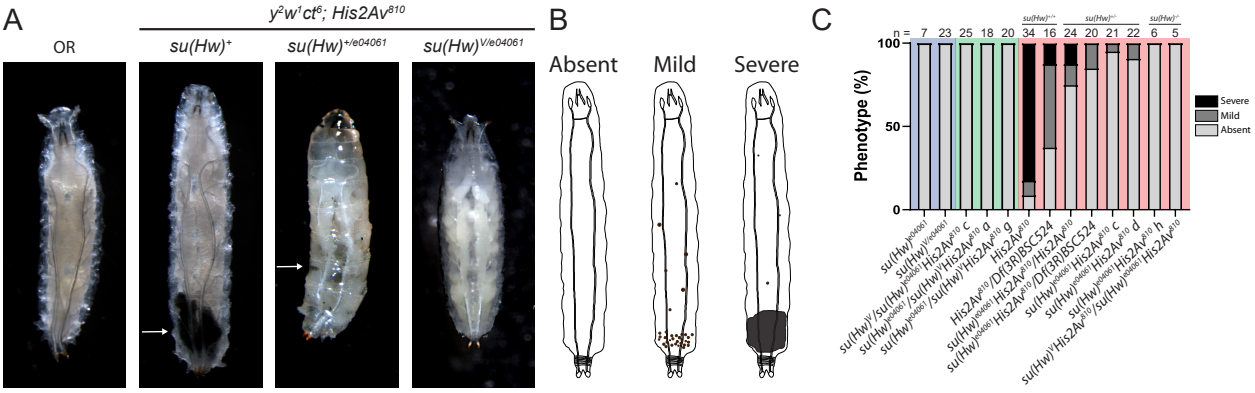


Figure 4.3. Mutation of *su(Hw)* suppresses the *His2Av*^{810} melanotic tumor phenotype. A. Representative pictures of select genotypes photographed from the dorsal aspect. The presence of black melanotic masses is indicated by white arrows. **B.** Illustration showing presentation of the melanotic tumor phenotype in wandering third-instar larvae (representing each of the phenotypic classes used for tumor scoring: absent, mild, and severe). **C.** Quantification of tumor phenotype scoring across each genotype examined. Within the bars the light grey color indicates larvae absent of tumors, the dark grey indicates a mild phenotype, and the black represents a severe phenotype. Blue background in the graph indicates homozygosity for wild type *His2Av*, green indicates heterozygosity for *His2Av*^{810}, and red indicates homozygosity for *His2Av*^{810}. Sample size is shown above each genotype.

In addition to the circulating crystal cells that become visible upon heat treatment, the lymph glands themselves sometimes become visible due to the presence crystal cells (Figure 4.4 A). The frequency of observable lymph glands after heat treatment is significantly higher in the *su(Hw)^{e04061} His2Av^{810}* mutants than the wild type (Figure 4.4 D). Shockingly, the lymph glands in *su(Hw)^{e04061} His2Av^{810}* double mutants were significantly overdeveloped compared to those in wild type larvae, often showing supernumerary lobes (Figure 4.4 B, D). Indeed, some larvae in the *su(Hw)^{e04061} His2Av^{810}* homozygous mutant displayed up to eight large lymph gland lobes and the average size of lymph gland lobes was significantly larger in the *su(Hw)^{e04061} His2Av^{810}* double mutant than wild type (Figure 4.4 B, D, E). Supernumerary lymph gland lobes were also observed at a low frequency in larvae homozygous for *su(Hw)^{e04061}* and heterozygous for *His2Av^{810}* (Figure 4.4 D).

Since immune system development in *Drosophila* larvae depends largely upon hematopoiesis in the lymph gland, we tested the innate immune response in these larvae using a sterile wound assay. This involves stabbing larvae using an ultrafine sterile needle and monitoring surviving larvae for clot formation and melanization at the site of wounding (Figure 4.5 A). This assay revealed that, like the wild type strain, *su(Hw)^{e04061} His2Av^{810}* double mutants are competent to form clot in response to sterile injury (Figure 4.5 B, C). *su(Hw)^{e04061}* single mutants also form clots in response to sterile wounds; however, *His2Av^{810}* mutants form clots at a slightly lower frequency compared to wild type, likely a result of the hematopoietic phenotypes reported previously (Figure 4.5 C). It was also noted that the *su(Hw)^{e04061} His2Av^{810}* double mutants grew to significantly larger sizes as third instar larvae compared to wild type (data not shown), possibly as a result of overactive lymph development. Despite the rescue of the *His2Av^{810}* hematopoietic phenotypes observed the *su(Hw)^{e04061} His2Av^{810}* double mutant, mutation of *su(Hw)* in the *His2Av* null background was not enough to overcome the completely penetrant lethality associated with the inability to express the essential H2Av histone, with double mutants showing 100% lethality before the end of the pupal stage (data not shown).

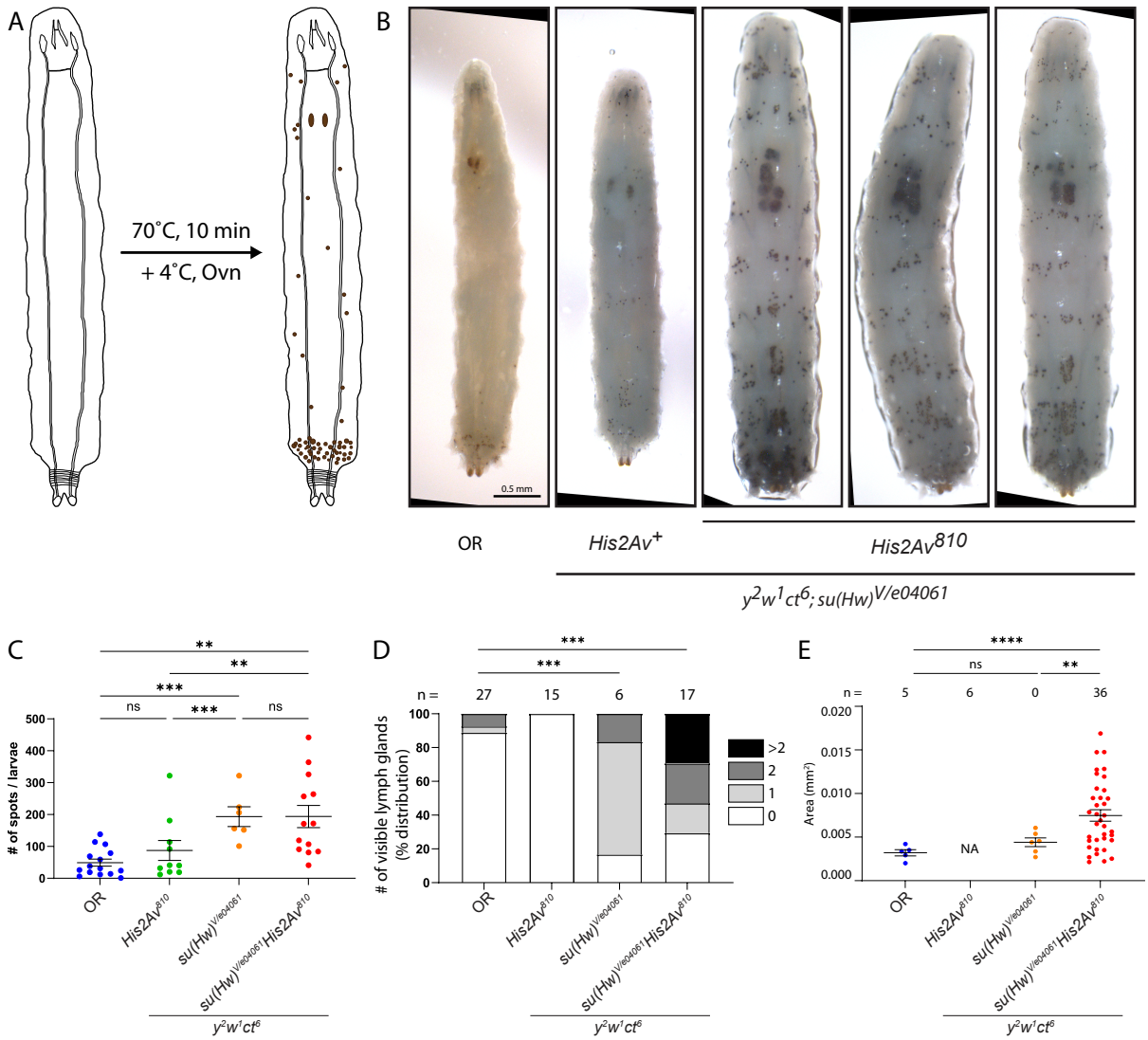


Figure 4.4. *su(Hw)*$^{-}$*His2Av*^{810} larvae exhibit overgrowth of lymph glands. **A.** Illustration showing the heating assay, which involves incubating larvae at 70 °C and monitoring for melanization of individual cells and lymph glands. **B.** Representative examples of melanized cells and lymph glands. The $y^2w^1ct^6$; *su(Hw)*$^{V/e04061}$*His2Av*^{810} mutant genotype shows larger lymph glands with supernumerary lobes. The scale bar represents 0.5 mm. **C.** Quantification of melanized spots observed after heat treatment for each genotype. P-values were determined using an ordinary one-way ANOVA with Tukey's multiple comparisons test. **D.** Number of lymph gland nodes per larvae observed in each genotype. P-values were determined using pairwise Chi-squared tests. **E.** Measurements of lymph gland lobe size in different genotypes. P-values were determined using ANOVA with Dunnett's multiple comparisons. * P < 0.05, ** P < 0.01, *** P < 0.001, **** P < 0.0001.

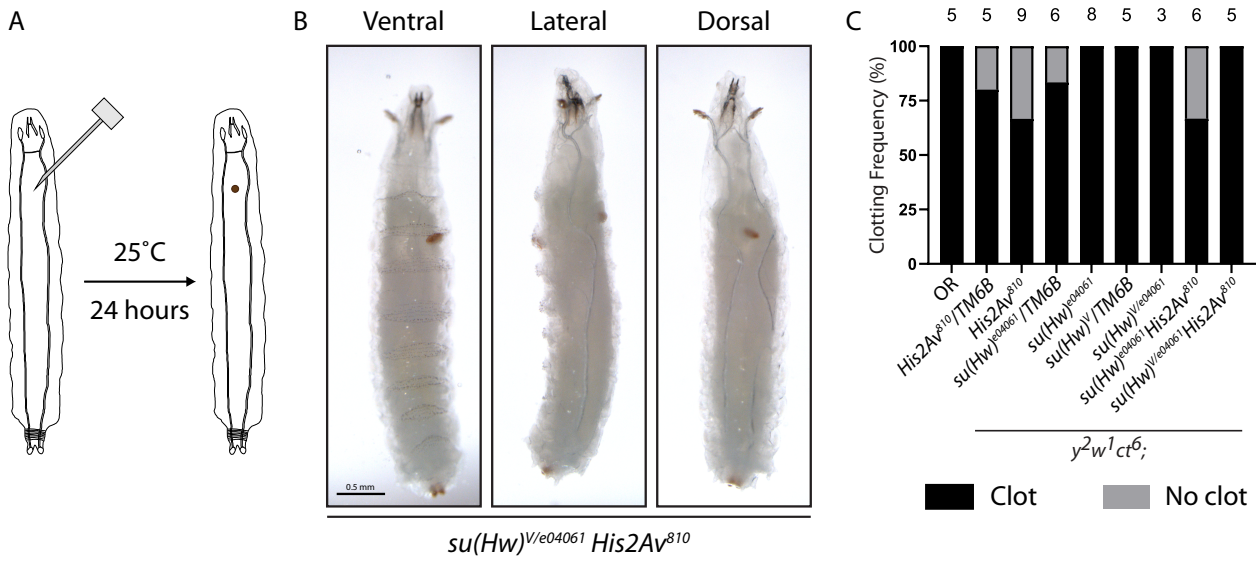


Figure 4.5. *su(Hw)*$^{-}$*His2Av*^{810} larvae are immunocompetent. A. Illustration showing the sterile wound assay, which involves stabbing larvae with a fine-tipped needle and monitoring for clot formation. **B.** Representative example of clot formation in the $y^2w^1ct^6$; $su(Hw)^{V/e04061}His2Av^{810}$ mutant genotype. Views are shown from the ventral, lateral, and dorsal aspects. Two clots are visible, one from the entry wound (dorsal) and one from the exit wound (ventral). **C.** Frequencies of clot formation for different genotypes.

Development of the larval lymph gland is influenced by *Antennapedia*, which is expressed in the posterior signaling center (PSC), a group of cells at the posterior end of the primary lymph gland that regulates cell fate and differentiation among undifferentiated prohemocytes through paracrine signaling (Krzemień *et al.*, Mandal *et al.*). We therefore wondered what the effect would be on lymph gland structure and crystal cell production when overexpressing Su(Hw) in cells that normally express *Antennapedia* during larval development. Expression of a UAS-Su(Hw)::GFP construct driven by *Antp*-GAL4 resulted in significant lethality at early developmental stages (data not shown), and produced larvae with severe growth defects and small degrees of spontaneous melanization of crystal cells (Figure 4.6 B). A review of publicly available ChIP-seq data reveals the presence of Su(Hw) insulator components in the *Antp* gene, between the transcription start site and the start codon (Figure 4.6 C), suggesting that *Antp* expression may be regulated by Su(Hw).

Discussion

Our investigation into the relationship between H2Av and Su(Hw) revealed a genetic interaction with significant and pleiotropic effects in larval hematopoiesis. That rescue of the melanotic tumor phenotype occurs in a Su(Hw) dose-dependent manner is not surprising, as hematopoietic phenotypes in the $His2Av^{810}$ mutant result from either reduction or increases in *His2Av* expression. For example, overexpression of wild type H2Av results in less cohesion between posterior signaling center (PSC, a stem cell/tissue organizing hub) cells and fewer differentiated plasmatocytes and crystal cells. This would imply that a precise concentration of H2Av is needed for normal development of this critical tissue. The same is likely true for Su(Hw), which regulates expression of crucial genes through stoichiometric interactions with related proteins.

An H2Av-dependent function with lymph gland formation is evident as mutation of *su(Hw)* alone is insufficient for lymph gland overgrowth phenotype. Indeed, mutation of *His2Av* alone results in

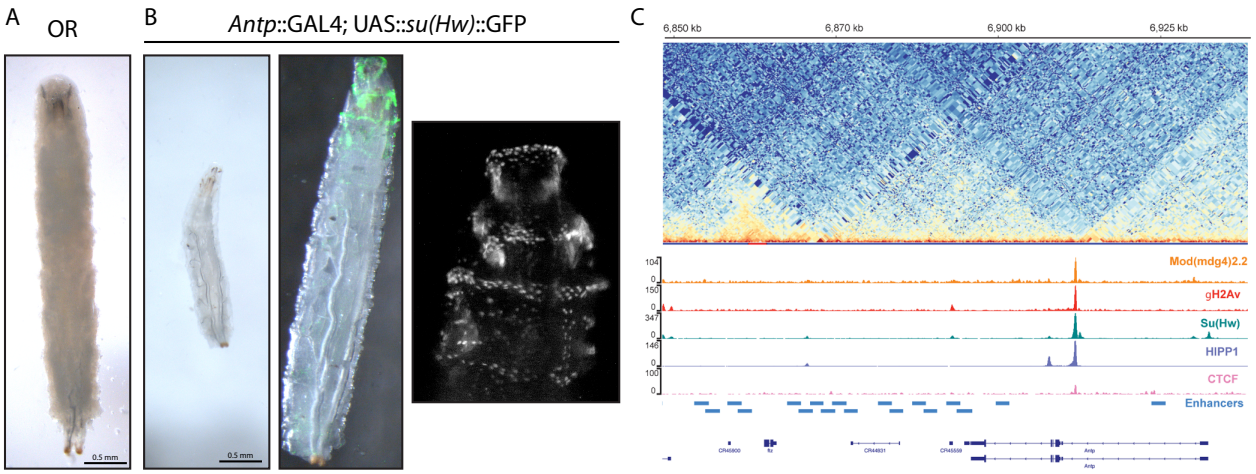


Figure 4.6. Overexpression of *su(Hw)* in *Antp*-expressing cells results in spontaneous melanization and lethality. A. Wild type OR larvae for size comparison. **B.** Example of *Antp*::GAL4; UAS-*su(Hw)*::GFP larvae. Left: shown at the same scale as **A**. Middle: close-up showing brightfield image overlaid with fluorescence from Su(Hw)::GFP observed at the anterior and posterior ends. Spontaneous melanization is observed on the left side of the larvae. Right: Magnified view of the anterior end of the larvae showing only Su(Hw)::GFP. The scale bars in **A.** and **B.** represent 0.5 mm. **C.** Publicly available ChIP-seq data shows binding of Su(Hw) insulator complex components, including γH2Av, between the transcription start site and start codon of Antennapedia (*Antp*).

diminished lymph glands, a finding consistent with previous work (Grigorian *et al.*, 2017), whereas mutation of both *su(Hw)* and *His2Av* together generates overgrown lymph glands (Figure 4.4 D). Evidence is also provided in a previous study that phosphorylation of H2Av is not required for its activity in regulating hematopoietic tissue development (Grigorian *et al.*, 2017). First, expression of a dominant negative mutant allele of *His2Av* lacking the C-terminal 14 amino acid H2AX-like motif ($H2AV^{CT}$) (Clarkson *et al.*, 1999) partially rescues hematopoiesis in the $His2Av^{810}$ null background and allows larvae to survive to adulthood (Grigorian *et al.*, 2017). Second, overexpression of either the phosphomimetic $H2AV^{SE}$ or the phosphonull $H2AV^{SA}$ alleles was able to partially rescue the phenotype seen in the $His2Av^{810}$ null background (Grigorian *et al.*, 2017). These results from the $His2Av^{810}$ background may also extend to the role that Su(Hw) is playing in this process. Su(Hw) is required for genomic stability but can also act as a transcription factor, leading to the question of which role for Su(Hw) is involved in the hematopoietic pathway.

We hypothesize that Su(Hw) acts as a transcription factor in the hematopoietic cell lineage, affecting the expression of genes that influence lymph gland development and/or the melanization process. Based on our findings of a Su(Hw) binding site upstream of the *Antp* start codon and that overexpression of Su(Hw) in *Antp*-expressing cells causes growth defects and spontaneous melanization (Figure 4.6), it is possible that Su(Hw) is necessary for regulating expression of *Antp* in cells of the PSC. Too much Su(Hw) is associated with growth defects, while lack of Su(Hw) in an *His2Av* mutant background causes severe overgrowth of lymph glands and larval size. Alternatively, as the generation of reactive oxygen species (ROS) in cells of the PSC is involved in the lamellocyte maturation pathway (Sinenko *et al.*, 2011), DNA damage that occurs as a result of ROS generation may be relevant. If so, this provides another potential mechanism through which Su(Hw) may impact hematopoietic development. This remains an open question that will be addressed in future experiments.

Chapter V: Fragile X and DNA Damage Repair

Abstract

Mutations of the human *FMR1* (fragile X mental retardation) gene result in Fragile X syndrome, a leading heritable form of mental disability throughout the world. Animal models have revealed a role for the FMR protein in the DNA damage response. We show evidence here that dFMRP is not actively shuttled from the cytoplasm to the nucleus in response to various forms of genotoxic stress. Mutation of *dFmr1* is associated with accumulation of second-site mutations in genes touching many different developmental and homeostatic pathways. Mutation of *dFmr1* is associated with decreased expression of *su(Hw)* in diploid cells of the central nervous system. We propose a mechanism in which dFMRP indirectly regulates *su(Hw)* expression in these cells through an intermediate inhibitory protein.

Introduction

Fragile X syndrome (FXS) in humans is directly linked to mutations in the *FMR1* (fragile X mental retardation) gene and is the most common monogenic cause of intellectual disability and autism (Ciaccio *et al.*, 2017). Fragile X patients generally exhibit issues with cognition and behavior in addition to showing certain physical characteristics associated with the syndrome. In humans, most cases of fragile X syndrome are caused by an expansion of a CGG trinucleotide repeat in the 5' UTR of the *FMR1* gene (Fu *et al.*, 1991, Verkerk *et al.*, 1991), resulting in hypermethylation of this region and subsequent transcriptional silencing of the *FMR1* gene (Oberle *et al.*, 1991, Pieretti *et al.*, 1991). A number of cases, however, have been caused by mutations at highly conserved residues in different domains of FMRP. These mutations have been instructive in understanding the cellular roles of FMRP and how different domains contribute to these roles.

FMRP has been shown to bind mRNAs and inhibit their translation (Bassell and Warren, 2008) in the post-synaptic compartment of neurons, where FMRP regulates translation of mRNAs whose products

modulate the activity of the post-synaptic density (Antar and Bassell, 2003). Model systems to study FXS have been developed in both mice and *Drosophila*. The FMR protein is well conserved from flies to humans (Wan *et al.*, 2000) and contains two tandem amino-terminal Agenet domains that are associated with binding methylated histones (Alpatov *et al.*, 2014) followed by three KH domains used for binding mRNAs and an RGG domain also used for RNA binding (Myrick *et al.*, 2015). The FMR protein also contains a nuclear localization sequence (NLS) and nuclear export sequence (NES) and has been shown to traffic in and out of the nucleus (Dictenberg *et al.*, 2008).

While much of the characterization of FMRP activity has focused on its role in the cytoplasm of the dendrites and synapses, little is known about how FMRP functions when it is in the nucleus. Recently, however, a number of studies have supported a potential role for FMRP in the DNA damage response (DDR) pathway in mice and *Drosophila*. One finding is the localization of FMRP to sites of double strand breaks along chromosomes in meiotic mouse spermatocytes (Alpatov *et al.*, 2014); these chromosomes undergo a program of breaking and repair as part of homologous recombination and foci of FMRP may be involved in repair of these breaks. Another recently reported nuclear role for FMRP is that it is required for phosphorylation of H2AX in mice, one of the earliest steps in the DDR, and that FMRP binding of chromatin via the Agenet domains was necessary for this response (Alpatov *et al.*, 2014). This role in the nucleus was shown to be distinct from FMRP's role in regulating synaptic activity as mutations in the Agenet domain that impair DNA repair do not affect synaptic plasticity. Previous work in our lab has also suggested a necessary role for insulators in DNA repair: flies that are mutant for *su(Hw)* show significant increases in the levels of phosphorylated H2Av. This implies that insulators are either required to prevent DNA damage or that they are crucial for repair. These findings together suggest that both dFMRP and insulators are involved in DNA repair, potentially in the same pathway.

Methods and Materials

Fly stocks and husbandry

All stocks were maintained on a standard cornmeal agar fly food medium supplemented with yeast at 20°C; crosses were carried out at 25°C. The following stocks are maintained in our lab and were originally obtained from Dr. Victor Corces (Emory University): w^{1118}; $su(Hw)^{V}/TM6B$, Tb^{1}. The stock w^{1118}; PBac(RB)$su(Hw)^{e04061}/TM6B$, Tb^{1} was obtained from the Bloomington *Drosophila* stock center (BDSC: 18224). The $dFmr1^{3}$ null allele, the wild-type rescue of this mutant, and the Venus::*dFmr1* and yw; *actin*-GAL4 stocks were obtained from Dr. Thomas Dockendorff. The $dFmr1^{\Delta 50M}$ and $dFmr1^{\Delta 113M}$ null alleles and the *His2Av*::mCherry stocks were obtained from the Bloomington *Drosophila* stock center. These remaining stocks were provided by our lab: OR, $y^{2}w^{1}ct^{6}$; PBac(RB)$su(Hw)^{e04061}/TM6B$, Tb^{1} (derived from BDSC: 18224).

Antibodies

A rabbit polyclonal IgG antibody against Su(Hw) was previously generated by our lab (Wallace et al., 2010, Schoborg et al., 2013). Antibody against the phosphorylated form of H2Av (UNC93-5.2.1) (Lake et al., 2013) was obtained from the Developmental Studies Hybridoma Bank, created by the NICHD of the NIH and maintained at The University of Iowa, Department of Biology, Iowa City, IA 52242. These antibodies were all diluted 1:1 in glycerol (Fisher Scientific, BP229-1, lot 020133) and used at a final dilution of 1:200. Secondary antibodies were all diluted 1:1 in glycerol and used at a final dilution of 1:200. The following secondary antibodies were used in this study: Alexa Fluor 594 goat anti-rabbit (Invitrogen, A-111037, lot 2079421), Alexa Fluor 488 donkey anti-rabbit (Invitrogen, A-21206, lot 1834802), and Alexa Fluor 488 goat anti-mouse (Invitrogen, A-11001, lot 1858182).

Immunostaining of larval tissues

Wandering third instar larvae were dissected in PBS. Tissues were immediately placed into fixative (4%, para-formaldehyde (Alfa Aesar, 43368, lot N13E011), 50% glacial acetic acid (Fisher Scientific, A38-212, lot 172788)) on a coverslip for one minute. Samples were squashed by lowering a slide on top of the sample then turning it over, placing it between sheets of blotting paper, and hitting the coverslip firmly with a small rubber mallet. Slides were dipped in liquid nitrogen, coverslips were removed, and samples were incubated in blocking solution (3% powdered nonfat milk in PBS + 0.1% IGEPAL CA-630 (Sigma-Aldrich, 18896, lot 1043)) for 10 minutes at room temperature. The slides were dried and incubated with primary antibodies overnight at 4°C in a box humidified with wet paper towels. The next day, slides were washed twice in PBS + 0.1% IGEPAL CA-630 before incubation with secondary antibodies for three hours in the dark at room temperature. Slides were washed twice in PBS + 0.1% IGEPAL CA-630, treated with DAPI solution of 0.5 μg/mL (ThermoFisher, D1306) for one minute, and washed one more time in PBS alone.

Samples were mounted with Vectashield antifade mounting medium (Vector Laboratories, H-1000, lot ZF0409) and coverslips were sealed with clear nail polish. All microscopy for immunostaining was performed on a wide-field epifluorescent microscope (DM6000 B; Leica Microsystems) equipped with a 100X (NA 1.35) oil immersion objective and a charge-coupled device camera (ORCA-ER; Hamamatsu Photonics). Image acquisition was performed using SimplePCI (v6.6; Hamamatsu Photonics). Image manipulation was performed in FIJI (Schindelin et al., 2012); all contrast adjustments are linear. Images were further processed in Adobe Photoshop CS5 Extended, Version 12.0 x64. Figures were assembled in Adobe Illustrator CS5, Version 15.0.0. Statistical analyses were performed in GraphPad Prism version 8.0.0 (224) (GraphPad Software, San Diego, CA).

Fluorescence intensity analysis

Images were analyzed for the amount of each protein (i.e. the intensity of each channel) using a macro script in FIJI (Schindelin et al., 2012). The DAPI channel was used to automatically generate non-biased ROIs for each cell, which were then manually curated for extra precision. A rolling-ball background subtraction algorithm was used for all images. Intensity measurements were made using the measure function. Numerous genomic images were collected from each sample. All acquisition parameters were kept constant between slides within each experiment.

Live-cell imaging

Small petri dishes with a hole sealed by a cover slip on the bottom were prepared before dissection; the coverslip was coated with 0.01% poly-L-lysine to help tissues adhere to the glass surface. Petri dishes were filled with insect culture medium prior to and during microscopy. Wandering third instar larvae were expressing the fluorescently tagged proteins were generated by crossing a stock containing both fluorescently tagged genes with a stock containing the *actin*-GAL4 driver. These larvae were dissected in insect culture medium and tissues were adhered to the coverslip in the petri dishes. Live-cell imaging was performed on a spinning disk confocal microscope using red (561 nm) and green (488 nm) channels, taking single Z-plane images every 5 seconds. The isotonic insect culture medium was initially replaced with hypertonic insect culture media supplemented with 250 mM NaCl by pipetting. The hypertonic media was then replaced with isotonic media to allow for recovery from osmotic stress.

Western blotting

Tissues were dissected from wandering third instar larvae in 1X PBS. Tissues were collected in RIPA buffer (150 mM NaCl, 1% NP-40, 0.5% sodium deoxycholate, 0.1% SDS, 50 mM Tris-HCl, pH 8.0) supplemented with protease inhibitor (A32953, Thermo Scientific) and a phosphatase inhibitor (A32957, Thermo

Scientific). Samples were homogenized in a 500 µL PCR tube with a motorized pestle, mixed with 5X loading buffer (0.5 M Tris-HCl, pH6.8, 5% SDS, 0.0125% bromophenol blue, 12.5% β-mercaptoethanol, 50% glycerol) and 15% per volume β-mercaptoethanol, and boiled for 10 minutes. Protein samples were separated on 8% polyacrylamide gels and transferred onto 0.45 µm PVDF membranes. Membranes were blocked in a solution of 20% Odyssey Blocking Buffer (LI-COR, 927-50000) in TBS at room temperature for one hour. Membranes were incubated in primary antibodies diluted in TBST at 4 °C overnight. Primary antibodies used in these western blots include the mouse monoclonal α-dFMRP (5A11; 1:1,000), our rabbit polyclonal α-dFMRP antibody (35261; 1:500), and mouse monoclonal α-beta tubulin (E7; 1:10,000). Next, membranes were washed four times in TBST, 5 minutes each wash. Membranes were then incubated in secondary antibodies diluted in TBST at room temperature for one hour. Secondary antibodies used in these western blots include Goat α-rabbit 680 RD (1:10,000) and Donkey α-mouse 800 CW (1:10,000). Membranes were washed four times in TBST followed by two washes in TBS, 5 minutes each wash. Blots were imaged on an Odyssey CLx scanner (LI-COR). Image files were manipulated in FIJI for analysis and presentation (Schindelin *et al.*, 2012).

Results

Generation and characterization of novel polyclonal antibodies against dFMRP

In order to probe the nuclear mechanisms behind these recently described phenomena, our laboratory has developed new antibodies against *Drosophila* FMRP. The use of giant polytene chromosomes obtained from larval salivary glands provides an opportunity to map proteins to specific genomic loci through immunofluorescence. This method also allows proteins to be compared to determine whether or not they bind the same genomic regions. Initial experiments using commercially available antibodies against dFMRP were unsuccessful at showing reproducible binding patterns in polytene chromosomes, leading our lab to develop two new polyclonal antibodies. These antibodies were obtained using the

amino-terminus of dFMRP as an antigen. This region was chosen as it contains two tandem Agenet domains that preferentially bind methylated histones and are crucial for FMR's role in the DNA damage response. These antibodies are specific to dFMRP and provide reproducible staining patterns on western blots (Figure 5.1). Our polyclonal dFMRP rabbit antibody reproduced the same banding pattern as the commercially available mouse monoclonal antibody (5A11). dFMRP protein was observed in wild type backgrounds but not in the homozygous null $dFmr1^{3}$ background. The signal was also significantly reduced when knocking down *dFmr1* expression using two independent RNAi constructs. To confirm specificity, wild type *dFmr1* was expressed in the mutant $dFmr1^{3}$ background using a P-element on the second chromosome. The band was labelled by both antibodies in this sample, demonstrating that our rabbit polyclonal is specific to dFMRP in western blots.

Su(Hw) signal is reduced in diploid cells in several null *dFmr1* mutant backgrounds

We next sought to determine whether or not our rabbit polyclonal antibodies are able to specifically label dFMRP in immunostains of larval tissues. In diploid cells, binding of our polyclonal dFMRP antibody (35262) was normal in wild type cells, but significantly reduced in several different null mutant genotypes (Figure 5.2). The lowest amount of signal was observed in genotypes carrying the $dFmr1^{\Delta 50M}$ mutation, which is associated with the most severe phenotypes. This direct correlation between the presence of wild type *dFmr1* and the amount of signal in the immunostain seems to confirm that our antibody specifically labels dFMRP in diploid cells. Another important result from this experiment is the observation that Su(Hw) antibody labelling is significantly reduced in *dFmr1* null mutants. This points to a genetic interaction between *su(Hw)* and *dFmr1*, although the nature of this relationship remains unclear. dFMRP may be required for the recruitment or stabilization of Su(Hw) on chromatin. However, it is also possible that this relationship is due to dFMRP's role as a translational repressor of many substrates. In this case, dFMRP may be repressing expression of an unknown factor that is required either for expression of *su(Hw)*

or for the stable binding of Su(Hw) protein to chromatin. Despite the ability for the novel rabbit polyclonal antibodies to label dFMRP in diploid cells, immunostaining in polytene chromatin was unreliable. While significant decreases in fluorescent intensity of the antibody signals were noted in an RNAi experiment (data not shown), many bands were present throughout the polytene chromatin that were not specific to dFMRP. Based on this conclusion we were unable to use these antibodies for further staining in this tissue.

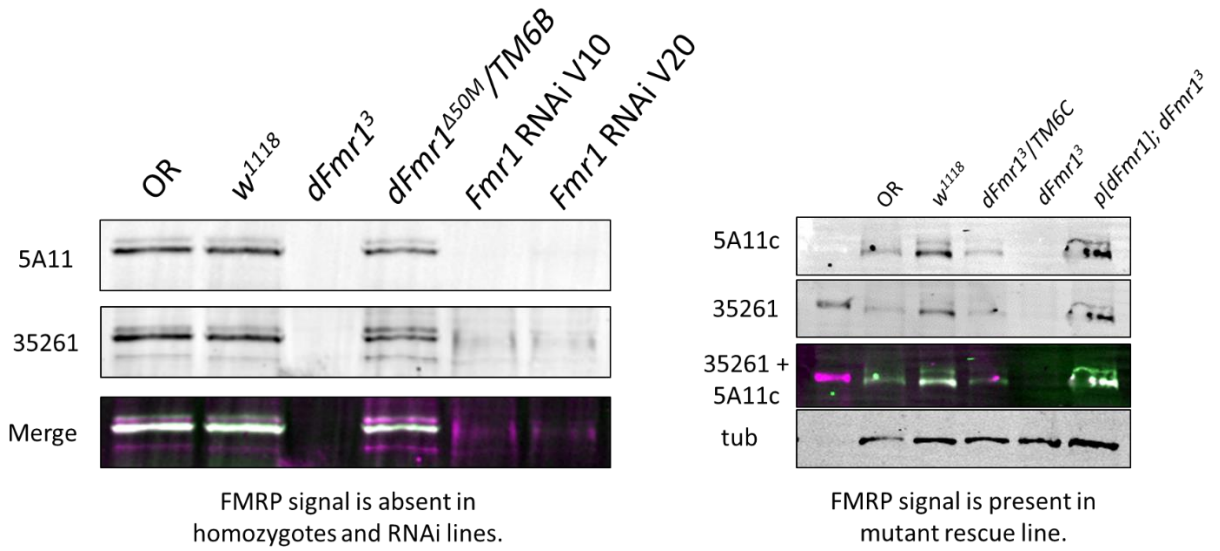


Figure 5.1. New polyclonal antibodies specifically label FMRP. Western blots showing the presence or absence of dFMRP in various genotypes. Each channel is shown independently in greyscale and together as a green and magenta merged image. *Fmr1* RNAi V10 and *Fmr1* RNAi V20 represent two independent RNAi lines. 5A11 = mouse monoclonal antibody, 35261 = rabbit polyclonal antibody. Anti-tubulin antibody (E7) was used as a loading control for the blot on the right.

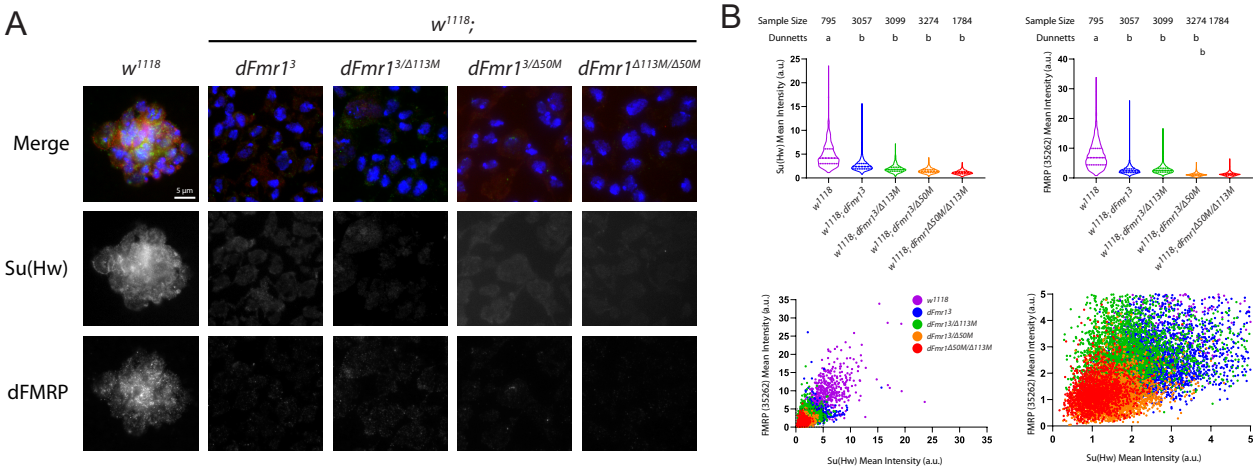


Figure 5.2. Su(Hw) signal is reduced in *dFmr1* mutant larval brains. **A.** Fluorescent micrographs of each genotype showing Su(Hw) (green) and dFMRP (red) with DAPI (blue) labeling DNA. **B.** Quantitative measurements of Su(Hw) antibody intensity. **C.** Quantitative measurements of dFMRP rabbit polyclonal antibody (35262) intensity. **D.** Covariance of the dFMRP and Su(Hw) antibody signals. Dashed lines indicate the range of the inset in E. **E.** Close-up of the inset from D.

dFMRP remains cytoplasmic in polytene cells during genotoxic stress

Only a minor fraction of cellular dFMRP can be found in the nucleus under normal conditions, making study of nuclear dFMRP difficult. In another attempt to visualize nuclear dFMRP bound to chromatin, we subjected cells to several forms of genotoxic stress paired with either immunostaining or live-cell imaging. In one example of these experiments, salivary glands expressing Venus::dFMRP and H2Av::mCherry as a chromatin marker were examined (Figure 5.3). The tissue was initially submerged in isotonic insect cell culture medium; in this condition dFMRP is seen throughout the cytoplasm but there is no discernable dFMRP seen in the nucleus. Stress was induced by replacement of the isotonic medium with medium made hypertonic by increasing the concentration of NaCl by 250 mM. During this stress, the cells contracted as expected in a hypertonic solution, and the nuclei were tightly squeezed by the pressure. Despite this, there was still no Venus::dFMRP observed in the nucleus. This pattern remained as the tissue was returned to isotonic conditions, indicating the dFMRP is not trafficked into the nucleus in response to osmotic stress or during the recovery period after stress. One limitation of this experiment is that the green fluorescent Venus tag on dFMRP in this experiment may interfere with nuclear import; however, immunostaining results replicated this result (data not shown). We next tested other forms of genotoxic stress, including exposure to ultraviolet light and to x-ray irradiation. Similar to our results with osmotic stress, no increase in the nuclear fraction of dFMRP was ever noted in these experiments (data not shown).

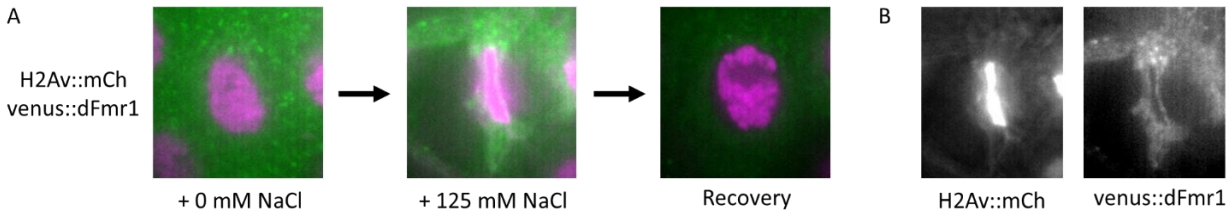


Figure 5.3. dFMR1 remains cytoplasmic in polytene cells during osmotic stress. A. Time course of live-cell imaging showing the same cell before, during, and after hyperosmotic stress. H2Av::mCh is shown in magenta, Venus::dFMRP is shown in green. **B.** Shows the greyscale images for each channel during the maximal response to hyperosmotic stress.

Mutation of *dFmr1* is associated with accumulation of second-site mutations but not with chromosomal aberrations

One early observation made when studying *dFmr1* mutations for their effect on genome stability was the suppression of the chromatin insulator-dependent *cut*^{6} phenotype. This phenotype results in a jagged appearance to the wing margin of adult flies due to decreased cell division during development and is due to the placement of a *gypsy* insulator between the *cut* promoter and enhancer. The suppression of this phenotype was first thought to be due to the null *dFmr1* mutation, however suppression of this phenotype was subsequently characterized in genotypes with wild-type *dFmr1*, implying that dFMRP is unrelated to this phenotype. During this study, whole genome sequencing was used to determine whether or not other insulator sequences or other genes were affected in the *dFmr1*^{3} background. Sequencing revealed the presence of thousands of single nucleotide polymorphisms, some of which have been previously described but the majority are novel SNPs with unknown consequences. Many insertions/deletions were noted as well, spread throughout the genome. Of particular relevance, mutations were noted in the coding regions of several genes we had been trying to study interactions with, including the insulator complex genes *mod(mdg)4*, *ctcf*, GAGA/*trl*, and *beaf-32*. Mutations were also found in genes for key regulator proteins that influence the DNA damage response and cell cycle progression such as the PP2A subunit *twins* (*tws*). Our results here were recently corroborated by research performed with another null *dFmr1* allele, *dFmr1*$^{\Delta 50M}$. This null allele is commonly used in the fruit fly fragile-X model system as a means to knock out dFMRP activity; however, this genotype is also riddled with second-site mutations that influence the phenotypes that have so far been blamed on the lack of dFMRP. Specifically, these researchers found 8 quantitative trait loci that were responsible for promoting supernumerary synapse formation in the brain (Kennedy *et al.*, 2020). These similar results from two different mutations of *dFmr1* that had been maintained independently for nearly two decades seem to indicate that *dFmr1* mutants are prone to accumulation of second-site mutations. Whether this is related to DNA damage that goes

unresolved in the absence or dFMRP or is the consequence of the lack of translational regulation that occurs without dFMRP is still unknown.

Previous research has implicated dFMRP in the DNA damage response and we were able to observe high rates of mutation in our null *dFmr1*^{3} background. This led us to test genome stability in the absence of dFMRP by examining mitotic chromosomes in dividing larval neuroblasts. These are neural stem cells that give rise to differentiated neurons and glia and provide a reliable source of metaphase chromosomes. As we hypothesized that dFMRP and Su(Hw) were functioning together, this experiment was performed in null mutant backgrounds of each gene and with a *su(Hw)*^{e04061} *dFmr1*^{3} double mutant. While initial results suggested that mutation of both genes together was responsible for the appearance of chromosomal aberrations (CABs), further testing revealed that the aberrations were due to mutation of *su(Hw)* alone. This is based on the finding that mutation of *dFmr1* alone does not cause CAB formation and that mutation of *dFmr1* in the *su(Hw)*^{e04061} background has no effect on CAB frequency (data not shown).

Discussion

In the course of our experiments we were able to develop two new rabbit polyclonal antibodies against the N-terminal region of dFMRP. We demonstrated that the antibody was specific to dFMRP in western blots and immunostains of diploid cells. However, we were unable to use these antibodies to image nuclear dFMRP in diploid cells, and results in polytene nuclei were unreliable due to non-specific binding. We continued our efforts to visualize nuclear dFMRP by immunostaining and live-cell imaging but were never able to record any significant chromatin-bound dFMRP. Of special interest, mutation of *dFmr1* was strongly associated with decreased nuclear Su(Hw) signal in diploid brain cells, indicating a potential genetic interaction. Su(Hw) expression is relatively high in the neuroblast stem cells that give rise to the more differentiated cells of the brain and decreases as cells become differentiated neurons and glia. One

hypothetical model is that dFMRP is negatively regulating the expression of a factor that would typically repress *su(Hw)* expression. Such a case would not be surprising given the wide range of targets dFMRP is responsible for regulating (Bassell and Warren, 2008). In the absence of dFMRP this factor may then become expressed and affect the expression of *su(Hw)* and potentially other genes. Further experiments will be needed to determine whether this model is correct or if there is a more direct relationship between dFMRP and Su(Hw) such as co-operative binding in chromatin. Initial experiments in *dFmr1*^{3} *su(Hw)*^{e04061} double mutants revealed CABs in dividing larval neuroblasts. While these aberrations were unrelated to the *dFmr1*^{3} mutation and were, in fact, due to mutation of *su(Hw)*, these experiments provided the basis for the remainder of the research presented here.

Final Conclusions

We have shown that Su(Hw) is essential for maintaining genome stability and we have characterized its relationship with the sole H2A variant described in *Drosophila*. We show that Su(Hw) and γH2Av colocalize throughout the genome and that *His2Av* contributes to *gypsy* insulator function in chromatin and in insulator bodies. We observe significantly less H2Av phosphorylation in the absence of Su(Hw), however, lack of H2Av has little effect on the recruitment or stability of insulator proteins in chromatin. We propose a model from these findings in which phosphorylation of H2Av is stabilized by an intact insulator complex and that this contributes to the function of the insulator itself. Kinase and phosphatase activity targeted to H2Av may act to regulate the activity of insulator complexes. Perhaps the most visceral manifestation of this interaction is the suppression of the melanotic tumor phenotype seen in *His2Av* mutants. These tumors are thought to result from the lack of transcriptional regulation brought about by *His2Av* mutation and is not related to the DNA damage response roles of H2Av. We conclude that Su(Hw) may be influencing the expression of genes in the same pathway as H2Av, and that mutation of *su(Hw)* and *His2Av* in the same tissue restores the proper expression program, thereby preventing tumor formation. In addition to this, the interaction between H2Av and Su(Hw) clearly regulates the growth of larval lymph glands and likely the differentiation of hemocytes. This points to converging pathways of transcriptional regulation of key developmental genes in this tissue and future experiments will seek to unravel the molecular mechanism behind this interaction. Future experiments may also test to see if this interaction is conserved in the other tissues H2Av function is known to regulate or if this is specific to the lymph gland.

References

Abbott, DW, VS Ivanova, X Wang, WM Bonner and J Ausió (2001). "Characterization of the Stability and Folding of H2A.Z Chromatin Particles: IMPLICATIONS FOR TRANSCRIPTIONAL ACTIVATION*." *Journal of Biological Chemistry* **276**(45): 41945-41949. DOI: 10.1074/jbc.M108217200.

Adam, M, F Robert, M Larochelle and L Gaudreau (2001). "H2A.Z is required for global chromatin integrity and for recruitment of RNA polymerase II under specific conditions." *Mol Cell Biol* **21**(18): 6270-6279. DOI: 10.1128/mcb.21.18.6270-6279.2001.

Adler, J and I Parmryd (2010). "Quantifying colocalization by correlation: the Pearson correlation coefficient is superior to the Mander's overlap coefficient." *Cytometry A* **77**(8): 733-742. DOI: 10.1002/cyto.a.20896.

Adryan, B, G Woerfel, I Birch-Machin, S Gao, M Quick, L Meadows, S Russell and R White (2007). "Genomic mapping of Suppressor of Hairy-wing binding sites in Drosophila." *Genome Biol* **8**(8): R167. DOI: 10.1186/gb-2007-8-8-r167.

Afgan, E, D Baker, B Batut, M van den Beek, D Bouvier, M Cech, J Chilton, D Clements, N Coraor, BA Gruning, A Guerler, J Hillman-Jackson, S Hiltemann, V Jalili, H Rasche, N Soranzo, J Goecks, J Taylor, A Nekrutenko and D Blankenberg (2018). "The Galaxy platform for accessible, reproducible and collaborative biomedical analyses: 2018 update." *Nucleic Acids Res* **46**(W1): W537-W544. DOI: 10.1093/nar/gky379.

Albert, I, TN Mavrich, LP Tomsho, J Qi, SJ Zanton, SC Schuster and BF Pugh (2007). "Translational and rotational settings of H2A.Z nucleosomes across the Saccharomyces cerevisiae genome." *Nature* **446**(7135): 572-576. DOI: 10.1038/nature05632.

Alekseyenko, AA, AA Gorchakov, BM Zee, SM Fuchs, PV Kharchenko and MI Kuroda (2014). "Heterochromatin-associated interactions of Drosophila HP1a with dADD1, HIPP1, and repetitive RNAs." *Genes Dev* **28**(13): 1445-1460. DOI: 10.1101/gad.241950.114.

Alpatov, R, BJ Lesch, M Nakamoto-Kinoshita, A Blanco, S Chen, A Stutzer, KJ Armache, MD Simon, C Xu, M Ali, J Murn, S Prisic, TG Kutateladze, CR Vakoc, J Min, RE Kingston, W Fischle, ST Warren, DC Page and Y Shi (2014). "A chromatin-dependent role of the fragile X mental retardation protein FMRP in the DNA damage response." *Cell* **157**(4): 869-881. DOI: 10.1016/j.cell.2014.03.040.

Andreyeva, EN, TD Kolesnikova, ES Belyaeva, RL Glaser and IF Zhimulev (2008). "Local DNA underreplication correlates with accumulation of phosphorylated H2Av in the Drosophila melanogaster polytene chromosomes." *Chromosome Research* **16**(6): 851-862. DOI: 10.1007/s10577-008-1244-4.

Antar, LN and GJ Bassell (2003). "Sunrise at the synapse: the FMRP mRNP shaping the synaptic interface." *Neuron* **37**(4): 555-558. DOI: 10.1016/s0896-6273(03)00090-4.

Armache, A, S Yang, A Martínez de Paz, LE Robbins, C Durmaz, JQ Cheong, A Ravishankar, AW Daman, DJ Ahimovic, T Klevorn, Y Yue, T Arslan, S Lin, T Panchenko, J Hrit, M Wang, S Thudium, BA Garcia, E Korb, K-J Armache, SB Rothbart, SB Hake, CD Allis, H Li and SZ Josefowicz (2020). "Histone H3.3 phosphorylation amplifies stimulation-induced transcription." *Nature* **583**(7818): 852-857. DOI: 10.1038/s41586-020-2533-0.

Baek, Y-S, S Haas, H Hackstein, G Bein, M Hernandez-Santana, H Lehrach, S Sauer and H Seitz (2009). "Identification of novel transcriptional regulators involved in macrophage differentiation and activation in U937 cells." *BMC Immunology* **10**(1): 18. DOI: 10.1186/1471-2172-10-18.

Bag, I, RK Dale, C Palmer and EP Lei (2019). "The zinc-finger protein CLAMP promotes gypsy chromatin insulator function in Drosophila (doi:10.1242/jcs.226092)." *J Cell Sci* **132**(6). DOI: 10.1242/jcs.231977.

Bagchi, DN, AM Battenhouse, D Park and VR Iyer (2019). "The histone variant H2A.Z in yeast is almost exclusively incorporated into the +1 nucleosome in the direction of transcription." *Nucleic Acids Research* **48**(1): 157-170. DOI: 10.1093/nar/gkz1075.

Baldi, S and PB Becker (2013). "The variant histone H2A.V of Drosophila--three roles, two guises." *Chromosoma* **122**(4): 245-258. DOI: 10.1007/s00412-013-0409-x.

Baldi, S, DS Jain, L Harpprecht, A Zabel, M Scheibe, F Butter, T Straub and PB Becker (2018). "Genome-wide Rules of Nucleosome Phasing in Drosophila." *Mol Cell* **72**(4): 661-672 e664. DOI: 10.1016/j.molcel.2018.09.032.

Banerjee, U, JR Girard, LM Goins and CM Spratford (2019). "*Drosophila* as a Genetic Model for Hematopoiesis." *Genetics* **211**(2): 367-417. DOI: 10.1534/genetics.118.300223.

Bassell, GJ and ST Warren (2008). "Fragile X syndrome: loss of local mRNA regulation alters synaptic development and function." *Neuron* **60**(2): 201-214. DOI: 10.1016/j.neuron.2008.10.004.

Baxley, RM, JD Bullard, MW Klein, AG Fell, JA Morales-Rosado, T Duan and PK Geyer (2017). "Deciphering the DNA code for the function of the Drosophila polydactyl zinc finger protein Suppressor of Hairy-wing." *Nucleic Acids Res* **45**(8): 4463-4478. DOI: 10.1093/nar/gkx040.

Baxley, RM, AA Soshnev, DE Koryakov, IF Zhimulev and PK Geyer (2011). "The role of the Suppressor of Hairy-wing insulator protein in Drosophila oogenesis." *Dev Biol* **356**(2): 398-410. DOI: 10.1016/j.ydbio.2011.05.666.

Bazzi, M, D Mantiero, C Trovesi, G Lucchini and MP Longhese (2010). "Dephosphorylation of gamma H2A by Glc7/protein phosphatase 1 promotes recovery from inhibition of DNA replication." *Mol Cell Biol* **30**(1): 131-145. DOI: 10.1128/mcb.01000-09.

Bell, AC, GG West and G Felsenfeld (1999). "The Protein CTCF Is Required for the Enhancer Blocking Activity of Vertebrate Insulators." *Cell* **98**(3): 387 - 396. DOI: 10.1016/s0092-8674(00)81967-4.

Bialojan, C and A Takai (1988). "Inhibitory effect of a marine-sponge toxin, okadaic acid, on protein phosphatases. Specificity and kinetics." *Biochemical Journal* **256**(1): 283-290. DOI: 10.1042/bj2560283.

Billon, P and J Côté (2013). "Precise deposition of histone H2A.Z in chromatin for genome expression and maintenance." *Biochim Biophys Acta* **1819**(3-4): 290-302. DOI: 10.1016/j.bbagrm.2011.10.004.

Bonchuk, A, O Maksimenko, O Kyrchanova, T Ivlieva, V Mogila, G Deshpande, D Wolle, P Schedl and P Georgiev (2015). "Functional role of dimerization and CP190 interacting domains of CTCF protein in Drosophila melanogaster." *BMC Biol* **13**: 63. DOI: 10.1186/s12915-015-0168-7.

Brunelle, M, A Nordell Markovits, S Rodrigue, M Lupien, P Jacques and N Gévry (2015). "The histone variant H2A.Z is an important regulator of enhancer activity." *Nucleic Acids Res* **43**(20): 9742-9756. DOI: 10.1093/nar/gkv825.

Burma, S, BP Chen, M Murphy, A Kurimasa and DJ Chen (2001). "ATM phosphorylates histone H2AX in response to DNA double-strand breaks." *J Biol Chem* **276**(45): 42462-42467. DOI: 10.1074/jbc.C100466200.

Bushey, AM, E Ramos and VG Corces (2009). "Three subclasses of a Drosophila insulator show distinct and cell type-specific genomic distributions." *Genes Dev* **23**(11): 1338-1350. DOI: 10.1101/gad.1798209.

Cai, HN and M Levine (1997). "The gypsy insulator can function as a promoter-specific silencer in the Drosophila embryo." *The EMBO Journal* **16**: 1732-1741. DOI: 10.1093/emboj/16.7.1732.

Canela, A, Y Maman, S Jung, N Wong, E Callen, A Day, KR Kieffer-Kwon, A Pekowska, H Zhang, SSP Rao, SC Huang, PJ McKinnon, PD Aplan, Y Pommier, EL Aiden, R Casellas and A Nussenzweig (2017). "Genome Organization Drives Chromosome Fragility." *Cell* **170**(3): 507-521 e518. DOI: 10.1016/j.cell.2017.06.034.

Cermelli, S, Y Guo, SP Gross and MA Welte (2006). "The lipid-droplet proteome reveals that droplets are a protein-storage depot." *Curr Biol* **16**(18): 1783-1795. DOI: 10.1016/j.cub.2006.07.062.

Chen, D, M Brovkina, LH Matzat and EP Lei (2019). "Shep RNA-Binding Capacity Is Required for Antagonism of gypsy Chromatin Insulator Activity." *G3 (Bethesda)* **9**(3): 749-754. DOI: 10.1534/g3.118.200923.

Chen, F, V Archambault, A Kar, P Lio, PP D'Avino, R Sinka, K Lilley, ED Laue, P Deak, L Capalbo and DM Glover (2007). "Multiple protein phosphatases are required for mitosis in Drosophila." *Curr Biol* **17**(4): 293-303. DOI: 10.1016/j.cub.2007.01.068.

Chen, HT, A Bhandoola, MJ Difilippantonio, J Zhu, MJ Brown, X Tai, EP Rogakou, TM Brotz, WM Bonner, T Ried and A Nussenzweig (2000). "Response to RAG-mediated VDJ cleavage by NBS1 and gamma-H2AX." *Science* **290**(5498): 1962-1965. DOI: 10.1126/science.290.5498.1962.

Chen, Y, N Negre, Q Li, JO Mieczkowska, M Slattery, T Liu, Y Zhang, T-K Kim, HH He, J Zieba, Y Ruan, PJ Bickel, RM Myers, BJ Wold, KP White, JD Lieb and XS Liu (2012). "Systematic evaluation of factors influencing ChIP-seq fidelity." *Nature methods* **9**(6): 609-614. DOI: 10.1038/nmeth.1985.

Choksi, SP, TD Southall, T Bossing, K Edoff, E de Wit, BE Fischer, B van Steensel, G Micklem and AH Brand (2006). "Prospero acts as a binary switch between self-renewal and differentiation in Drosophila neural stem cells." *Dev Cell* **11**(6): 775-789. DOI: 10.1016/j.devcel.2006.09.015.

Chowdhury, D, MC Keogh, H Ishii, CL Peterson, S Buratowski and J Lieberman (2005). "gamma-H2AX dephosphorylation by protein phosphatase 2A facilitates DNA double-strand break repair." *Mol Cell* **20**(5): 801-809. DOI: 10.1016/j.molcel.2005.10.003.

Ciaccio, C, L Fontana, D Milani, S Tabano, M Miozzo and S Esposito (2017). "Fragile X syndrome: a review of clinical and molecular diagnoses." *Ital J Pediatr* **43**(1): 39. DOI: 10.1186/s13052-017-0355-y.

Clarkson, MJ, JRE Wells, F Gibson, R Saint and DJ Tremethick (1999). "Regions of variant histone His2AvD required for Drosophila development." *Nature* **399**(6737): 694-697. DOI: 10.1038/21436.

Collins, BE, CB Greer, BC Coleman and JD Sweatt (2019). "Histone H3 lysine K4 methylation and its role in learning and memory." *Epigenetics & Chromatin* **12**(1): 7. DOI: 10.1186/s13072-018-0251-8.

Cook, RK, SJ Christensen, JA Deal, RA Coburn, ME Deal, JM Gresens, TC Kaufman and KR Cook (2012). "The generation of chromosomal deletions to provide extensive coverage and subdivision of the Drosophila melanogaster genome." *Genome Biol* **13**(3): R21. DOI: 10.1186/gb-2012-13-3-r21.

Costes, SV, D Daelemans, EH Cho, Z Dobbin, G Pavlakis and S Lockett (2004). "Automatic and quantitative measurement of protein-protein colocalization in live cells." *Biophys J* **86**(6): 3993-4003. DOI: 10.1529/biophysj.103.038422.

Dann, GP, GP Liszczak, JD Bagert, MM Müller, UTT Nguyen, F Wojcik, ZZ Brown, J Bos, T Panchenko, R Pihl, SB Pollock, KL Diehl, CD Allis and TW Muir (2017). "ISWI chromatin remodellers sense nucleosome modifications to determine substrate preference." *Nature* **548**(7669): 607-611. DOI: 10.1038/nature23671.

Dhillon, N and RT Kamakaka (2000). "A histone variant, Htz1p, and a Sir1p-like protein, Esc2p, mediate silencing at HMR." *Mol Cell* **6**(4): 769-780. DOI: 10.1016/s1097-2765(00)00076-9.

Dictenberg, JB, SA Swanger, LN Antar, RH Singer and GJ Bassell (2008). "A direct role for FMRP in activity-dependent dendritic mRNA transport links filopodial-spine morphogenesis to fragile X syndrome." *Dev Cell* **14**(6): 926-939. DOI: 10.1016/j.devcel.2008.04.003.

Difilippantonio, S, A Celeste, O Fernandez-Capetillo, HT Chen, B Reina San Martin, F Van Laethem, YP Yang, GV Petukhova, M Eckhaus, L Feigenbaum, K Manova, M Kruhlak, RD Camerini-Otero, S Sharan, M Nussenzweig and A Nussenzweig (2005). "Role of Nbs1 in the activation of the Atm kinase revealed in humanized mouse models." *Nat Cell Biol* **7**(7): 675-685. DOI: 10.1038/ncb1270.

Do, TV, J Hirst, S Hyter, KF Roby and AK Godwin (2017). "Aurora A kinase regulates non-homologous end-joining and poly(ADP-ribose) polymerase function in ovarian carcinoma cells." *Oncotarget* **8**(31): 50376-50392. DOI: 10.18632/oncotarget.18970.

Docquier, F, D Farrar, V D'Arcy, I Chernukhin, AF Robinson, D Loukinov, S Vatolin, S Pack, A Mackay, RA Harris, H Dorricott, MJ O'Hare, V Lobanenkov and E Klenova (2005). "Heightened Expression of CTCF in Breast Cancer Cells Is Associated with Resistance to Apoptosis." **65**(12): 5112-5122. DOI: 10.1158/0008-5472.CAN-03-3498 %J Cancer Research.

Donahue, PR, DK Palmer, JM Condie, LM Sabatini and M Blumenfeld (1986). "Drosophila histone H2A.2 is associated with the interbands of polytene chromosomes." *Proc Natl Acad Sci U S A* **83**(13): 4744-4748. DOI: 10.1073/pnas.83.13.4744.

Douglas, P, J Zhong, R Ye, GB Moorhead, X Xu and SP Lees-Miller (2010). "Protein phosphatase 6 interacts with the DNA-dependent protein kinase catalytic subunit and dephosphorylates gamma-H2AX." *Mol Cell Biol* **30**(6): 1368-1381. DOI: 10.1128/mcb.00741-09.

Downs, JA, NF Lowndes and SP Jackson (2000). "A role for Saccharomyces cerevisiae histone H2A in DNA repair." *Nature* **408**(6815): 1001-1004. DOI: 10.1038/35050000.

Doyon, Y and J Côté (2004). "The highly conserved and multifunctional NuA4 HAT complex." *Curr Opin Genet Dev* **14**(2): 147-154. DOI: 10.1016/j.gde.2004.02.009.

Duan, T and PK Geyer (2018). "Spermiogenesis and Male Fertility Require the Function of Suppressor of Hairy-Wing in Somatic Cyst Cells of Drosophila." *Genetics* **209**(3): 757-772. DOI: 10.1534/genetics.118.301088.

Dubowy, C and A Sehgal (2017). "Circadian Rhythms and Sleep in Drosophila melanogaster." *Genetics* **205**(4): 1373-1397. DOI: 10.1534/genetics.115.185157.

Dunn, KW, MM Kamocka and JH McDonald (2011). "A practical guide to evaluating colocalization in biological microscopy." *Am J Physiol Cell Physiol* **300**(4): C723-742. DOI: 10.1152/ajpcell.00462.2010.

Eleuteri, B, S Aranda and P Ernfors (2018). "NoRC Recruitment by H2A.X Deposition at rRNA Gene Promoter Limits Embryonic Stem Cell Proliferation." *Cell Reports* **23**(6): 1853-1866. DOI: 10.1016/j.celrep.2018.04.023.

Fernandez-Capetillo, O, HT Chen, A Celeste, I Ward, PJ Romanienko, JC Morales, K Naka, Z Xia, RD Camerini-Otero, N Motoyama, PB Carpenter, WM Bonner, J Chen and A Nussenzweig (2002). "DNA damage-induced G2-M checkpoint activation by histone H2AX and 53BP1." *Nat Cell Biol* **4**(12): 993-997. DOI: 10.1038/ncb884.

Fernandez-Capetillo, O, SK Mahadevaiah, A Celeste, PJ Romanienko, RD Camerini-Otero, WM Bonner, K Manova, P Burgoyne and A Nussenzweig (2003). "H2AX is required for chromatin remodeling and

inactivation of sex chromosomes in male mouse meiosis." *Dev Cell* **4**(4): 497-508. DOI: 10.1016/s1534-5807(03)00093-5.

Flegel, K, O Grushko, K Bolin, E Griggs and L Buttitta (2016). "Roles for the Histone Modifying and Exchange Complex NuA4 in Cell Cycle Progression in Drosophila melanogaster." *Genetics* **203**(3): 1265-1281. DOI: 10.1534/genetics.116.188581.

Frydrychova, RC, JM Mason and TK Archer (2008). "HP1 is distributed within distinct chromatin domains at Drosophila telomeres." *Genetics* **180**(1): 121-131. DOI: 10.1534/genetics.108.090647.

Fu, Y-H, DPA Kuhl, A Pizzuti, M Pieretti, JS Sutcliffe, S Richards, AJMH Verkert, JJA Holden, RG Fenwick, ST Warren, BA Oostra, DL Nelson and CT Caskey (1991). "Variation of the CGG repeat at the fragile X site results in genetic instability: Resolution of the Sherman paradox." *Cell* **67**(6): 1047-1058. DOI: 10.1016/0092-8674(91)90283-5.

Fudenberg, G, M Imakaev, C Lu, A Goloborodko, N Abdennur and LA Mirny (2016). "Formation of Chromosomal Domains by Loop Extrusion." *Cell Rep* **15**(9): 2038-2049. DOI: 10.1016/j.celrep.2016.04.085.

Fujioka, M, G Sun and JB Jaynes (2013). "The Drosophila eve insulator Homie promotes eve expression and protects the adjacent gene from repression by polycomb spreading." *PLoS Genet* **9**(10): e1003883. DOI: 10.1371/journal.pgen.1003883.

Fuller, MT and AC Spradling (2007). "Male and female Drosophila germline stem cells: two versions of immortality." *Science* **316**(5823): 402-404. DOI: 10.1126/science.1140861.

Galko, MJ and MA Krasnow (2004). "Cellular and genetic analysis of wound healing in Drosophila larvae." *PLoS Biol* **2**(8): E239. DOI: 10.1371/journal.pbio.0020239.

Gatti, M and ML Goldberg (1991). "Mutations affecting cell division in Drosophila." *Methods Cell Biol* **35**: 543-586. DOI: 10.1016/s0091-679x(08)60587-7.

Gause, M, P Morcillo and D Dorsett (2001). "Insulation of enhancer-promoter communication by a gypsy transposon insert in the Drosophila cut gene: cooperation between suppressor of hairy-wing and modifier of mdg4 proteins." *Mol Cell Biol* **21**(14): 4807-4817. DOI: 10.1128/MCB.21.14.4807-4817.2001.

Gdula, DA, TI Gerasimova and VG Corces (1996). "Genetic and molecular analysis of the gypsy chromatin insulator of Drosophila." *Proc Natl Acad Sci U S A* **93**: 9378-9383.

Gehre, M, D Bunina, S Sidoli, MJ Lübke, N Diaz, M Trovato, BA Garcia, JB Zaugg and KM Noh (2020). "Lysine 4 of histone H3.3 is required for embryonic stem cell differentiation, histone enrichment at regulatory regions and transcription accuracy." *Nat Genet* **52**(3): 273-282. DOI: 10.1038/s41588-020-0586-5.

Georgiev, P and M Kozycina (1996). "Interaction Between Mutations in the *suppressor of Hairy wing* and *modifier of mdg4* Genes of *Drosophila melanogaster* Affecting the Phenotype of *gypsy*-Induced Mutations." *Genetics* **142**(2): 425-436.

Gerasimova, TI, K Byrd and VG Corces (2000). "A Chromatin Insulator Determines the Nuclear Localization of DNA." *Molecular Cell* **6**(5): 1025-1035. DOI: 10.1016/S1097-2765(00)00101-5.

Gerasimova, TI and VG Corces (1998). "Polycomb and trithorax group proteins mediate the function of a chromatin insulator." *Cell* **92**: 511 - 521. DOI: 10.1016/s0092-8674(00)80944-7.

Gerasimova, TI, EP Lei, AM Bushey and VG Corces (2007). "Coordinated control of dCTCF and gypsy chromatin insulators in Drosophila." *Mol Cell* **28**(5): 761-772. DOI: 10.1016/j.molcel.2007.09.024.

Geyer, PK and VG Corces (1992). "DNA position-specific repression of transcription by a Drosophila zinc finger protein." *Genes & Development* **6**: 1865-1873.

Ghosh, D, TI Gerasimova and VG Corces (2001). "Interactions between the Su(Hw) and Mod(mdg4) proteins required for gypsy insulator function." *The EMBO Journal* **20**: 2518-2527. DOI: 10.1093/emboj/20.10.2518.

Giaimo, BD, F Ferrante, A Herchenrother, SB Hake and T Borggrefe (2019). "The histone variant H2A.Z in gene regulation." *Epigenetics Chromatin* **12**(1): 37. DOI: 10.1186/s13072-019-0274-9.

Glenn, SE and PK Geyer (2019). "Investigation of the Developmental Requirements of Drosophila HP1 and Insulator Protein Partner, HIPP1." *G3 (Bethesda)* **9**(2): 345-357. DOI: 10.1534/g3.118.200705.

Goldberg, M, M Stucki, J Falck, D D'Amours, D Rahman, D Pappin, J Bartek and SP Jackson (2003). "MDC1 is required for the intra-S-phase DNA damage checkpoint." *Nature* **421**(6926): 952-956. DOI: 10.1038/nature01445.

Goldman, JA, JD Garlick and RE Kingston (2010). "Chromatin remodeling by imitation switch (ISWI) class ATP-dependent remodelers is stimulated by histone variant H2A.Z." *J Biol Chem* **285**(7): 4645-4651. DOI: 10.1074/jbc.M109.072348.

Golovnin, A, L Melnikova, I Shapovalov, M Kostyuchenko and P Georgiev (2015). "EAST Organizes Drosophila Insulator Proteins in the Interchromosomal Nuclear Compartment and Modulates CP190 Binding to Chromatin." *PLoS One* **10**(10): e0140991. DOI: 10.1371/journal.pone.0140991.

Golovnin, A, I Volkov and P Georgiev (2012). "SUMO conjugation is required for the assembly of Drosophila Su(Hw) and Mod(mdg4) into insulator bodies that facilitate insulator complex formation." *J Cell Sci* **125**(Pt 8): 2064-2074. DOI: 10.1242/jcs.100172.

Golovnin, AK, VV Molodina, PG Georgiev and LS Melnikova (2016). "Zinc finger domain of Su(Hw) protein is required for the formation of functional Su(Hw)-dependent insulator complex." *Dokl Biochem Biophys* **469**(1): 247-252. DOI: 10.1134/S1607672916040049.

Gomes, R, RE Karess, H Ohkura, DM Glover and CE Sunkel (1993). "Abnormal anaphase resolution (aar): a locus required for progression through mitosis in Drosophila." *Journal of Cell Science* **104**(2): 583-593. DOI: 10.1242/jcs.104.2.583.

Grigorian, M, H DeBruhl and JS Lipsick (2017). "The role of variant histone H2AV in Drosophila melanogaster larval hematopoiesis." *Development* **144**(8): 1441-1449. DOI: 10.1242/dev.142729.

Guerrero, PA and KA Maggert (2011). "The CCCTC-binding factor (CTCF) of Drosophila contributes to the regulation of the ribosomal DNA and nucleolar stability." *PLoS One* **6**(1): e16401. DOI: 10.1371/journal.pone.0016401.

Guo, YA, MM Chang, W Huang, WF Ooi, M Xing, P Tan and AJ Skanderup (2018). "Mutation hotspots at CTCF binding sites coupled to chromosomal instability in gastrointestinal cancers." *Nat Commun* **9**(1): 1520. DOI: 10.1038/s41467-018-03828-2.

Han, D, Q Chen, J Shi, F Zhang and X Yu (2017). "CTCF participates in DNA damage response via poly(ADP-ribosyl)ation." *Sci Rep* **7**: 43530. DOI: 10.1038/srep43530.

Hanai, K, H Furuhashi, T Yamamoto, K Akasaka and S Hirose (2008). "RSF governs silent chromatin formation via histone H2Av replacement." *PLoS Genet* **4**(2): e1000011. DOI: 10.1371/journal.pgen.1000011.

Harrison, DA, DA Gdula, RS Coyne and VG Corces (1993). "A Leucine Zipper Domain of the Suppressor of Hairy-wing Protein Mediates Its Repressive Effect on Enhancer Function." *Genes & Development* **7**(10): 1966-1978.

Harrison, DA, PK Geyer, C Spana and VG Corces (1989). "The gypsy retrotransposon of Drosophila melanogaster: mechanisms of mutagenesis and interaction with the suppressor of Hairy-wing locus." *Dev Genet* **10**(3): 239-248. DOI: 10.1002/dvg.1020100313.

Harrison, DA, MA Mortin and VG Corces (1992). "The RNA polymerase II 15-kilodalton subunit is essential for viability in Drosophila melanogaster." *Molecular and Cellular Biology* **12**(3): 928-935. DOI: 10.1128/mcb.12.3.928.

Hartenstein, V and JW Posakony (1989). "Development of adult sensilla on the wing and notum of Drosophila melanogaster." *Development* **107**(2): 389-405.

Haystead, TAJ, ATR Sim, D Carling, RC Honnor, Y Tsukitani, P Cohen and DG Hardie (1989). "Effects of the tumour promoter okadaic acid on intracellular protein phosphorylation and metabolism." *Nature* **337**(6202): 78-81. DOI: 10.1038/337078a0.

Heger, P and T Wiehe (2014). "New tools in the box: an evolutionary synopsis of chromatin insulators." *Trends Genet* **30**(5): 161-171. DOI: 10.1016/j.tig.2014.03.004.

Henikoff, S and MM Smith (2015). "Histone variants and epigenetics." *Cold Spring Harb Perspect Biol* **7**(1): a019364. DOI: 10.1101/cshperspect.a019364.

Hilmi, K, M Jangal, M Marques, T Zhao, A Saad, C Zhang, VM Luo, A Syme, C Rejon, Z Yu, A Krum, MR Rabian, S Richard, M Alaoui-Jamali, A Orthwein, L McCaffrey and M Witcher (2017). "CTCF facilitates DNA double-strand break repair by enhancing homologous recombination repair." *Science Advances* **3**(e1601898): 1-14.

Honkanen, RE and T Golden (2002). "Regulators of Serine Threonine Protein Phosphatases at the Dawn of a Clinical Era." *Current Medicinal Chemistry* **9**: 2055-2075. DOI: 10.2174/0929867023368836.

Hoskins, RA, JW Carlson, KH Wan, S Park, I Mendez, SE Galle, BW Booth, BD Pfeiffer, RA George, R Svirskas, M Krzywinski, J Schein, MC Accardo, E Damia, G Messina, M Mendez-Lago, B de Pablos, OV Demakova, EN Andreyeva, LV Boldyreva, M Marra, AB Carvalho, P Dimitri, A Villasante, IF Zhimulev, GM Rubin, GH Karpen and SE Celniker (2015). "The Release 6 reference sequence of the Drosophila melanogaster genome." *Genome Res* **25**(3): 445-458. DOI: 10.1101/gr.185579.114.

Hsu, SJ, MP Plata, B Ernest, S Asgarifar and M Labrador (2015). "The insulator protein Suppressor of Hairy wing is required for proper ring canal development during oogenesis in Drosophila." *Dev Biol* **403**(1): 57-68. DOI: 10.1016/j.ydbio.2015.03.024.

Hsu, SJ, EC Stow, JR Simmons, HA Wallace, AM Lopez, S Stroud and M Labrador (2020). "Mutations in the insulator protein Suppressor of Hairy wing induce genome instability." *Chromosoma* **129**(3-4): 255-274. DOI: 10.1007/s00412-020-00743-8.

Ikeshima-Kataoka, H, JB Skeath, Y Nabeshima, CQ Doe and F Matsuzaki (1997). "Miranda directs Prospero to a daughter cell during Drosophila asymmetric divisions." *Nature* **390**(6660): 625-629. DOI: 10.1038/37641.

Ikura, M, K Furuya, A Fukuto, R Matsuda, J Adachi, T Matsuda, A Kakizuka and T Ikura (2016). "Coordinated Regulation of TIP60 and Poly(ADP-Ribose) Polymerase 1 in Damaged-Chromatin Dynamics." *Mol Cell Biol* **36**(10): 1595-1607. DOI: 10.1128/mcb.01085-15.

Ikura, M, K Furuya, S Matsuda, R Matsuda, H Shima, J Adachi, T Matsuda, T Shiraki and T Ikura (2015). "Acetylation of Histone H2AX at Lys 5 by the TIP60 Histone Acetyltransferase Complex Is Essential for the Dynamic Binding of NBS1 to Damaged Chromatin." *Molecular and Cellular Biology* **35**(24): 4147-4157. DOI: 10.1128/mcb.00757-15.

Ikura, T, VV Ogryzko, M Grigoriev, R Groisman, J Wang, M Horikoshi, R Scully, J Qin and Y Nakatani (2000). "Involvement of the TIP60 histone acetylase complex in DNA repair and apoptosis." *Cell* **102**(4): 463-473. DOI: 10.1016/s0092-8674(00)00051-9.

Ikura, T, S Tashiro, A Kakino, H Shima, N Jacob, R Amunugama, K Yoder, S Izumi, I Kuraoka, K Tanaka, H Kimura, M Ikura, S Nishikubo, T Ito, A Muto, K Miyagawa, S Takeda, R Fishel, K Igarashi and K Kamiya (2007). "DNA damage-dependent acetylation and ubiquitination of H2AX enhances chromatin dynamics." *Mol Cell Biol* **27**(20): 7028-7040. DOI: 10.1128/mcb.00579-07.

Jack, J, D Dorsett, Y Delotto and S Liu (1991). "Expression of the cut locus in the Drosophila wing margin is required for cell type specification and is regulated by a distant enhancer." *Development* **113**: 735-747.

Jack, JW (1985). "Molecular organization of the cut locus of drosophila melanogaster." *Cell* **42**(3): 869-876. DOI: 10.1016/0092-8674(85)90283-1.

Jambhekar, A, A Dhall and Y Shi (2019). "Roles and regulation of histone methylation in animal development." *Nature Reviews Molecular Cell Biology* **20**(10): 625-641. DOI: 10.1038/s41580-019-0151-1.

Jang, JK, DE Sherizen, R Bhagat, EA Manheim and KS McKim (2003). "Relationship of DNA double-strand breaks to synapsis in Drosophila." *J Cell Sci* **116**(Pt 15): 3069-3077. DOI: 10.1242/jcs.00614.

Jeon, H-J, Y-S Kim, J-S Park, J-H Pyo, H-J Na, I-J Kim, C-M Kim, HY Chung, ND Kim, R Arking and M-A Yoo (2015). "Age-related change in γH2AX of Drosophila muscle: its significance as a marker for muscle damage and longevity." *Biogerontology* **16**(4): 503-516. DOI: 10.1007/s10522-015-9573-0.

Jiang, D and F Berger (2017). "Histone variants in plant transcriptional regulation." *Biochim Biophys Acta Gene Regul Mech* **1860**(1): 123-130. DOI: 10.1016/j.bbagrm.2016.07.002.

Jin, Y, Y Wang, DL Walker, H Dong, C Conley, J Johansen and KM Johansen (1999). "JIL-1: a novel chromosomal tandem kinase implicated in transcriptional regulation in Drosophila." *Mol Cell* **4**(1): 129-135. DOI: 10.1016/s1097-2765(00)80195-1.

Johansson, AM, P Stenberg, A Allgardsson and J Larsson (2012). "POF regulates the expression of genes on the fourth chromosome in Drosophila melanogaster by binding to nascent RNA." *Mol Cell Biol* **32**(11): 2121-2134. DOI: 10.1128/mcb.06622-11.

Johnson, MR, RA Stephenson, S Ghaemmaghami and MA Welte (2018). "Developmentally regulated H2Av buffering via dynamic sequestration to lipid droplets in Drosophila embryos." *Elife* **7**. DOI: 10.7554/eLife.36021.

Jox, T, MK Buxa, D Bohla, I Ullah, I Mačinković, A Brehm, M Bartkuhn and R Renkawitz (2017). "Drosophila CP190- and dCTCF-mediated enhancer blocking is augmented by SUMOylation." *Epigenetics & Chromatin* **10**(1): 32. DOI: 10.1186/s13072-017-0140-6.

Joyce, EF, M Pedersen, S Tiong, SK White-Brown, A Paul, SD Campbell and KS McKim (2011). "Drosophila ATM and ATR have distinct activities in the regulation of meiotic DNA damage and repair." *J Cell Biol* **195**(3): 359-367. DOI: 10.1083/jcb.201104121.

Kassis, JA, JA Kennison and JW Tamkun (2017). "Polycomb and Trithorax Group Genes in Drosophila." *Genetics* **206**(4): 1699-1725. DOI: 10.1534/genetics.115.185116.

Kawashima, T, ZJ Lorković, R Nishihama, K Ishizaki, E Axelsson, R Yelagandula, T Kohchi and F Berger (2015). "Diversification of histone H2A variants during plant evolution." *Trends Plant Sci* **20**(7): 419-425. DOI: 10.1016/j.tplants.2015.04.005.

Kellum, R and P Schedl (1991). "A position-effect assay for boundaries of higher order chromosomal domains." *Cell* **64**: 941-950.

Kemp, CJ, JM Moore, R Moser, B Bernard, M Teater, LE Smith, NA Rabaia, KE Gurley, J Guinney, SE Busch, R Shaknovich, VV Lobanenkov, D Liggitt, I Shmulevich, A Melnick and GN Filippova (2014). "CTCF haploinsufficiency destabilizes DNA methylation and predisposes to cancer." *Cell Rep* **7**(4): 1020-1029. DOI: 10.1016/j.celrep.2014.04.004.

Kennedy, T, D Rinker and K Broadie (2020). "Genetic background mutations drive neural circuit hyperconnectivity in a fragile X syndrome model." *BMC Biology* **18**(1): 94. DOI: 10.1186/s12915-020-00817-0.

Keogh, MC, JA Kim, M Downey, J Fillingham, D Chowdhury, JC Harrison, M Onishi, N Datta, S Galicia, A Emili, J Lieberman, X Shen, S Buratowski, JE Haber, D Durocher, JF Greenblatt and NJ Krogan (2006). "A phosphatase complex that dephosphorylates gammaH2AX regulates DNA damage checkpoint recovery." *Nature* **439**(7075): 497-501. DOI: 10.1038/nature04384.

Kiger, AA, H White-Cooper and MT Fuller (2000). "Somatic support cells restrict germline stem cell self-renewal and promote differentiation." *Nature* **407**(6805): 750-754. DOI: 10.1038/35037606.

Kim, J, B Shen, C Rosen and D Dorsett (1996). "The DNA-binding and enhancer-blocking domains of the Drosophila suppressor of Hairy-wing protein." *Molecular and Cellular Biology* **16**(7): 3381-3392.

Kim, J, C Sun, AD Tran, P-J Chin, PD Ruiz, K Wang, RJ Gibbons, MJ Gamble, Y Liu and P Oberdoerffer (2019). "The macroH2A1.2 histone variant links ATRX loss to alternative telomere lengthening." *Nature Structural & Molecular Biology* **26**(3): 213-219. DOI: 10.1038/s41594-019-0192-3.

Kim, MY, S Mauro, N Gévry, JT Lis and WL Kraus (2004). "NAD+-dependent modulation of chromatin structure and transcription by nucleosome binding properties of PARP-1." *Cell* **119**(6): 803-814. DOI: 10.1016/j.cell.2004.11.002.

King, MR, LH Matzat, RK Dale, SJ Lim and EP Lei (2014). "The RNA-binding protein Rumpelstiltskin antagonizes gypsy chromatin insulator function in a tissue-specific manner." *J Cell Sci* **127**(Pt 13): 2956-2966. DOI: 10.1242/jcs.151126.

Klug, WS, D Bodenstein and RC King (1968). "Oogenesis in the suppressor2 of Hairy-wing mutant of Drosophila melanogaster." *Journal of Experiemental Zoology* **167**: 151–156.

Kobor, MS, S Venkatasubrahmanyam, MD Meneghini, JW Gin, JL Jennings, AJ Link, HD Madhani and J Rine (2004). "A protein complex containing the conserved Swi2/Snf2-related ATPase Swr1p deposits histone variant H2A.Z into euchromatin." *PLoS Biol* **2**(5): E131. DOI: 10.1371/journal.pbio.0020131.

Kotova, E, N Lodhi, M Jarnik, AD Pinnola, Y Ji and AV Tulin (2011). "Drosophila histone H2A variant (H2Av) controls poly(ADP-ribose) polymerase 1 (PARP1) activation in chromatin." *Proc Natl Acad Sci U S A* **108**(15): 6205-6210. DOI: 10.1073/pnas.1019644108.

Krzemień, J, R Dubois L Fau - Makki, M Makki R Fau - Meister, A Meister M Fau - Vincent, M Vincent A Fau - Crozatier and M Crozatier (2007). "Control of blood cell homeostasis in Drosophila larvae by the posterior signalling centre." (1476-4687 (Electronic)).

Kuhn-Parnell, EJ, C Helou, DJ Marion, BL Gilmore, TJ Parnell, MS Wold and PK Geyer (2008). "Investigation of the properties of non-gypsy suppressor of hairy-wing-binding sites." *Genetics* **179**(3): 1263-1273. DOI: 10.1534/genetics.108.087254.

Kusch, T, L Florens, WH Macdonald, SK Swanson, RL Glaser, JR Yates, 3rd, SM Abmayr, MP Washburn and JL Workman (2004). "Acetylation by Tip60 is required for selective histone variant exchange at DNA lesions." *Science* **306**(5704): 2084-2087. DOI: 10.1126/science.1103455.

Kusch, T, A Mei and C Nguyen (2014). "Histone H3 lysine 4 trimethylation regulates cotranscriptional H2A variant exchange by Tip60 complexes to maximize gene expression." *Proc Natl Acad Sci U S A* **111**(13): 4850-4855. DOI: 10.1073/pnas.1320337111.

Labrador, M and VG Corces (2002). "Setting the Boundaries of Chromatin Domains and Nuclear Organization." *Cell* **111**(2): 151 - 154. DOI: 10.1016/S0092-8674(02)01004-8.

Lai, WKM and BF Pugh (2017). "Understanding nucleosome dynamics and their links to gene expression and DNA replication." *Nature Reviews Molecular Cell Biology* **18**(9): 548-562. DOI: 10.1038/nrm.2017.47.

Lake, CM, JK Holsclaw, SP Bellendir, J Sekelsky and RS Hawley (2013). "The development of a monoclonal antibody recognizing the Drosophila melanogaster phosphorylated histone H2A variant (gamma-H2AV)." *G3 (Bethesda)* **3**(9): 1539-1543. DOI: 10.1534/g3.113.006833.

Lang, F, X Li, W Zheng, Z Li, D Lu, G Chen, D Gong, L Yang, J Fu, P Shi and J Zhou (2017). "CTCF prevents genomic instability by promoting homologous recombination-directed DNA double-strand break repair." *Proc Natl Acad Sci U S A* **114**(41): 10912-10917. DOI: 10.1073/pnas.1704076114.

Langmead, B and SL Salzberg (2012). "Fast gapped-read alignment with Bowtie 2." *Nat Methods* **9**(4): 357-359. DOI: 10.1038/nmeth.1923.

Lankenau, DH, MV Peluso and S Lankenau (2000). "The Su(Hw) chromatin insulator protein alters double-strand break repair frequencies in the Drosophila germ line." *Chromosoma* **109**(1-2): 148-160. DOI: 10.1007/s004120050423.

LaRocque, JR, B Jaklevic, TT Su and J Sekelsky (2007). "Drosophila ATR in double-strand break repair." *Genetics* **175**(3): 1023-1033. DOI: 10.1534/genetics.106.067330.

Leach, TJ, M Mazzeo, HL Chotkowski, JP Madigan, MG Wotring and RL Glaser (2000). "Histone H2A.Z is widely but nonrandomly distributed in chromosomes of Drosophila melanogaster." *J Biol Chem* **275**(30): 23267-23272. DOI: 10.1074/jbc.M910206199.

Lee, JH and TT Paull (2004). "Direct activation of the ATM protein kinase by the Mre11/Rad50/Nbs1 complex." *Science* **304**(5667): 93-96. DOI: 10.1126/science.1091496.

Li, B, SG Pattenden, D Lee, J Gutiérrez, J Chen, C Seidel, J Gerton and JL Workman (2005). "Preferential occupancy of histone variant H2AZ at inactive promoters influences local histone modifications and chromatin remodeling." *Proc Natl Acad Sci U S A* **102**(51): 18385-18390. DOI: 10.1073/pnas.0507975102.

Li, Y, RL Armstrong, RJ Duronio and DM MacAlpine (2016). "Methylation of histone H4 lysine 20 by PR-Set7 ensures the integrity of late replicating sequence domains in Drosophila." *Nucleic Acids Res* **44**(15): 7204-7218. DOI: 10.1093/nar/gkw333.

Li, Y, C Wang, W Cai, S Sengupta, M Zavortink, H Deng, J Girton, J Johansen and KM Johansen (2017). "H2Av facilitates H3S10 phosphorylation but is not required for heat shock-induced chromatin decondensation or transcriptional elongation." *Development* **144**(18): 3232-3240. DOI: 10.1242/dev.151134.

Li, Z, MR Johnson, Z Ke, L Chen and MA Welte (2014). "Drosophila lipid droplets buffer the H2Av supply to protect early embryonic development." *Curr Biol* **24**(13): 1485-1491. DOI: 10.1016/j.cub.2014.05.022.

Li, Z, K Thiel, PJ Thul, M Beller, RP Kühnlein and MA Welte (2012). "Lipid droplets control the maternal histone supply of Drosophila embryos." *Curr Biol* **22**(22): 2104-2113. DOI: 10.1016/j.cub.2012.09.018.

Liu, S, E McLeod and J Jack (1991). "Four distinct regulatory regions of the cut locus and their effect on cell type specification in Drosophila." *Genetics* **127**(1): 151-159.

Liu, Z, CA Tabuloc, Y Xue, Y Cai, P McIntire, Y Niu, VH Lam, JC Chiu and Y Zhang (2019). "Splice variants of DOMINO control Drosophila circadian behavior and pacemaker neuron maintenance." *PLoS Genet* **15**(10): e1008474. DOI: 10.1371/journal.pgen.1008474.

Lou, Z, K Minter-Dykhouse, X Wu and J Chen (2003). "MDC1 is coupled to activated CHK2 in mammalian DNA damage response pathways." *Nature* **421**(6926): 957-961. DOI: 10.1038/nature01447.

Lowell, JE and GAM Cross (2004). "A variant histone H3 is enriched at telomeres in Trypanosoma brucei." *Journal of Cell Science* **117**(24): 5937-5947. DOI: 10.1242/jcs.01515.

Loyola, A, T Bonaldi, D Roche, A Imhof and G Almouzni (2006). "PTMs on H3 variants before chromatin assembly potentiate their final epigenetic state." *Mol Cell* **24**(2): 309-316. DOI: 10.1016/j.molcel.2006.08.019.

Loyola, A, JY Huang, G LeRoy, S Hu, YH Wang, RJ Donnelly, WS Lane, SC Lee and D Reinberg (2003). "Functional analysis of the subunits of the chromatin assembly factor RSF." *Mol Cell Biol* **23**(19): 6759-6768. DOI: 10.1128/mcb.23.19.6759-6768.2003.

Loyola, A, G LeRoy, YH Wang and D Reinberg (2001). "Reconstitution of recombinant chromatin establishes a requirement for histone-tail modifications during chromatin assembly and transcription." *Genes Dev* **15**(21): 2837-2851. DOI: 10.1101/gad.937401.

Lu, J, M-L Ruhf, N Perrimon and P Leder (2007). "A genome-wide RNA interference screen identifies putative chromatin regulators essential for E2F repression." *Proceedings of the National Academy of Sciences* **104**(22): 9381-9386. DOI: 10.1073/pnas.0610279104.

Luger, K, AW Mäder, RK Richmond, DF Sargent and TJ Richmond (1997). "Crystal structure of the nucleosome core particle at 2.8 A resolution." *Nature* **389**(6648): 251-260. DOI: 10.1038/38444.

Lupiáñez, Darío G, K Kraft, V Heinrich, P Krawitz, F Brancati, E Klopocki, D Horn, H Kayserili, John M Opitz, R Laxova, F Santos-Simarro, B Gilbert-Dussardier, L Wittler, M Borschiwer, Stefan A Haas, M Osterwalder, M Franke, B Timmermann, J Hecht, M Spielmann, A Visel and S Mundlos (2015). "Disruptions of Topological Chromatin Domains Cause Pathogenic Rewiring of Gene-Enhancer Interactions." *Cell* **161**(5): 1012-1025. DOI: 10.1016/j.cell.2015.04.004.

Macurek, L, A Lindqvist, O Voets, J Kool, HR Vos and RH Medema (2010). "Wip1 phosphatase is associated with chromatin and dephosphorylates gammaH2AX to promote checkpoint inhibition." *Oncogene* **29**(15): 2281-2291. DOI: 10.1038/onc.2009.501.

Macůrek, L, A Lindqvist, O Voets, J Kool, HR Vos and RH Medema (2010). "Wip1 phosphatase is associated with chromatin and dephosphorylates gammaH2AX to promote checkpoint inhibition." *Oncogene* **29**(15): 2281-2291. DOI: 10.1038/onc.2009.501.

Madigan, JP, HL Chotkowski and RL Glaser (2002). "DNA double-strand break-induced phosphorylation of Drosophila histone variant H2Av helps prevent radiation-induced apoptosis." *Nucleic Acids Res* **30**(17): 3698 - 3705. DOI: 10.1093/nar/gkf496.

Mahadevaiah, SK, JM Turner, F Baudat, EP Rogakou, P de Boer, J Blanco-Rodríguez, M Jasin, S Keeney, WM Bonner and PS Burgoyne (2001). "Recombinational DNA double-strand breaks in mice precede synapsis." *Nat Genet* **27**(3): 271-276. DOI: 10.1038/85830.

Mandal, L, CJ Martinez-Agosto Ja Fau - Evans, V Evans Cj Fau - Hartenstein, U Hartenstein V Fau - Banerjee and U Banerjee (2007). "A Hedgehog- and Antennapedia-dependent niche maintains Drosophila haematopoietic precursors." (1476-4687 (Electronic)).

Manders, EMM, J Stap, GJ Brakenhoff, R Van Driel and JA Aten (1992). "Dynamics of three-dimensional replication patterns during the S-phase, analysed by double labelling of DNA and confocal microscopy." *J Cell Sci* **103**: 857-862.

Manders, EMM, FJ Verbeek and JA Aten (1993). "Measurement of co-localization of objects in dual-color confocal images." *Journal of Microscopy* **169**: 375-382.

Mannironi, C, WM Bonner and CL Hatch (1989). "H2A.X. a histone isoprotein with a conserved C-terminal sequence, is encoded by a novel mRNA with both DNA replication type and polyA 3' processing signals." *Nucleic Acids Res* **17**(22): 9113-9126. DOI: 10.1093/nar/17.22.9113.

Martire, S and LA Banaszynski (2020). "The roles of histone variants in fine-tuning chromatin organization and function." *Nat Rev Mol Cell Biol* **21**(9): 522-541. DOI: 10.1038/s41580-020-0262-8.

Matzat, LH, RK Dale, N Moshkovich and EP Lei (2012). "Tissue-specific regulation of chromatin insulator function." *PLoS Genet* **8**(11): e1003069. DOI: 10.1371/journal.pgen.1003069.

Mavrich, TN, C Jiang, IP Ioshikhes, X Li, BJ Venters, SJ Zanton, LP Tomsho, J Qi, RL Glaser, SC Schuster, DS Gilmour, I Albert and BF Pugh (2008). "Nucleosome organization in the Drosophila genome." *Nature* **453**(7193): 358-362. DOI: 10.1038/nature06929.

Maxouri, S, S Taraviras and Z Lygerou (2018). "Visualizing the dynamics of histone variants in the S-phase nucleus." *Genome Biology* **19**(1): 182. DOI: 10.1186/s13059-018-1556-4.

Mehrotra, S and KS McKim (2006). "Temporal analysis of meiotic DNA double-strand break formation and repair in Drosophila females." *PLoS Genet* **2**(11): e200. DOI: 10.1371/journal.pgen.0020200.

Melnikova, L, M Kostyuchenko, V Molodina, A Parshikov, P Georgiev and A Golovnin (2017). "Multiple interactions are involved in a highly specific association of the Mod(mdg4)-67.2 isoform with the Su(Hw) sites in Drosophila." *Open Biol* **7**(10). DOI: 10.1098/rsob.170150.

Melnikova, L, M Kostyuchenko, V Molodina, A Parshikov, P Georgiev and A Golovnin (2018). "Interactions between BTB domain of CP190 and two adjacent regions in Su(Hw) are required for the insulator complex formation." *Chromosoma* **127**(1): 59-71. DOI: 10.1007/s00412-017-0645-6.

Melnikova, L, M Kostyuchenko, A Parshikov, P Georgiev and A Golovnin (2018). "Role of Su(Hw) zinc finger 10 and interaction with CP190 and Mod(mdg4) proteins in recruiting the Su(Hw) complex to chromatin sites in Drosophila." *PLoS One* **13**(2): e0193497. DOI: 10.1371/journal.pone.0193497.

Melnikova, L, V Molodina, M Erokhin, P Georgiev and A Golovnin (2019). "HIPP1 stabilizes the interaction between CP190 and Su(Hw) in the Drosophila insulator complex." *Sci Rep* **9**(1): 19102. DOI: 10.1038/s41598-019-55617-6.

Melnikova, L, I Shapovalov, M Kostyuchenko, P Georgiev and A Golovnin (2017). "EAST affects the activity of Su(Hw) insulators by two different mechanisms in Drosophila melanogaster." *Chromosoma* **126**(2): 299-311. DOI: 10.1007/s00412-016-0596-3.

Meneghini, MD, M Wu and HD Madhani (2003). "Conserved histone variant H2A.Z protects euchromatin from the ectopic spread of silent heterochromatin." *Cell* **112**(5): 725-736. DOI: 10.1016/s0092-8674(03)00123-5.

Mengoli, V, E Bucciarelli, R Lattao, R Piergentili, M Gatti and S Bonaccorsi (2014). "The analysis of mutant alleles of different strength reveals multiple functions of topoisomerase 2 in regulation of Drosophila chromosome structure." *PLoS Genet* **10**(10): e1004739. DOI: 10.1371/journal.pgen.1004739.

Merigliano, C, A Marzio, F Renda, MP Somma, M Gatti and F Verni (2017). "A Role for the Twins Protein Phosphatase (PP2A-B55) in the Maintenance of Drosophila Genome Integrity." *Genetics* **205**(3): 1151-1167. DOI: 10.1534/genetics.116.192781.

Merigliano, C, E Mascolo, A Cesta, I Saggio and F Verni (2019). "A new role for Drosophila Aurora-A in maintaining chromosome integrity." *Chromosoma* **128**(1): 41-52. DOI: 10.1007/s00412-018-00687-0.

Mizuguchi, G, X Shen, J Landry, WH Wu, S Sen and C Wu (2004). "ATP-driven exchange of histone H2AZ variant catalyzed by SWR1 chromatin remodeling complex." *Science* **303**(5656): 343-348. DOI: 10.1126/science.1090701.

Mohan, M, M Bartkuhn, M Herold, A Philippen, N Heinl, I Bardenhagen, J Leers, RA White, R Renkawitz-Pohl, H Saumweber and R Renkawitz (2007). "The Drosophila insulator proteins CTCF and CP190 link enhancer blocking to body patterning." *EMBO J* **26**(19): 4203-4214. DOI: 10.1038/sj.emboj.7601851.

Mongelard, F, M Labrador, EM Baxter, TI Gerasimova and VG Corces (2002). "Trans-splicing as a Novel Mechanism to Explain Interallelic Complementation in Drosophila." *Genetics* **160**(4): 1481-1487.

Moon, SH, L Lin, X Zhang, TA Nguyen, Y Darlington, AS Waldman, X Lu and LA Donehower (2010). "Wild-type p53-induced phosphatase 1 dephosphorylates histone variant gamma-H2AX and suppresses DNA double strand break repair." *J Biol Chem* **285**(17): 12935-12947. DOI: 10.1074/jbc.M109.071696.

Moretti, L, K Niermann, S Schleicher, NJ Giacalone, V Varki, KW Kim, P Kopsombut, DK Jung and B Lu (2011). "MLN8054, a small molecule inhibitor of aurora kinase a, sensitizes androgen-resistant prostate cancer to radiation." *Int J Radiat Oncol Biol Phys* **80**(4): 1189-1197. DOI: 10.1016/j.ijrobp.2011.01.060.

Morillo Prado, JR, S Srinivasan and MT Fuller (2013). "The histone variant His2Av is required for adult stem cell maintenance in the Drosophila testis." *PLoS Genet* **9**(11): e1003903. DOI: 10.1371/journal.pgen.1003903.

Myrick, LK, H Hashimoto, X Cheng and ST Warren (2015). "Human FMRP contains an integral tandem Agenet (Tudor) and KH motif in the amino terminal domain." *Hum Mol Genet* **24**(6): 1733-1740. DOI: 10.1093/hmg/ddu586.

Nakada, S, GI Chen, AC Gingras and D Durocher (2008). "PP4 is a gamma H2AX phosphatase required for recovery from the DNA damage checkpoint." *EMBO Rep* **9**(10): 1019-1026. DOI: 10.1038/embor.2008.162.

Natale, F, A Rapp, W Yu, A Maiser, H Harz, A Scholl, S Grulich, T Anton, D Horl, W Chen, M Durante, G Taucher-Scholz, H Leonhardt and MC Cardoso (2017). "Identification of the elementary structural units of the DNA damage response." *Nat Commun* **8**: 15760. DOI: 10.1038/ncomms15760.

Negre, N, CD Brown, PK Shah, P Kheradpour, CA Morrison, JG Henikoff, X Feng, K Ahmad, S Russell, RA White, L Stein, S Henikoff, M Kellis and KP White (2010). "A comprehensive map of insulator elements for the Drosophila genome." *PLoS Genet* **6**(1): e1000814. DOI: 10.1371/journal.pgen.1000814.

Negrini, S, VG Gorgoulis and TD Halazonetis (2010). "Genomic instability — an evolving hallmark of cancer." *Nature Reviews Molecular Cell Biology* **11**(3): 220-228. DOI: 10.1038/nrm2858.

Oberle, I, F Rousseau, D Heitz, C Kretz, D Devys, A Hanauer, J Boue, M Bertheas and J Mandel (1991). "Instability of a 550-base pair DNA segment and abnormal methylation in fragile X syndrome." *Science* **252**(5009): 1097-1102. DOI: 10.1126/science.252.5009.1097.

Ong, CT, K Van Bortle, E Ramos and VG Corces (2013). "Poly(ADP-ribosyl)ation regulates insulator function and intrachromosomal interactions in Drosophila." *Cell* **155**(1): 148-159. DOI: 10.1016/j.cell.2013.08.052.

Ooegema, K, WGF Whitfield and B Alberts (1995). "The cell cycle-dependent localization of the CP190 centrosomal protein is determined by the coordinate action of two separable domains." *Journal of Cell Biology* **131**(5): 1261-1273.

Ozdemir, I and MC Gambetta (2019). "The Role of Insulation in Patterning Gene Expression." *Genes (Basel)* **10**(10). DOI: 10.3390/genes10100767.

Pai, CY, EP Lei, D Ghosh and VG Corces (2004). "The centrosomal protein CP190 is a component of the gypsy chromatin insulator." *Mol Cell* **16**(5): 737-748. DOI: 10.1016/j.molcel.2004.11.004.

Palmer, D, LA Snyder and M Blumenfeld (1980). "Drosophila nucleosomes contain an unusual histone-like protein." *Proc Natl Acad Sci U S A* **77**(5): 2671-2675. DOI: 10.1073/pnas.77.5.2671.

Park, AR, N Liu, N Neuenkirchen, Q Guo and H Lin (2019). "The Role of Maternal HP1a in Early Drosophila Embryogenesis via Regulation of Maternal Transcript Production." *Genetics* **211**(1): 201-217. DOI: 10.1534/genetics.118.301704.

Park, EJ, DW Chan, JH Park, MA Oettinger and J Kwon (2003). "DNA-PK is activated by nucleosomes and phosphorylates H2AX within the nucleosomes in an acetylation-dependent manner." *Nucleic Acids Res* **31**(23): 6819-6827. DOI: 10.1093/nar/gkg921.

Paull, TT, EP Rogakou, V Yamazaki, CU Kirchgessner, M Gellert and WM Bonner (2000). "A critical role for histone H2AX in recruitment of repair factors to nuclear foci after DNA damage." *Curr Biol* **10**(15): 886-895. DOI: 10.1016/s0960-9822(00)00610-2.

Pearson, K (1895). "Mathematical contributions to the theory of evolution." *Philosophical Transactions of the Royal Society of London. Series A, Containing Papers of a Mathematical or Physical Character*(187): 253 - 318. DOI: 10.1098/rsta.1896.0007.

Pengelly, AR, R Kalb, K Finkl and J Müller (2015). "Transcriptional repression by PRC1 in the absence of H2A monoubiquitylation." *Genes Dev* **29**(14): 1487-1492. DOI: 10.1101/gad.265439.115.

Pieretti, M, FP Zhang, YH Fu, ST Warren, BA Oostra, CT Caskey and DL Nelson (1991). "Absence of expression of the FMR-1 gene in fragile X syndrome." *Cell* **66**(4): 817-822. DOI: 10.1016/0092-8674(91)90125-i.

Placek, BJ, LN Harrison, BM Villers and LM Gloss (2005). "The H2A.Z/H2B dimer is unstable compared to the dimer containing the major H2A isoform." *Protein Science* **14**(2): 514-522. DOI: 10.1110/ps.041026405.

Postika, N, M Metzler, M Affolter, M Müller, P Schedl, P Georgiev and O Kyrchanova (2018). "Boundaries mediate long-distance interactions between enhancers and promoters in the Drosophila Bithorax complex." *PLoS Genet* **14**(12): e1007702. DOI: 10.1371/journal.pgen.1007702.

Raisner, RM, PD Hartley, MD Meneghini, MZ Bao, CL Liu, SL Schreiber, OJ Rando and HD Madhani (2005). "Histone variant H2A.Z marks the 5' ends of both active and inactive genes in euchromatin." *Cell* **123**(2): 233-248. DOI: 10.1016/j.cell.2005.10.002.

Ramirez, F, V Bhardwaj, L Arrigoni, KC Lam, BA Gruning, J Villaveces, B Habermann, A Akhtar and T Manke (2018). "High-resolution TADs reveal DNA sequences underlying genome organization in flies." *Nat Commun* **9**(1): 189. DOI: 10.1038/s41467-017-02525-w.

Rangasamy, D, L Berven, P Ridgway and DJ Tremethick (2003). "Pericentric heterochromatin becomes enriched with H2A.Z during early mammalian development." *Embo j* **22**(7): 1599-1607. DOI: 10.1093/emboj/cdg160.

Rao, Suhas SP, Miriam H Huntley, Neva C Durand, Elena K Stamenova, Ivan D Bochkov, James T Robinson, Adrian L Sanborn, I Machol, Arina D Omer, Eric S Lander and Erez L Aiden (2014). "A 3D Map of the Human Genome at Kilobase Resolution Reveals Principles of Chromatin Looping." *Cell* **159**(7): 1665-1680. DOI: 10.1016/j.cell.2014.11.021.

Rappold, I, K Iwabuchi, T Date and J Chen (2001). "Tumor suppressor p53 binding protein 1 (53BP1) is involved in DNA damage-signaling pathways." *J Cell Biol* **153**(3): 613-620. DOI: 10.1083/jcb.153.3.613.

Ray Chaudhuri, A and A Nussenzweig (2017). "The multifaceted roles of PARP1 in DNA repair and chromatin remodelling." *Nat Rev Mol Cell Biol* **18**(10): 610-621. DOI: 10.1038/nrm.2017.53.

Richmond, TJ and CA Davey (2003). "The structure of DNA in the nucleosome core." *Nature* **423**(6936): 145-150. DOI: 10.1038/nature01595.

Robinson, JT, H Thorvaldsdóttir, W Winckler, M Guttman, ES Lander, G Getz and JP Mesirov (2011). "Integrative genomics viewer." *Nature Biotechnology* **29**(1): 24-26. DOI: 10.1038/nbt.1754.

Rogakou, EP, C Boon, C Redon and WM Bonner (1999). "Megabase chromatin domains involved in DNA double-strand breaks in vivo." *J Cell Biol* **146**(5): 905-916. DOI: 10.1083/jcb.146.5.905.

Rogakou, EP, W Nieves-Neira, C Boon, Y Pommier and WM Bonner (2000). "Initiation of DNA fragmentation during apoptosis induces phosphorylation of H2AX histone at serine 139." *J Biol Chem* **275**(13): 9390-9395. DOI: 10.1074/jbc.275.13.9390.

Rogakou, EP, DR Pilch, AH Orr, VS Ivanova and WM Bonner (1998). "DNA Double-stranded Breaks Induce Histone H2AX Phosphorylation on Serine 139." *The Journal of Biological Chemistry* **273**: 5858-5868. DOI: 10.1074/jbc.273.10.5858.

Rong, YS (2008). "Loss of the histone variant H2A.Z restores capping to checkpoint-defective telomeres in Drosophila." *Genetics* **180**(4): 1869-1875. DOI: 10.1534/genetics.108.095547.

Roseman, RR, V Pirrotta and PK Geyer (1993). "The su(Hw) protein insulates expression of the Drosophila melanogaster white gene from chromosomal position-effects." *EMBO J* **12**: 435 - 442. DOI: 10.1002/j.1460-2075.1993.tb05675.x.

Rudnizky, S, A Bavly, O Malik, L Pnueli, P Melamed and A Kaplan (2016). "H2A.Z controls the stability and mobility of nucleosomes to regulate expression of the LH genes." *Nat Commun* **7**: 12958. DOI: 10.1038/ncomms12958.

Ruhf, ML, A Braun, O Papoulas, JW Tamkun, N Randsholt and M Meister (2001). "The domino gene of Drosophila encodes novel members of the SWI2/SNF2 family of DNA-dependent ATPases, which contribute to the silencing of homeotic genes." *Development* **128**(8): 1429-1441.

Rust, K, MD Tiwari, VK Mishra, F Grawe and A Wodarz (2018). "Myc and the Tip60 chromatin remodeling complex control neuroblast maintenance and polarity in Drosophila." *Embo j* **37**(16). DOI: 10.15252/embj.201798659.

Sanders, JT, TF Freeman, Y Xu, R Golloshi, MA Stallard, AM Hill, R San Martin, AS Balajee and RP McCord (2020). "Radiation-induced DNA damage and repair effects on 3D genome organization." *Nat Commun* **11**(1): 6178. DOI: 10.1038/s41467-020-20047-w.

Santos-Rosa, H, R Schneider, AJ Bannister, J Sherriff, BE Bernstein, NC Emre, SL Schreiber, J Mellor and T Kouzarides (2002). "Active genes are tri-methylated at K4 of histone H3." *Nature* **419**(6905): 407-411. DOI: 10.1038/nature01080.

Scacchetti, A, T Schauer, A Reim, Z Apostolou, A Campos Sparr, S Krause, P Heun, M Wierer and PB Becker (2020). "Drosophila SWR1 and NuA4 complexes are defined by DOMINO isoforms." *Elife* **9**. DOI: 10.7554/eLife.56325.

Schindelin, J, I Arganda-Carreras, E Frise, V Kaynig, M Longair, T Pietzsch, S Preibisch, C Rueden, S Saalfeld, B Schmid, JY Tinevez, DJ White, V Hartenstein, K Eliceiri, P Tomancak and A Cardona (2012). "Fiji: an open-source platform for biological-image analysis." *Nat Methods* **9**(7): 676-682. DOI: 10.1038/nmeth.2019.

Schoborg, T and M Labrador (2014). "Expanding the roles of chromatin insulators in nuclear architecture, chromatin organization and genome function." *Cell Mol Life Sci* **71**(21): 4089-4113. DOI: 10.1007/s00018-014-1672-6.

Schoborg, T, R Rickels, J Barrios and M Labrador (2013). "Chromatin insulator bodies are nuclear structures that form in response to osmotic stress and cell death." *J Cell Biol* **202**(2): 261-276. DOI: 10.1083/jcb.201304181.

Secombe, J, J Pispa, R Saint and H Richardson (1998). "Analysis of a Drosophila cyclin E hypomorphic mutation suggests a novel role for cyclin E in cell proliferation control during eye imaginal disc development." *Genetics* **149**(4): 1867-1882.

Sharma, D, L De Falco, S Padavattan, C Rao, S Geifman-Shochat, CF Liu and CA Davey (2019). "PARP1 exhibits enhanced association and catalytic efficiency with γH2A.X-nucleosome." *Nat Commun* **10**(1): 5751. DOI: 10.1038/s41467-019-13641-0.

Shin, HJ, JY Kim, L Hampson, H Pyo, HJ Baek, SA Roberts, JH Hendry and IN Hampson (2010). "Human papillomavirus 16 E6 increases the radiosensitivity of p53-mutated cervical cancer cells, associated with up-regulation of aurora A." *Int J Radiat Biol* **86**(9): 769-779. DOI: 10.3109/09553002.2010.484477.

Simmons, JR, R An, B Amankwaa, S Zayac, J Kemp and M Labrador (2021). "A Phosphorylated Histone H2A Variant Displays Properties of Chromatin Insulator Proteins in *Drosophila*." *bioRxiv*: 2021.2002.2023.432395. DOI: 10.1101/2021.02.23.432395.

Sinenko, SA, J Shim and U Banerjee (2011). "Oxidative stress in the haematopoietic niche regulates the cellular immune response in Drosophila." *EMBO Rep* **13**(1): 83-89. DOI: 10.1038/embor.2011.223.

Sirbu, BM and D Cortez (2013). "DNA damage response: three levels of DNA repair regulation." *Cold Spring Harb Perspect Biol* **5**(8): a012724. DOI: 10.1101/cshperspect.a012724.

Snaith, HA, CG Armstrong, Y Guo, K Kaiser and PT Cohen (1996). "Deficiency of protein phosphatase 2A uncouples the nuclear and centrosome cycles and prevents attachment of microtubules to the kinetochore in Drosophila microtubule star (mts) embryos." *Journal of Cell Science* **109**(13): 3001-3012. DOI: 10.1242/jcs.109.13.3001.

Soshnev, AA, RM Baxley, JR Manak, K Tan and PK Geyer (2013). "The insulator protein Suppressor of Hairy-wing is an essential transcriptional repressor in the Drosophila ovary." *Development* **140**(17): 3613-3623. DOI: 10.1242/dev.094953.

Soshnev, AA, B He, RM Baxley, N Jiang, CM Hart, K Tan and PK Geyer (2012). "Genome-wide studies of the multi-zinc finger Drosophila Suppressor of Hairy-wing protein in the ovary." *Nucleic Acids Res* **40**(12): 5415-5431. DOI: 10.1093/nar/gks225.

Sourisseau, T, D Maniotis, A McCarthy, C Tang, CJ Lord, A Ashworth and S Linardopoulos (2010). "Aurora-A expressing tumour cells are deficient for homology-directed DNA double strand-break repair and sensitive to PARP inhibition." *EMBO Mol Med* **2**(4): 130-142. DOI: 10.1002/emmm.201000068.

Stephenson, RA, JM Thomalla, L Chen, P Kolkhof, M Beller and MA Welte (2020). "Sequestration to lipid droplets promotes histone availability by preventing turnover of excess histones." *bioRxiv*: 2020.2008.2006.237164. DOI: 10.1101/2020.08.06.237164.

Stevens, KM, JB Swadling, A Hocher, C Bang, S Gribaldo, RA Schmitz and T Warnecke (2020). "Histone variants in archaea and the evolution of combinatorial chromatin complexity." *Proc Natl Acad Sci U S A* **117**(52): 33384-33395. DOI: 10.1073/pnas.2007056117.

Stewart, GS, B Wang, CR Bignell, AM Taylor and SJ Elledge (2003). "MDC1 is a mediator of the mammalian DNA damage checkpoint." *Nature* **421**(6926): 961-966. DOI: 10.1038/nature01446.

Stiff, T, M O'Driscoll, N Rief, K Iwabuchi, M Lobrich and PA Jeggo (2004). "ATM and DNA-PK Function Redundantly to Phosphorylate H2AX after Exposure to Ionizing Radiation." *Cancer Research* **64**(7): 2390-2396.

Stowers, RS and TL Schwarz (1999). "A genetic method for generating Drosophila eyes composed exclusively of mitotic clones of a single genotype." *Genetics* **152**(4): 1631-1639.

Sullivan, KF, M Hechenberger and K Masri (1994). "Human CENP-A contains a histone H3 related histone fold domain that is required for targeting to the centromere." *J Cell Biol* **127**(3): 581-592. DOI: 10.1083/jcb.127.3.581.

Sun, Y, X Jiang, S Chen, N Fernandes and BD Price (2005). "A role for the Tip60 histone acetyltransferase in the acetylation and activation of ATM." *Proc Natl Acad Sci U S A* **102**(37): 13182-13187. DOI: 10.1073/pnas.0504211102.

Sun, Y, Y Xu, K Roy and BD Price (2007). "DNA Damage-Induced Acetylation of Lysine 3016 of ATM Activates ATM Kinase Activity." *Molecular and Cellular Biology* **27**(24): 8502-8509. DOI: 10.1128/mcb.01382-07.

Swaminathan, J, EM Baxter and VG Corces (2005). "The role of histone H2Av variant replacement and histone H4 acetylation in the establishment of Drosophila heterochromatin." *Genes Dev* **19**(1): 65-76. DOI: 10.1101/gad.1259105.

Talbert, PB and S Henikoff (2010). "Histone variants--ancient wrap artists of the epigenome." *Nat Rev Mol Cell Biol* **11**(4): 264-275. DOI: 10.1038/nrm2861.

Talbert, PB and S Henikoff (2021). "Histone variants at a glance." *Journal of Cell Science* **134**(6): jcs244749. DOI: 10.1242/jcs.244749.

Thomas, CJ, E Kotova, M Andrake, J Adolf-Bryfogle, R Glaser, C Regnard and AV Tulin (2014). "Kinase-mediated changes in nucleosome conformation trigger chromatin decondensation via poly(ADP-ribosyl)ation." *Mol Cell* **53**(5): 831-842. DOI: 10.1016/j.molcel.2014.01.005.

Tran, J, TJ Brenner and S DiNardo (2000). "Somatic control over the germline stem cell lineage during Drosophila spermatogenesis." *Nature* **407**(6805): 754-757. DOI: 10.1038/35037613.

Tulin, A and A Spradling (2003). "Chromatin loosening by poly(ADP)-ribose polymerase (PARP) at Drosophila puff loci." *Science* **299**(5606): 560-562. DOI: 10.1126/science.1078764.

van Berkum, NL, E Lieberman-Aiden, L Williams, M Imakaev, A Gnirke, LA Mirny, J Dekker and ES Lander (2010). "Hi-C: A Method to Study the Three-dimensional Architecture of Genomes." *JoVE*(39): e1869. DOI: doi:10.3791/1869.

Van Bortle, K, MH Nichols, C Ong, N Takenaka, ZS Qin and VG Corces (2014). "Insulator function and topological domain border strength scale with architectural protein occupancy." *Genome Biology* **15**(R82): 1-18.

van Daal, A and SCR Elgin (1992). "A histone variant, H2AvD, is essential in Drosophila melanogaster." *Molecular Biology of the Cell* **3**: 593-602. DOI: 10.1091/mbc.3.6.593.

van Daal, A, EM White, MA Gorovsky and CR Elgin (1988). "Drosophila has a single copy of the gene encoding a highly conserved histone H2A variant of the H2A. F/Z type." *Nucleic Acids Research* **16**(15): 7487-7497. DOI: 10.1093/nar/16.15.7487.

Verkerk, AJ, M Pieretti, JS Sutcliffe, YH Fu, DP Kuhl, A Pizzuti, O Reiner, S Richards, MF Victoria, FP Zhang and et al. (1991). "Identification of a gene (FMR-1) containing a CGG repeat coincident with a breakpoint cluster region exhibiting length variation in fragile X syndrome." *Cell* **65**(5): 905-914. DOI: 10.1016/0092-8674(91)90397-h.

Wallace, HA, MP Plata, HJ Kang, M Ross and M Labrador (2010). "Chromatin insulators specifically associate with different levels of higher-order chromatin organization in Drosophila." *Chromosoma* **119**(2): 177-194. DOI: 10.1007/s00412-009-0246-0.

Wallace, JA and TL Orr-Weaver (2005). "Replication of heterochromatin: insights into mechanisms of epigenetic inheritance." *Chromosoma* **114**(6): 389-402. DOI: 10.1007/s00412-005-0024-6.

Wan, L, TC Dockendorff, TA Jongens and G Dreyfuss (2000). "Characterization of dFMR1, a Drosophila melanogaster homolog of the fragile X mental retardation protein." *Mol Cell Biol* **20**(22): 8536-8547. DOI: 10.1128/mcb.20.22.8536-8547.2000.

Wang, C, KC Chang, G Somers, D Virshup, BT Ang, C Tang, F Yu and H Wang (2009). "Protein phosphatase 2A regulates self-renewal of Drosophila neural stem cells." *Development* **136**(13): 2287-2296. DOI: 10.1242/dev.035758.

Wang, L, W Dai and L Lu (2014). "Osmotic stress-induced phosphorylation of H2AX by polo-like kinase 3 affects cell cycle progression in human corneal epithelial cells." *J Biol Chem* **289**(43): 29827-29835. DOI: 10.1074/jbc.M114.597161.

Wang, Y, W Zhang, Y Jin, J Johansen and KM Johansen (2001). "The JIL-1 Tandem Kinase Mediates Histone H3 Phosphorylation and Is Required for Maintenance of Chromatin Structure in Drosophila." *Cell* **105**(4): 433-443. DOI: 10.1016/S0092-8674(01)00325-7.

Ward, IM and J Chen (2001). "Histone H2AX is phosphorylated in an ATR-dependent manner in response to replicational stress." *J Biol Chem* **276**(51): 47759-47762. DOI: 10.1074/jbc.C100569200.

Ward, IM, K Minn, J van Deursen and J Chen (2003). "p53 Binding protein 53BP1 is required for DNA damage responses and tumor suppression in mice." *Mol Cell Biol* **23**(7): 2556-2563. DOI: 10.1128/mcb.23.7.2556-2563.2003.

Weber, CM, JG Henikoff and S Henikoff (2010). "H2A.Z nucleosomes enriched over active genes are homotypic." *Nat Struct Mol Biol* **17**(12): 1500-1507. DOI: 10.1038/nsmb.1926.

Weber, CM, S Ramachandran and S Henikoff (2014). "Nucleosomes are context-specific, H2A.Z-modulated barriers to RNA polymerase." *Mol Cell* **53**(5): 819-830. DOI: 10.1016/j.molcel.2014.02.014.

Wen, Z, L Zhang, H Ruan and G Li (2020). "Histone variant H2A.Z regulates nucleosome unwrapping and CTCF binding in mouse ES cells." *Nucleic Acids Res* **48**(11): 5939-5952. DOI: 10.1093/nar/gkaa360.

Wittkopp, PJ, JR True and SB Carroll (2002). "Reciprocal functions of the Drosophila Yellow and Ebony proteins in the development and evolution of pigment patterns." *Development* **129**(8): 1849-1858.

Wlodarchak, N and Y Xing (2016). "PP2A as a master regulator of the cell cycle." *Crit Rev Biochem Mol Biol* **51**(3): 162-184. DOI: 10.3109/10409238.2016.1143913.

Xiao, A, H Li, D Shechter, SH Ahn, LA Fabrizio, H Erdjument-Bromage, S Ishibe-Murakami, B Wang, P Tempst, K Hofmann, DJ Patel, SJ Elledge and CD Allis (2009). "WSTF regulates the H2A.X DNA damage response via a novel tyrosine kinase activity." *Nature* **457**(7225): 57-62. DOI: 10.1038/nature07668.

Ye, T, AR Krebs, MA Choukrallah, C Keime, F Plewniak, I Davidson and L Tora (2011). "seqMINER: an integrated ChIP-seq data interpretation platform." *Nucleic Acids Res* **39**(6): e35. DOI: 10.1093/nar/gkq1287.

Yu, W, V Ginjala, V Pant, I Chernukhin, J Whitehead, F Docquier, D Farrar, G Tavoosidana, R Mukhopadhyay, C Kanduri, M Oshimura, AP Feinberg, V Lobanenkov, E Klenova and R Ohlsson (2004). "Poly(ADP-ribosyl)ation regulates CTCF-dependent chromatin insulation." *Nat Genet* **36**(10): 1105-1110. DOI: 10.1038/ng1426.

Zhan, X and DJ Liu (2015). "SEQMINER: An R-Package to Facilitate the Functional Interpretation of Sequence-Based Associations." *Genetic Epidemiology* **39**(8): 619-623. DOI: doi.org/10.1002/gepi.21918.

Zhang, H, DN Roberts and BR Cairns (2005). "Genome-wide dynamics of Htz1, a histone H2A variant that poises repressed/basal promoters for activation through histone loss." *Cell* **123**(2): 219-231. DOI: 10.1016/j.cell.2005.08.036.

Zhang, Y, T Liu, CA Meyer, J Eeckhoute, DS Johnson, BE Bernstein, C Nusbaum, RM Myers, M Brown, W Li and XS Liu (2008). "Model-based analysis of ChIP-Seq (MACS)." *Genome Biol* **9**(9): R137. DOI: 10.1186/gb-2008-9-9-r137.

Zhang, Z and BF Pugh (2011). "Genomic organization of H2Av containing nucleosomes in Drosophila heterochromatin." *PLoS One* **6**(6): e20511. DOI: 10.1371/journal.pone.0020511.

Zink, B, Y Engström, WJ Gehring and R Paro (1991). "Direct interaction of the Polycomb protein with Antennapedia regulatory sequences in polytene chromosomes of Drosophila melanogaster." *Embo j* **10**(1): 153-162.

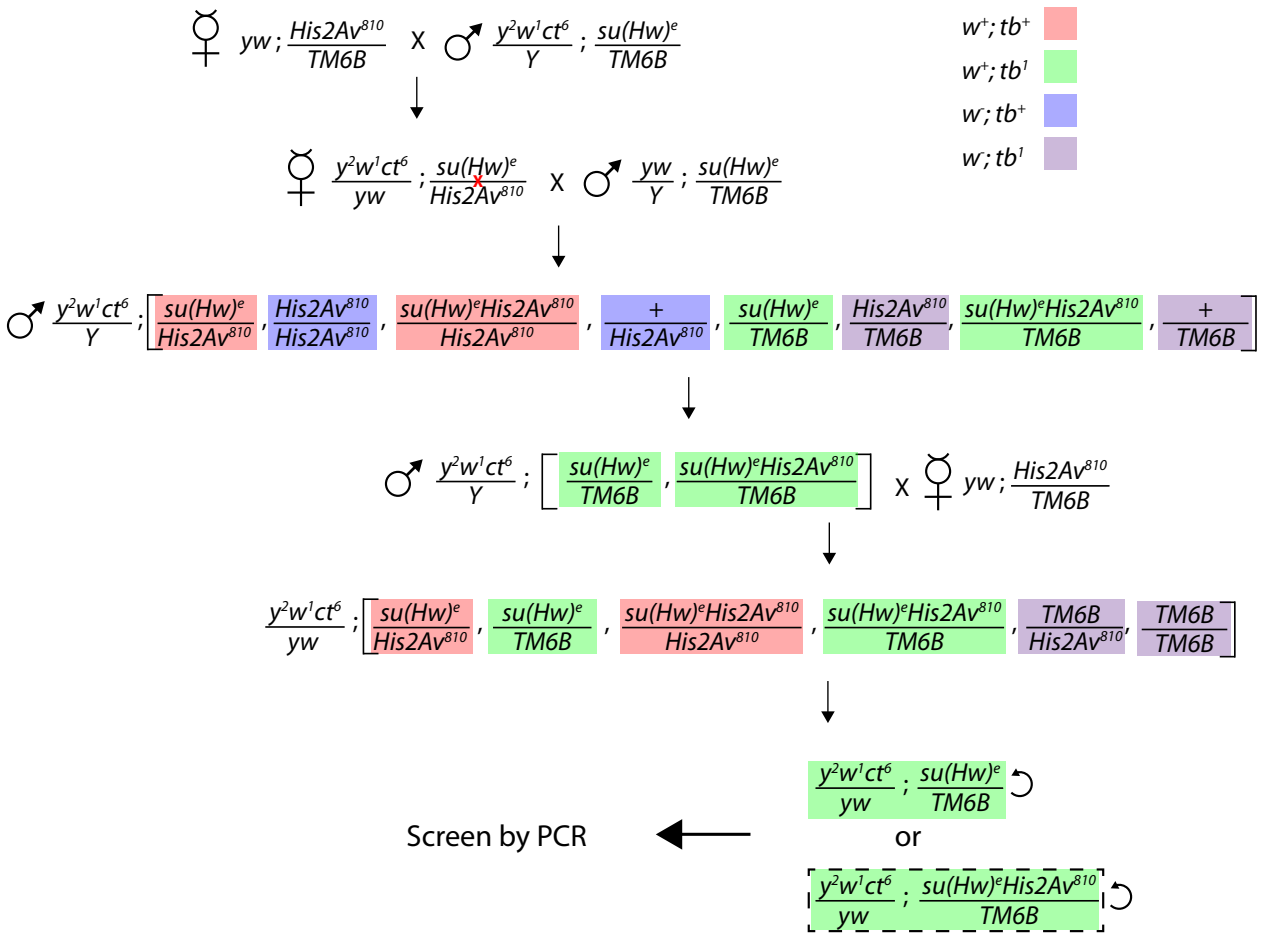


Figure A.1. Genetic crossing and phenotypic selection screen to generate *su(Hw)^{e04061}His2Av^{810}* double mutants. The *su(Hw)^{e04061}* genotype is abbreviated as *su(Hw)^{e}* and contains a visible *white^{+mC}* (*w^{+}*) marker. The *TM6B* balancer chromosome contains the visible *tubby^{1}* (*tb^{1}*) marker. The red X (**X**) in the F1 generation indicates meiotic recombination in the female third chromosome.

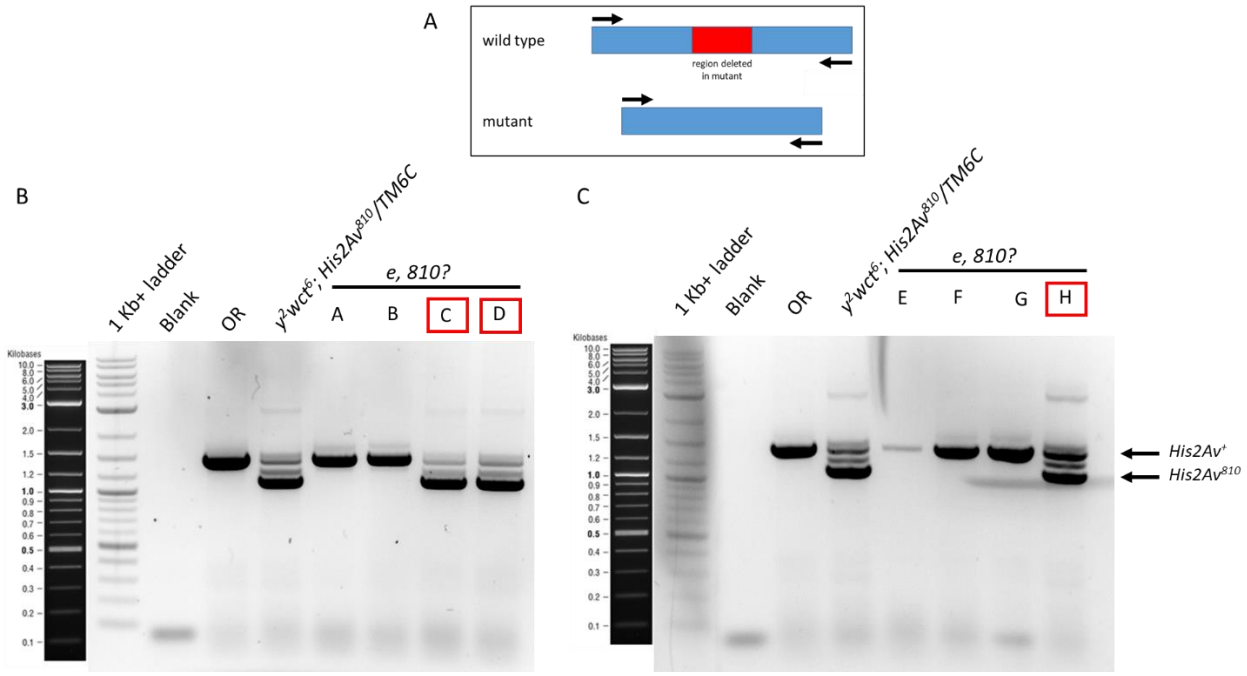


Figure A.2. Confirmation of *su(Hw)*^{e04061}*His2Av*^{810} double mutants by PCR. A. Schematic of the diagnostic PCR used to verify double mutants for the presence of *His2Av*^{810}, a mutation generated by the deletion of 311 base pairs. The mutant genotype therefore produces a smaller amplicon with primers placed outside the deleted region. **B., C.** Agarose gels showing PCR results from genomic DNA samples gathered from wild type OR, control *His2Av*^{810}, and potential recombinant lines. Red boxes indicate successful recombinant genotypes. Ladder image is from neb.com.

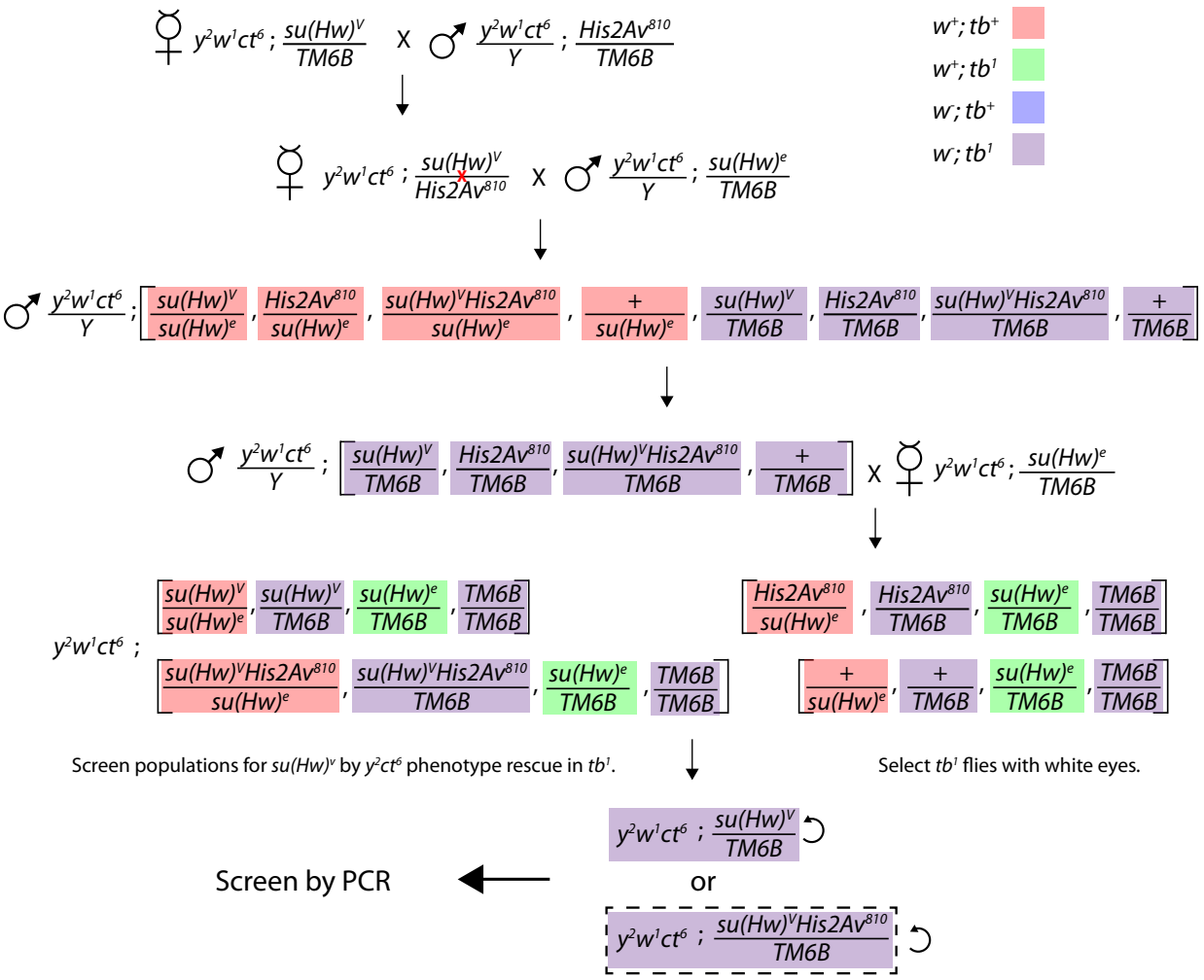


Figure A.3. Genetic crossing and phenotypic selection screen to generate *su(Hw)^{V}His2Av^{810}* double mutants. The *su(Hw)^{e04061}* genotype is abbreviated as *su(Hw)^{e}* and contains a visible *white^{+mC}* (*w^{+}*) marker. The *TM6B* balancer chromosome contains the visible *tubby^{1}* (*tb^{1}*) marker. Populations with genotypes transheterozygous for the *su(Hw)^{e04061}* and *su(Hw)^{V}* chromosomes were selected for by screening for rescue of the *y^{2}* and *ct^{6}* phenotypes. The red X (**X**) in the F1 generation indicates meiotic recombination in the female third chromosome.

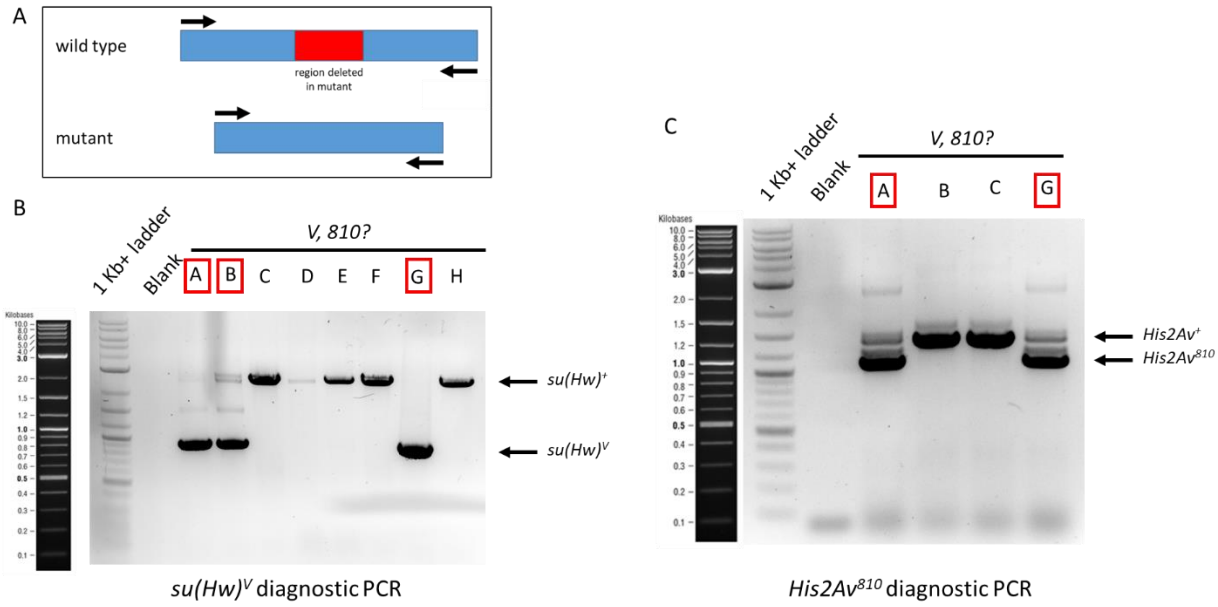


Figure A.4. Confirmation of *su(Hw)^{V}His2Av^{810}* double mutants by PCR. **A.** Schematic of the diagnostic PCR used to verify double mutants for the presence of *su(Hw)^{V}* and *His2Av^{810}*, both mutations generated by the deletion of hundreds of base pairs. The mutant genotypes therefore produce smaller amplicons with primers placed outside the deleted regions. **B., C.** Agarose gels showing PCR results from genomic DNA samples gathered from potential recombinant lines for *su(Hw)^{V}* **(B.)** and *His2Av^{810}* **(C.)**. Red boxes indicate successful recombinant genotypes. Ladder image is from neb.com.

Vita

James Ryan Simmons was raised in North Carolina, where he attended the North Carolina School of Science and Mathematics, garnering a four year tuition scholarship for public universities in North Carolina. After earning a Bachelor of Science degree in biology at the University of North Carolina at Chapel Hill, Ryan earned his Master of Science degree in Biology at Western Carolina University while performing research on kinetochore proteins in the pathogenic yeast *Cryptococcus neoformans* in the lab of Dr. Indrani Bose. From there, Ryan moved to the University of Tennessee and joined the lab of Dr. Mariano Labrador to study the activity of chromatin insulator proteins in the fruit fly *Drosophila melanogaster*.